

ANTITUMOR AND CARDIOPROTECTIVE EFFECTS OF ANTIOXIDANT
PHENYLAMINOETHYL SELENIDE IN LIPOSOMES

by

JEONG YEON KANG

(Under the Direction of JASON ZASTRE)

ABSTRACT

Anthracyclines are potent anticancer agents, but cardiotoxicity mediated by free radical generation limits their clinical use. These studies evaluated the anticancer activity of phenyl-2-aminoethyl selenide (PAESe) and its potential to reduce doxorubicin (DOX)-induced cardiotoxicity. Growth inhibitory effects of PAESe with DOX, and vincristine, clinically used anticancer agents, and *tert*-butylhydroperoxide (TBHP), a known oxidant, was determined on the growth of human prostate carcinoma (PC-3) and breast cancer (BT-474) cells. PAESe did not alter the growth of PC-3 and BT-474 cells, however, concomitant use of PAESe decreased the oxidative-mediated cytotoxicity of TBHP, but had limited effect on vincristine or DOX activity. Further, PAESe decreased the formation of intracellular reactive oxygen species from TBHP and DOX. In tumor xenograft mouse model, PAESe did not alter DOX antitumor activity and showed evidence of direct antitumor activity relative to controls. DOX treatment decreased mice body weight significantly, whereas concomitant administration of PAESe and DOX was similar to controls. Most importantly, PAESe decreased DOX-mediated infiltration of

neutrophil and macrophages into the myocardium. These data suggest PAESe had *in vivo* antitumor activity and in combination with DOX decreased early signs of cardiotoxicity while preserving its antitumor activity. Furthermore, sterically stabilized PAESe liposome (SSL-PAESe) was formulated and the pharmacokinetic properties of SSL-PAESe were evaluated and compared with those of free PAESe to determine the effect of encapsulation using newly developed high-performance liquid chromatography - tandem mass spectrometry (HPLC-MS/MS) analytical method with electrospray ionization. Significant alterations in pharmacokinetic properties were observed; Circulation half-life of SSL-PAESe was increased significantly compared to free PAESe. A significant decrease in the rate of elimination and total systemic clearance and an increase in AUC were observed in animals receiving SSL-PAESe compared to free PAESe. The antitumor effect of SSL-PAESe was established by determining tumor growth inhibition, body weight, and survival using a tumor xenograft mice model. These results might be associated with increased exposure of drug in the body to improve efficacy (antitumor activity) with encapsulation in long-circulating liposomes. We demonstrated that PAESe encapsulation in SSL provides a potential to be developed as a clinical therapeutic product for improving cancer treatment.

INDEX WORDS: Antioxidant, Phenylaminoethyl selenides, Anthracycline, Doxorubicin, Cardiotoxicity, Liposome, Mass Spectrometry, HPLC-MS/MS, Electrospray, Pharmacokinetics

ANTITUMOR AND CARDIOPROTECTIVE EFFECTS OF ANTIOXIDANT
PHENYLAMINOETHYL SELENIDE IN LIPOSOMES

by

JEONG YEON KANG

B.S., Duksung Women's University, Seoul, S. Korea, 2004

M.S. Seoul National University, Seoul, S. Korea, 2007

A Dissertation Submitted to the Graduate Faculty of The University of Georgia in Partial
Fulfillment of the Requirements for the Degree

DOCTOR OF PHILOSOPHY

ATHENS, GEORGIA

2012

© 2012

Jeong Yeon Kang

All Rights Reserved

ANTITUMOR AND CARDIOPROTECTIVE EFFECTS OF ANTIOXIDANT
PHENYLAMINOETHYL SELENIDE IN LIPOSOMES

by

JEONG YEON KANG

Major Professor: Jason Zastre

Committee: Robert D. Arnold
Catherine A. White
Shelley B. Hooks
Robert S. Phillips

Electronic Version Approved:

Maureen Grasso
Dean of the Graduate School
The University of Georgia
December 2012

ACKNOWLEDGEMENTS

I would like to express my sincere appreciation to my advisor, Dr. Robert D. Arnold, for his support, guidance, and encouragement throughout my graduate studies. I would also like to express my gratitude to dissertation advisory committee members: Drs. Zastre, White, Hooks and Phillips for taking their time and providing insightful comments and suggestions that helped me to complete my dissertation in its final form. Many thanks to past Arnold's lab members, Ibrahim, Guodong, Leah, Ha, and Yahya for supporting me in many ways. I would like to acknowledge the Department of Pharmaceutical and Biomedical Sciences in the College of Pharmacy at University of Georgia for financial support through my graduate studies. Finally, I would like to express my deepest appreciation to my parents, Jae-yeol and Kui-ok, and sister, Seo-yeon, brother, Jong-hui, and Ji-hyun for supporting and encouraging me throughout this long time.

TABLE OF CONTENTS

	Page
ACKNOWLEDGEMENTS.....	iv
LIST OF TABLES.....	vi
LIST OF FIGURES	vii
CHAPTER	
1 INTRODUCTION AND LITERATURE REVIEW	1
2 THE CARDIOPROTECTIVE AND ANTITUMOR EFFECTS OF THE ANTIOXIDANT PHENYLAMINOETHYL SELENIDE: IN VITRO HUMAN PROSTATE AND BREAST CANCER CELLS AND IN VIVO XENOGRAFT MODEL OF HUMAN PROSTATE CANCER.....	34
3 QUANTIFICATION OF LIPOSOMAL PHENYLAMINOETHYL SELENIDES BY HIGH PERFORMANCE LIQUID CHROMATO-GRAPHY-TANDEM MASS SPECTROMETRY AND PHARMACOKINETIC IN RATS.....	80
4 CARDIOPROTECTION AND ANTITUMOR ACTIVITY OF PHENYL- AMINOETHYL SELENIDES ENCAPSULATED IN LIPOSOME.....	118
5 SUMMARY AND FUTURE STUDY.....	155

LIST OF TABLES

	Page
Table 2-1: Free radical scavenging effects of PAESe on TBHP and DOX in PC-3 cells	54
Table 2-2: Free radical scavenging effects of PAESe on TBHP and DOX in BT-474 cells	55
Table 3-1: MRM parameters for PAESe and FPAESe (I.S)	101
Table 3-2: Intra-day and Inter-day accuracy and precision for PAESe.....	102
Table 3-3: Stability of PAESe for 4 weeks.....	103
Table 3-4: Model-predicted pharmacokinetic parameters for free PAESe and SSL-PAESe.....	104
Table 4-1: Mean days survival.....	138
Table 4-2: Necrotic index.....	139

LIST OF FIGURES

	Page
Figure 1-1: The structures of anthracyclines: (a) Doxorubicin (b) Daunorubicin (c) Epirubicin.....	16
Figure 1-2: Selenide redox cycling.....	17
Figure 2-1: Effect of PAESe on the growth of PC-3 cells <i>in vitro</i>	56
Figure 2-2: Growth inhibition of PAESe on the growth of BT-474 cells <i>in vitro</i>	57
Figure 2-3: Effect of PAESe on the growth inhibition of vincristine in PC-3 cells.....	58
Figure 2-4: Growth inhibitory effect of PAESe in combination with vincristine on BT-474 cells.....	59
Figure 2-5: Effect of PAESe on the growth inhibition of TBHP in PC-3 cells.....	60
Figure 2-6: Growth inhibitory effect of PAESe in combination with TBHP on BT-474 cells.....	61
Figure 2-7: Effect of PAESe on the growth inhibition of DOX in PC-3 cells.....	62
Figure 2-8: Growth inhibitory effect of PAESe in combination with DOX on BT-474 Cells.....	63
Figure 2-9: Effect of PAESe on antitumor activity of DOX in a PC-3 xenograft model.....	64
Figure 2-10: Histological examination of heart.....	66
Figure 3-1: Chemical structures of phenylaminoalkyl selenide.....	105
Figure 3-2: Total ion chromatogram of PAESe and FPAESe (I.S.).....	106

Figure 3-3: Product ion chromatogram of PAESe and FPAESe (I.S.).....	107
Figure 3-4: Mean plasma concentration-time profile after <i>i.v.</i> administration of free PAESe (10 mg/kg) and SSL-PAESe (5 mg/kg).....	108
Figure 3-5: Encapsulation efficiency according to the drug:lipid ratio.....	110
Figure 4-1: Effect of SSL-PAESe on tumor growth (A) and body weight (B) in a PC-3 xenograft model.....	140
Figure 4-2: Survival (%) time profile.....	142
Figure 4-3: Body weight change of mice after long-term exposure of DOX.....	143
Figure 4-4: Histological micrographic images of the myocardium.....	144

CHAPTER 1

INTRODUCTION AND LITERATURE REVIEW

Cancer

Cancer is the 2nd leading cause of death accounting for 23% of all deaths, and the probability of developing cancer is 1 in 2 men and 1 in 3 women in their lifetimes in the United States [1]. Prostate and breast cancer are the most prevalent cancers expected to occur among men and women, respectively in 2012. These cancers will account for 29% of all newly diagnosed cancers in men and women [1].

Standard treatment of prostate and breast cancers includes surgery, radiation therapy, hormonal therapy and chemotherapy. Although these options have been efficacious in treatment of cancer for decades, severe side effects have been reported and limit overall clinical activity. Common side effects of surgery include incontinence, impotence, and bowel complication for prostate cancer and lymphedema of the arm and physical discomfort for breast cancer [1, 2]. Hormonal therapy is known to increase the potential of osteoporosis, diabetes, cardiovascular disease and obesity [3]. Radiation therapy has been reported to increase the risk of other cancers such as bladder cancer and rectal cancer by damaging adjacent epithelial cells [4]. Moreover, radiation therapy may not be effective on tumor tissue that has a low oxygen level, which decreases radiation-generated radicals that destroy tumor cells [5]. There is limited utility of localized therapies, such as surgery or radiation, in patients with metastatic disease. The

effectiveness of cancer treatment by chemotherapy may be limited by the development of drug resistance and undesired systemic effect on normal/non-targeted tissues [6].

Anthracyclines

Anthracyclines antibiotics such as doxorubicin (DOX, Fig 1-1A), daunorubicin (DNR, Fig 1-1B) and epirubicin (EPI, Fig 1-1C) are widely used anticancer agents in the treatment of hemopoietic neoplasms, such as acute lymphocytic leukemia and acute myelogenous leukemia, Hodgkin's and non-Hodgkin's lymphoma, multiple myeloma, breast, prostate, ovary and lung cancers [7, 8].

DOX and DNR, developed over 45 years ago, are still used widely in current cancer treatment [9, 10]. DOX has a broad spectrum of antitumor activity in the treatment of solid tumors including breast and prostate cancer [8, 11]. DOX is one of standard chemotherapeutics used in women with early-stage invasive breast cancer. A number of clinical trials have demonstrated that chemotherapy containing anthracyclines, *e.g.*, DOX, prolongs survival time over non-anthracycline chemotherapy protocols [12], and the survival advantage was reported especially for women with HER-2 positive not negative breast cancer [13]. Androgen-independent PC-3 prostate cancer cell has also been widely utilized to determine the therapeutic effect of DOX due to its high sensitivity to DOX [14-17].

Unlike DOX, DNR has a hydroxyl group at position C14. DNR has significantly greater activity against hematopoietic malignancies, but is less efficacious in the treatment of solid tumors. Thus, DNR is most commonly used for treatment of acute lymphocytic leukemia and acute myelogenous leukemia [11]. EPI, an epimer of DOX,

has the C4' hydroxyl group on the amino sugar in the equatorial not the axial position. EPI was discovered to expect having a similar antineoplastic spectrum of action to DOX with its structural similarity. However, it was shown that EPI does not provide any significant advantage over DOX. EPI has significantly less antitumor activity compared to DOX. EPI was also found to have slightly less cardiotoxicity compared to DOX, but this affect was observed at equimolar concentrations not at equitherapeutic doses [18]. Moreover, the cost of an equitherapeutic dose of EPI is substantially higher (22 times) than DOX in the U.S. [19].

Although the mechanisms of action of anthracyclines have not been elucidated fully, they are known to include: *i)* Inhibition of the activity of topoisomerase II that cleaves double-stranded DNA and unwinds supercoiled DNA, preventing DNA transcription and replication [20]; *ii)* Intercalation between base pairs of nucleic acid (DNA and RNA) strand, preventing nucleic acid synthesis, thus inhibiting the replication of cancer cells [21]; and *iii)* Formation of iron-mediated free oxygen radicals, damaging DNA and cellular membranes [22, 23].

Cardiotoxicity of Anthracycline

The clinical use of anthracyclines has been limited by cumulative dose-dependent cardiotoxicity [7]. Anthracycline cardiotoxicity is known to cause electrocardiographic changes such as blood pressure dysregulation and impaired heart contractility [24]. Anthracycline treatment also causes numerous morphological changes in cardiomyocytes including microtubular injury, mitochondrial damage, mitochondrial cristae lesion, disruption and dilatation of the sarcoplasmic reticulum, degeneration of Z band as well as

loss of myofibrils and tight junctions [25-27]. These alterations are known to associate with myocardial dysfunction, which over time lead to cardiomyopathy, congestive heart failure and mortality [26].

Anthracycline-induced cardiotoxicity can occur immediately (acute toxicity) after the first dose of treatment, resulting in transient arrhythmias or acute failure of the left ventricle [28, 29]. This acute cardiotoxicity, however, is rare form under current treatment protocols. More importantly, anthracycline-induced cardiotoxicity has been more commonly recognized months to even years after treatment has terminated [30]. This chronic or late onset cardiotoxicity is clinically the most important form because dose-related cardiac dysfunction can be progressed asymptotically, and eventually leads to more serious clinical problems such as late-onset ventricular dysfunction, heart failure and fatal arrhythmias [30-32].

Cardiotoxicity is known to occur based on the cumulative dose of the drug. In case of DOX, the risk of developing DOX-induced cardiotoxicity increases evidently above a cumulative dose of 550 mg/m^2 body surface area [7]. Therefore, it is recommended that total cumulative dose should not exceed 550 mg/m^2 to reduce the potential for cardiotoxicity. However, cardiotoxicity has been observed after cumulative doses under 550 mg/m^2 even though patients were carefully monitored to keep the cumulative dose under the safe upper limit [33]. In a retrospective analysis of three phase III clinical trials, congestive heart failure occurred with total cumulative DOX doses of 300 mg/m^2 or less [33]. It has been reported that cardiotoxicity occurred after treatment with even a single dose of DOX at 240 mg/m^2 [34].

Cause of cardiotoxicity

Several hypotheses have been proposed to explain DOX (one of anthracycline)-induced cardiotoxicity. Free radicals generated by metabolism of DOX can induce oxidative damage to lipid membranes and cellular components of cardiomyocytes. DOX can stimulate the release of intracellular calcium (Ca^{2+}) from cardiac sarcoplasmic reticulum, which dysregulate excitation-contraction coupling in cardiomyocytes [35]. The enhanced level of vasoactive substances such as catecholamine and histamine by DOX can induce myocardial damages [36]. DOX can also reduce the density of β -adrenergic receptors that control cardiac function as well as can inhibit the activity of glutathione peroxidase in cardiomyocytes [37, 38]. DOX can decrease selectively the expression of cardiac muscle gene such as α -actin, troponin I, and myosin light chain 2, as well as the muscle-specific isoform of creatine kinase [39].

Among these several mechanisms proposed, the primary cause of DOX cardiotoxicity is believed to be reactive free radicals produced during intracellular metabolism of DOX [26, 40, 41]. DOX is chemically composed of a tetracyclic aglycone and reducing daunosamine sugar with an *O*-glycosidic bond at carbon 7 (Fig 1-1) [42]. The quinone moiety on the tetracycline ring of DOX is responsible for the oxidation–reduction processes. In a microsomal NADPH-oxidase system, the quinone group in the tetracyclic aglycone molecule accepts an electron from NADPH and forms semiquinone catalyzed by either NADPH-cytochrome *c*-reductase or b_5 -reductase. The electron of the semiquinone is transferred to molecular O_2 , generating superoxide anion (O_2^-) by oxidization [7, 43, 44], followed by initiating lipid peroxidation or producing numerous

reactive free radicals such as hydrogen peroxide (H_2O_2), hydroxyl radical (OH^\bullet) and peroxynitrite (ONOO^-) [36, 38].

These reactive free radicals induce oxidative injury in macromolecules such as cellular components and membranes non-specifically, leading to cellular damage and death [45]. Free radicals are also known to damage cells by disrupting oxidative balance of nucleic acids, proteins, and lipids [46]. Normally, reactive intermediates are detoxified by antioxidant enzymes such as superoxide dismutase (SOD), catalase (CAT) and selenium-dependent glutathione peroxidase (GSHPx) to repair the resulting damage. However, this homeostatic balance can be altered by excessive free radical formation and oxidative stress or inhibition of antioxidant enzyme like GSHPx during DOX metabolism, which induces lipid peroxidation and altered cellular homeostasis [47-49].

Among reactive free radicals derived from DOX, superoxide anion is hypothesized to be primarily responsible for cardiac dysfunction [50]. The superoxide anions induce the peroxidation of polyunsaturated fatty acids within membranes [51, 52]. This superoxide anion is subsequently converted into hydrogen peroxide and oxygen by superoxide dismutase, a catalyzing enzyme. Hydroxyl radical, the most damaging and highly reactive radical, is then produced from hydrogen peroxide in the presence of ferrous iron (Fe^{2+}), followed by initiating free radical-mediated chain reactions, leading to oxidative damage to cardiomyocytes as well as lipid peroxidation by removing hydrogen atoms from unsaturated fatty acids [53]. Peroxynitrite is also one of important species that account for myocardial damage [54]. Peroxynitrite interacts readily with DNA to induce double- and single-strand breakage and base modifications [47, 55], and also target primarily cardiac myofibril, which is a major contributor to dysregulate

contractility in cardiac failure [56]. Nitric oxide (NO^{*}) also plays an important role in cardiac dysfunction. Although nitric oxide is involved in controlling cardiac contractility and blood flow, excessive nitric oxide is known to associate with oxidative damage in cardiomyocytes, leading to cardiomyopathy and congestive heart failure [54]. Moreover, nitric oxide can react with superoxide anion to form peroxynitrite [57].

Further, the heart is more susceptible to oxidative damage by free radicals generated by DOX for several reasons. The amount of antioxidants is limited in the heart and there is a specific myocardial phospholipid, cardiolipin, that has a high affinity to DOX [41]. Moreover, oxidative metabolism is highly activated so that the reaction with free radicals is increased due to the greater amount of mitochondria in heart than other organs [41]. In addition, DOX is known to be involved in structural and functional impairment of mitochondria that can decrease energy production, resulting in contractile failure of the heart [58, 59]. Due to the potent antitumor activity of DOX and other anthracyclines, cardiac protective approaches are needed to prevent DOX cardiotoxicity, thus increasing the therapeutic potential of DOX.

Antioxidants to reduce cardiotoxicity

The ability of antioxidants and scavenging agents to protect the heart from DOX-induced oxidative damage has been studied to reduce DOX cardiotoxicity [41, 60]. The concomitant administration of antioxidants, e.g., vitamin C, α -tocopherol (vitamin E), flavonoids (7-monohydroxyethylrutoside; monoHER) and lipid lowering drugs (statins) with DOX have been studied preclinically and/or clinically to evaluate their effects as a chemoprotectant [61-63]. However, the therapeutic potential of these antioxidants are

limited by several drawbacks such as an excessive synergism of DOX activity by induction of apoptosis mediated by induction of cell cycle inhibitor (vitamin E) and by arrest cells in the G₁ phase of the cell cycle (statins) [61, 64], bone marrow toxicity (vitamin E) [65] and insufficient cardioprotection and high dose (500 mg/kg) requirement (monoHER) [66]. Also, antioxidants such as vitamin E and N-acetylcysteine prevent the acute cardiotoxicity but not the chronic form of cardiotoxicity of DOX [67-69].

Further, there are several FDA approved drugs that are in clinical use as chemoprotectants. Dexrazoxane is a drug approved by the U.S. Food and Drug Administration (FDA) to reduce anthracycline-mediated cardiotoxicity as well as damage induced by extravasation (unintentional exposure) of anthracyclines. Dexrazoxane is a derivative of ethylenediaminetetraacetic acid (EDTA) and potent iron chelator; thus interrupting free radical formation induced by anthracycline-iron complex [70]. However, dexrazoxane was shown to cause myelosuppression and lead to acute myeloid leukemia and myelodysplastic syndrome [70, 71]. Although the mechanism responsible for the observed toxicity is not fully elucidated, it is believed that its ability to reversibly inhibit topoisomerase II, leading to direct cytotoxic effects or schedule-dependent synergistic or interfering effects on antitumor activity of DOX [70]. Currently, dexrazoxane is not allowed for use in pediatric cancer patients, and the limited usage is recommended to adult patients with advanced or metastatic breast cancer who have received 300 mg/m² dose of DOX due to concerns over toxicity [71]. Amifostine, another antioxidant approved by the FDA, has been shown to attenuate the toxicity associated with platinum-based anticancer agent on the kidney and salivary glands [72, 73]. Amifostine is dephosphorylated by alkaline phosphatase to a pharmacologically active sulfhydryl-

containing metabolite, which exerts a potent scavenging activity against free radicals generated by cisplatin [74]. However, amifostine showed less cardioprotective activity than dexrazoxane and did not prevent weight loss or alter mortality by DOX treatment in a spontaneously hypertensive rat model [74]. It was also reported that amifostine showed off-target toxicities, such as hypocalcemia, in animal models and human subjects by affecting parathyroid hormone secretion and tubular reabsorption of calcium [75, 76].

Phenyl-2-aminoethyl selenide (PAESe)

Phenyl-2-aminoethyl selenide (PAESe) is a novel selenium-containing therapeutic agent that shows antihypertensive activity through scavenging of dopamine- β -monooxygenase, a key enzyme of norepinephrine biosynthesis, and ascorbate depletion [77, 78]. PAESe also exhibits potent antioxidant activity through reacting with many metabolic oxidants such as peroxide, peroxy nitrite anion, and hydroperoxides in redox cycling process (Fig 1-2). Oxidized PAESe, phenyl-2-aminoethyl selenoxide (PAESeO), is generated when PAESe reduces cellular oxidants. PAESeO is then recycled readily back to the reduced form, PAESe, by cellular reductants such as ascorbate and glutathione, with no complex side reactions [47, 77, 78]. Thus, PAESe provides a protective effect against oxidant-induced DNA damage through this reductant-mediated redox cycling [47].

Selenium and Antioxidant in Chemotherapy

Selenium is an essential component of selenocysteine, the active site of glutathione peroxidase (GSHPx) [79, 80]. GSHPx is well-established major antioxidant

enzyme that scavenges hydroperoxides to prevent cellular damage and maintain membrane integrity in the presence of glutathione [79]. Selenium also has been shown to be a chemopreventive to a variety of malignancies [81]. In epidemiologic studies, it was suggested that selenium level was inversely associate with an incidence of prostate cancer, and selenium might slow tumor progression in prostate cancer patients [82, 83]. Also, selenium levels in plasma, serum, and erythrocyte of breast cancer patients were significantly lower compared to healthy controls [84]. Indeed, it was shown that selenium has antiangiogenic activity *in vitro* and *in vivo* through inducing apoptosis and regulating matrix metalloproteinase activity and vascular endothelial growth factor levels [85].

As described earlier, antioxidants are able to slow or inhibit the oxidation of cellular components, which prevents DNA mutation and lipid peroxidation that is highly correlated to the initiation and progression of malignancy [86]. Antioxidants are also found to decrease the expression of oncogenes and the activity of protein kinase C that is involved in cancer progression [87]. Antioxidants have been shown to impede tumor development by enhancing immune system activity *i.e.*, increasing the levels of interleukin-2, lymphocytes, T and B cell, natural killer cells, and lymphokine-activated killer cells as well as enhancing the responsiveness of antibody to antigen stimulation [88, 89].

Nanoparticulate drug carrier and sterically stabilized liposomes

Nanoparticulate drug carriers, which have the ability to encapsulate drugs and macromolecules, are known to alter drug disposition such as circulation half-life, tissue/tumor distribution, and rate/extent of drug release [90-93]. This disposition is

linked closely to the pharmacological efficacy and reduced toxicity of a number of clinical agents such as anticancer and anti-infective agents [92, 94].

Liposomes, one of the most commonly used drug-carriers, are spherical nano-sized structures with an aqueous interior surrounded by one or more concentric bilayers of phospholipids [95]. Depending on their hydrophobic properties, drugs can be encapsulated inside the aqueous core (hydrophilic drugs) or associated with the lipidic bilayer or interfacial region (hydrophobic drugs) [96].

Effective usage of liposomes is limited by their rapid clearance by reticular endothelial system (RES) and destabilization by serum protein opsonization. It has been shown that this opsonization and rapid clearance by the RES can be reduced through several modifications of lipid composition such as inclusion of cholesterol in the bilayer membrane and surface coating with hydrophilic polymers such as polyethylene glycol (PEG) and gangliosides [96]. Cholesterol incorporated in the bilayer membrane reduces liposome interaction with plasma proteins by decreasing membrane fluidity and permeability to aqueous solutes, which provide steric stability [96, 97]. Hydrophilic stealth coatings limit the ability of serum protein interaction with the carrier surface by steric hindrance effect, which reduces recognition by serum proteins [90, 98]. Sterically stabilized liposome (SSL), which incorporates PEG as surface coating, therefore has a long-circulating property with an increased retention of encapsulated compounds [99]. Pegylated liposomal DOX has been approved in the U.S. (Doxil[®]) and Canada (Caelyx[®]) and currently used as clinical products by the enhanced anticancer activity and diminished cardiotoxicity [91].

Furthermore, SSL can accumulated in tumor tissues passively through diffusion by the enhanced permeability and retention (EPR) effect [100]. EPR effect results from the unique physiological properties of tumor tissue such as leaky and disorganized vascular architecture and nonfunctional lymphatic drainage due to abnormal and uncontrolled formation of new blood vessels [101]. In normal tissue, vascular endothelial cells are generally continuous and non-fenestrated with small paracellular spaces of 6.7-8.0 nm and tight cell junctions [102]. On the contrary, tumor vessels have incomplete and discontinuous intercellular junctions with pores between 200-780 nm, which leads to an enhanced vessel permeability and provides an opportunity for drugs to extravasate and accumulate in tumor interstitium [91, 96]. Therefore, encapsulated drugs are able to reach and remain at the tumor site with sufficient concentration passing through the tumor microvasculature to achieve desirable pharmacological efficacy [103]. EPR effect is known to be relevant to over 40 kDa nanoparticles or macromolecules, not to low-molecular weight compounds which covers most of drugs in use today [104].

Dissertation Rationale and Hypotheses

DOX is widely used potent anticancer agent that inhibits topoisomerase II activity. However, its clinical use is hampered by severe cumulative dose-limiting cardiotoxicity that is believed to result from generation of reactive free radicals. Although there are two clinically approved drugs to lessen anthracycline cardiotoxicity, they have been shown to limit DOX antitumor activity and their use has been associated with significant toxicities. Phenyl-2-aminoethyl selenide (PAESe) is a potent antioxidant, reacting rapidly with many metabolic oxidants such as peroxide, peroxy nitrite anion, and hydroperoxides. It

has been also demonstrated that GSH-mediated redox cycling of PAESE results in protection of DNA against oxidant-induced damage. Therefore, we *hypothesized* that PAESE can reduce DOX-mediated cardiotoxicity. This hypothesis was tested by determining the effect of PAESE, alone and in combination with DOX, on *in vitro* human prostate and breast cancer cells growth and generation of reactive oxygen species. Utilizing a murine xenograft model of human prostate cancer the effect of PAESE on acute and chronic cardiotoxicity, overall toxicity (body weight change) and antitumor activity were determined. PAESE was encapsulated into a long-circulating liposome and a sensitive liquid chromatography tandem mass spectrometry assay was developed to determine the systemic pharmacokinetics (PK) of PAESE and assist in understanding the effect of drug exposure on PAESE activity.

In **Chapter 2**, we tested the *hypotheses* that *i*) PAESE does not inhibit the growth of human prostate and breast cancer cells, *ii*) PAESE does not alter the cytotoxicity of DOX when used in combination and *iii*) PAESE decreases free radicals generated from DOX. This was accomplished by evaluated the potential of PAESE antioxidant activity to mitigate DOX-induced cardiotoxicity using *in vitro* and *in vivo* human cancer models. Growth inhibitory effects of PAESE were determined alone and in combination with DOX, vincristine, and *tert*-butylhydroperoxide (TBHP) on the human prostate carcinoma (PC-3) and breast cancer (BT-474) cells. The effect of PAESE to decrease free radicals generated from DOX was also determined by cell-permeant indicator.

In **Chapter 2**, we also determined the pharmacological activity of PAESE in an animal model of human prostate cancer. This tested the *hypotheses* that *i*) PAESE does not alter the antitumor activity of DOX in a tumor (PC-3) xenograft mouse model, *ii*)

PAESe does not decrease animal body weight and *iii*) PAESe reduces the evidence of DOX's cardiotoxicity in mice. We observed an unexpected finding that PAESe appeared to have antitumor activity *in vivo*.

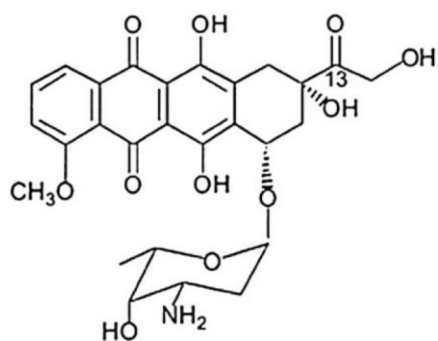
In **Chapter 3**, we developed a sensitive and selective high-performance liquid chromatography – tandem mass spectrometry (HPLC-MS/MS) assay with electrospray ionization (ESI) to quantify PAESe in plasma to support further development with respect to *in vivo* exposure of PAESe. Further, we developed sterically stabilized liposome to encapsulate PAESe (SSL-PAESe) and determined the pharmacokinetic (PK) properties of PAESe and SSL-PAESe in rat plasma to evaluate the effect of altering exposure of PAESe by encapsulation. Nanoparticulate drug carriers are known to alter drug disposition such as circulation half-life, tissue/tumor distribution, and rate/extent of drug release. Sterically stabilized liposome (SSL), one type of nanoparticulate drug carriers, has long-circulating property through a surface coating with hydrophilic polymer like polyethylene glycol (PEG). It is well known that encapsulation in SSL changes markedly the PK properties of drugs by pegylation. In **Chapter 3**, we hypothesized that encapsulation PAESe in sterically stabilized liposomes (SSL) would increase the systemic exposure of PAESe, and that differences in exposure may provide insights into PAESe cardioprotective effects and the unexpected *in vivo* antitumor activity. Nanoparticulate drug carriers are known to modulate drug disposition, which is responsible for the increased therapeutic efficacy and reduced toxicity of a variety of chemotherapeutic agents in animal models and clinically. Further, SSL-formulations containing anthracyclines, including DOX, are clinically approved and their exposure is different compared to free DOX. It would not be unexpected that to fully maximize

PAESe activity, a long-circulating formulation was needed. In **Chapter 3**, we observed that long circulating PAESe-liposomes altered PK properties (*i.e.* enhanced circulation time and exposure) of PAESe.

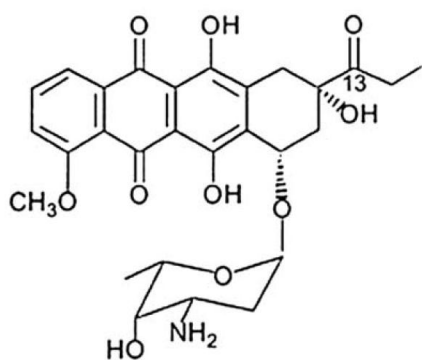
In **Chapter 4**, we determined the effect of PAESe encapsulated in long circulating liposomes in an established human prostate (PC-3) tumor xenograft model in athymic mice. This tested the *hypotheses* that *i)* long-circulating PAESe-liposomes improved antitumor efficacy compared to free PAESe and retained its cardioprotectant properties and *ii)* PAESe provides cardioprotection against chronic cardiotoxicities associated with long-term cumulative DOX treatments that are more representative of clinical practice and result in increased morbidity and mortality.

In **Chapter 5**, we summarize our findings. Specifically this research has demonstrated that PAESe is able to prevent acute and chronic DOX-mediated cardiotoxicities without altering DOX antitumor activity. Most excitingly, we also demonstrated a previously unreported finding that PAESe was able to inhibit tumor growth in a murine xenograft model of human prostate cancer. Although the mechanism for this observation is not known, PAESe appears to be a promising investigational agent that may be used with DOX to improve treatment of cancer and reduce long-term clinically significant cardiotoxicity.

(a)



(b)



(c)

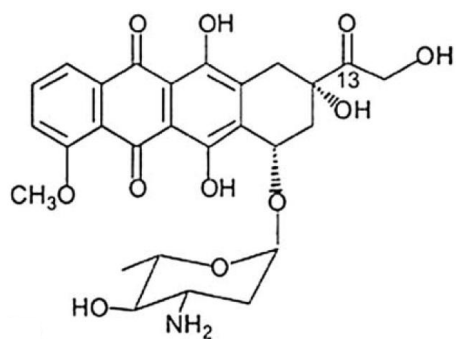


Figure 1-1. The structures of anthracyclines: (a) Doxorubicin (b) Daunorubicin (c) Epirubicin

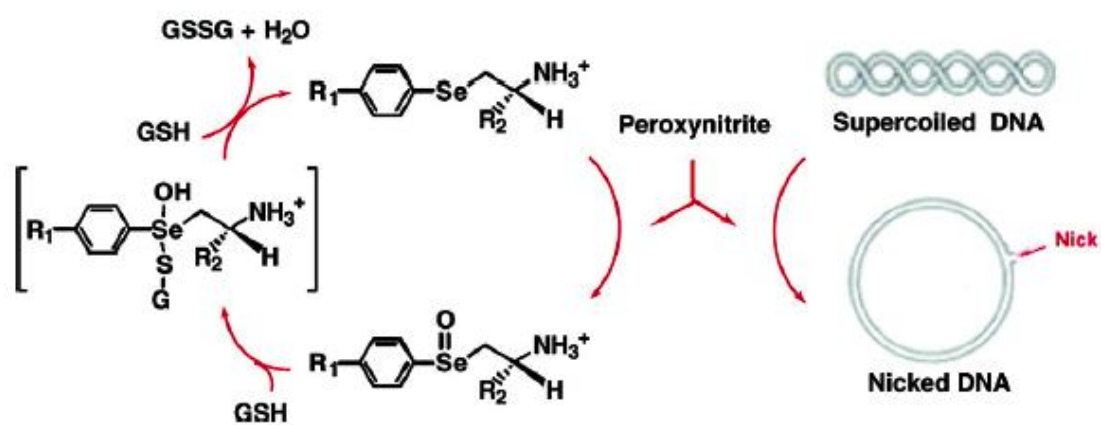


Figure 1-2. Selenide redox cycling

References

1. Siegel R, DeSantis C, Virgo K, Stein K, Mariotto A, Smith T, et al. Cancer treatment and survivorship statistics, 2012. *CA: A Cancer Journal For Clinicians* 2012; **62**:220-241.
2. Petrek JA, Senie RT, Peters M, Rosen PP. Lymphedema in a cohort of breast carcinoma survivors 20 years after diagnosis. *Cancer* 2001; **92**:1368-1377.
3. Kintzel PE, Chase SL, Schultz LM, O'Rourke TJ. Increased Risk of Metabolic Syndrome, Diabetes Mellitus, and Cardiovascular Disease in Men Receiving Androgen Deprivation Therapy for Prostate Cancer. *Pharmacotherapy: The Journal of Human Pharmacology and Drug Therapy* 2008; **28**:1511-1522.
4. Nieder AM, Porter MP, Soloway MS. Radiation therapy for prostate cancer increases subsequent risk of bladder and rectal cancer: a population based cohort study. *The Journal of urology* 2008; **180**:2005-2009; discussion 2009-2010.
5. Semenza GL. Intratumoral hypoxia, radiation resistance, and HIF-1. *Cancer Cell* 2004; **5**:405-406.
6. Kerbel RS, Kamen BA. The anti-angiogenic basis of metronomic chemotherapy. *Nature Reviews Cancer* 2004; **4**:423-436.
7. Hande KR. Clinical applications of anticancer drugs targeted to topoisomerase II. *Biochimica et Biophysica Acta (BBA) - Gene Structure and Expression* 1998; **1400**:173-184.

8. Kalyanaraman B, Joseph J, Kalivendi S, Wang S, Konorev E, Kotamraju S. Doxorubicin-induced apoptosis: implications in cardiotoxicity. *Molecular And Cellular Biochemistry* 2002; **234-235**:119-124.
9. Arcamone F, Cassinelli G, Fantini G, Grein A, Orezzi P, Pol C, et al. Adriamycin, 14-hydroxydaunomycin, a new antitumor antibiotic from *S. peuceetius* var. *caesius*. Reprinted from *Biotechnology and Bioengineering*, Vol. XI, Issue 6, Pages 1101-1110 (1969). *Biotechnology And Bioengineering* 2000; **67**:704-713.
10. Dimarco A, Gaetani M, Orezzi P, Scarpinato BM, Silvestrini R, Soldati M, et al. 'Daunomycin', A new antibiotic of the rhodomycin group. *Nature* 1964; **201**:706-707.
11. Doroshow JH. Anthracyclines and anthracenediones. *Cancer Chemotherapy and Biotherapy: Principles and Practice. 2nd ed. Philadelphia, Pa: Lippincott-Raven* 1996:409-434.
12. (EBCTCG) EBCTCG. Effects of chemotherapy and hormonal therapy for early breast cancer on recurrence and 15-year survival: an overview of the randomised trials. *Lancet* 2005; **365**:1687-1717.
13. Gennari A, Sormani MP, Pronzato P, Puntoni M, Colozza M, Pfeffer U, et al. HER2 Status and Efficacy of Adjuvant Anthracyclines in Early Breast Cancer: A Pooled Analysis of Randomized Trials. *Journal of the National Cancer Institute* 2008; **100**:14-20.
14. Polin L, Valeriote F, White K, Panchapor C, Pugh S, Knight J, et al. Treatment of human prostate tumors PC-3 and TSU-PR1 with standard and investigational agents in SCID mice. *Investigational New Drugs* 1997; **15**:99-108.

15. Liu X, Chen Z, Chua CC, Ma Y-S, Youngberg GA, Hamdy R, et al. Melatonin as an effective protector against doxorubicin-induced cardiotoxicity. *American Journal Of Physiology. Heart And Circulatory Physiology* 2002; **283**:H254-H263.
16. Das A, Durrant D, Mitchell C, Mayton E, Hoke NN, Salloum FN, et al. Sildenafil increases chemotherapeutic efficacy of doxorubicin in prostate cancer and ameliorates cardiac dysfunction. *Proceedings of the National Academy of Sciences of the United States of America* 2010; **107**:18202-18207.
17. Petrioli R, Fiaschi AI, Francini E, Pascucci A, Francini G. The role of doxorubicin and epirubicin in the treatment of patients with metastatic hormone-refractory prostate cancer. *Cancer Treatment Reviews* 2008; **34**:710-718.
18. Ryberg M, Nielsen D, Skovsgaard T, Hansen J, Jensen BV, Dombernowsky P. Epirubicin cardiotoxicity: an analysis of 469 patients with metastatic breast cancer. *Journal Of Clinical Oncology: Official Journal Of The American Society Of Clinical Oncology* 1998; **16**:3502-3508.
19. Thomson PDR, PDR Staff, Micromedex, Cohen HE, 2004 *Red Book: Pharmacy's Fundamental Reference*. Vol. 23. 2004: Advanstar Medical Economics.
20. Kellner U, Maxwell S, Peter BJ, Frank G, Pierre R. Review: Culprit and victim - DNA topoisomerase II. *Lancet Oncology* 2002; **3**:235-243.
21. Zitvogel LL, Fo G. Immunological aspects of cancer chemotherapy. *Nature Reviews Immunology* 2008; **8**:59.
22. Nygren O, Lundgren C. Determination of platinum in workroom air and in blood and urine from nursing staff attending patients receiving cisplatin chemotherapy.

- International Archives Of Occupational And Environmental Health* 1997; **70**:209-214.
23. Salmon SE, Sartorelli AC. Cancer chemotherapy. *Basic and clinical pharmacology* 1998:881-911.
 24. Cassidy SC, Chan DP, Rowland DG, Allen HD. Effects of doxorubicin on diastolic function, contractile reserve, and ventricular–vascular coupling in piglets. *Pediatric Cardiology* 1998; **19**:450-457.
 25. Young DM. Pathologic effects of adriamycin (NSC-123127) in experimental systems. *Cancer Chemother. Rep* 1975; **6**:159-175.
 26. Olson RD, Boerth RC, Gerber JG, Nies AS. Mechanism of adriamycin cardiotoxicity: Evidence for oxidative stress. *Life Sciences* 1981; **29**:1393-1401.
 27. Olson HM, Young DM, Prieur DJ, LeRoy AF, Reagan RL. Electrolyte and morphologic alterations of myocardium in adriamycin-treated rabbits. *The American Journal Of Pathology* 1974; **77**:439-454.
 28. Steinberg JS, Cohen AJ, Wasserman AG, Cohen P, Ross AM. Acute arrhythmogenicity of doxorubicin administration. *Cancer* 1987; **60**:1213-1218.
 29. Ferrans VJ. Overview of cardiac pathology in relation to anthracycline cardiotoxicity. *Cancer treatment reports* 1978; **62**:955-961.
 30. Freter CE. Doxorubicin cardiac toxicity manifesting seven years after treatment. Case report and review. *The American journal of medicine* 1986; **80**:483.
 31. Steinherz LJ, Steinherz PG, Tan CT, Heller G, Murphy ML. Cardiac toxicity 4 to 20 years after completing anthracycline therapy. *JAMA: The Journal Of The American Medical Association* 1991; **266**:1672-1677.

32. Schwartz RG, McKenzie WB, Alexander J, Sager P, D'Souza A, Manatunga A, et al. Congestive heart failure and left ventricular dysfunction complicating doxorubicin therapy. Seven-year experience using serial radionuclide angiography. *The American journal of medicine* 1987; **82**:1109-1118.
33. Swain SM, Whaley FS, Ewer MS. Congestive heart failure in patients treated with doxorubicin. *Cancer* 2003; **97**:2869-2879.
34. Billingham ME, Mason JW, Bristow MR, Daniels JR. Anthracycline cardiomyopathy monitored by morphologic changes. *Cancer treatment reports* 1978; **62**:865-872.
35. Wang Y, Korth M. Effects of doxorubicin on excitation-contraction coupling in guinea pig ventricular myocardium. *Circulation Research* 1995; **76**:645-653.
36. Bristow MR, Kantrowitz NE, Harrison WD, Minobe WA, Sageman WS, Billingham ME. Mediation of subacute anthracycline cardiotoxicity in rabbits by cardiac histamine release. *Journal of Cardiovascular Pharmacology* 1983; **5**:913-919.
37. Fujita N, Hiroe M, Ohta Y, Horie T, Hosoda S. Chronic Effects of Metoprolol on Myocardial [beta]-Adrenergic Receptors in Doxorubicin-Induced Cardiac Damage in Rats. *Journal of Cardiovascular Pharmacology* 1991; **17**:656-661.
38. Revis NW, Marusic N. Glutathione peroxidase activity and selenium concentration in the hearts of doxorubicin-treated rabbits. *Journal of Molecular and Cellular Cardiology* 1978; **10**:945-948.
39. Ito H, Miller SC, Billingham ME, Akimoto H, Torti SV, Wade R, et al. Doxorubicin Selectivity Inhibits Muscle Gene Expression in Cardiac Muscle

- Cells in vivo and in vitro. *Proceedings of the National Academy of Sciences of the United States of Ame* 1990; **87**:4275-4279.
40. Keizer HG, Pinedo HM, Schuurhuis GJ, Joenje H. Doxorubicin (adriamycin): A critical review of free radical-dependent mechanisms of cytotoxicity. *Pharmacology & Therapeutics* 1990; **47**:219-231.
 41. Quiles JL, Huertas JsR, Battino M, Mataix J, Ramirez-Tortosa MC. Antioxidant nutrients and adriamycin toxicity. *Toxicology* 2002; **180**:79-95.
 42. Arnold RD, Slack JE, Straubinger RM. Quantification of Doxorubicin and metabolites in rat plasma and small volume tissue samples by liquid chromatography/electrospray tandem mass spectroscopy. *Journal of Chromatography B* 2004; **808**:141-152.
 43. Handa K, Sato S. Generation of free radicals of quinone group-containing anti-cancer chemicals in NADPH-microsome system as evidenced by initiation of sulfite oxidation. *Gann* 1975; **66**:43-47.
 44. Sarvazyan NA, Askari A, Huang WH. Effects of doxorubicin on cardiomyocytes with reduced level of superoxide dismutase. *Life Sciences* 1995; **57**:1003-1010.
 45. Chance B, Sies H, Boveris A. Hydroperoxide metabolism in mammalian organs. *Physiological Reviews* 1979; **59**:527-605.
 46. Wallace KB. Doxorubicin-induced cardiac mitochondrionopathy. *Pharmacology & Toxicology* 2003; **93**:105-115.
 47. De Silva V, Woznichak MM, Burns KL, Grant KB, May SW. Selenium Redox Cycling in the Protective Effects of Organoselenides against Oxidant-Induced DNA Damage. *Journal of the American Chemical Society* 2004; **126**:2409-2413.

48. Zhou S, Palmeira CM, Wallace KB. Doxorubicin-induced persistent oxidative stress to cardiac myocytes. *Toxicology Letters* 2001; **121**:151-157.
49. Li T, Singal PK. Adriamycin-induced early changes in myocardial antioxidant enzymes and their modulation by probucol. *Circulation* 2000; **102**:2105-2110.
50. Yen HC. The protective role of manganese superoxide dismutase against adriamycin-induced acute cardiac toxicity in transgenic mice. *The Journal of Clinical Investigation* 1996; **98**:1253.
51. Doroshow JH, Davies KJ. Redox cycling of anthracyclines by cardiac mitochondria. II. Formation of superoxide anion, hydrogen peroxide, and hydroxyl radical. *Journal of Biological Chemistry* 1986; **261**:3068-3074.
52. Doroshow JH. Effect of Anthracycline Antibiotics on Oxygen Radical Formation in Rat Heart. *Cancer Research* 1983; **43**:460-472.
53. Rajagopalan S, Politi PM, Sinha BK, Myers CE. Adriamycin-induced Free Radical Formation in the Perfused Rat Heart: Implications for Cardiotoxicity. *Cancer Research* 1988; **48**:4766-4769.
54. Weinstein DM, Mihm MJ, Bauer JA. Cardiac Peroxynitrite Formation and Left Ventricular Dysfunction following Doxorubicin Treatment in Mice. *Journal of Pharmacology and Experimental Therapeutics* 2000; **294**:396-401.
55. Henle ES, Linn S. Formation, Prevention, and Repair of DNA Damage by Iron/Hydrogen Peroxide. *Journal of Biological Chemistry* 1997; **272**:19095-19098.

56. Perez NG, Hashimoto K, McCune S, Altschuld RA, Marban E. Origin of contractile dysfunction in heart failure: calcium cycling versus myofilaments. *Circulation* 1999; **99**:1077-1083.
57. Cai L, Klein JB, Kang YJ. Metallothionein inhibits peroxynitrite-induced DNA and lipoprotein damage. *Journal of Biological Chemistry* 2000; **275**:38957-38960.
58. Papadopoulou LC, Theophilidis G, Thomopoulos GN, Tsiftoglou AS. Structural and functional impairment of mitochondria in adriamycin-induced cardiomyopathy in mice: suppression of cytochrome c oxidase II gene expression. *Biochemical Pharmacology* 1999; **57**:481-489.
59. Santos DL, Moreno AJM, Leino RL, Froberg MK, Wallace KB. Carvedilol Protects against Doxorubicin-Induced Mitochondrial Cardiomyopathy. *Toxicology and Applied Pharmacology* 2002; **185**:218-227.
60. Yagmurca M, Fadillioglu E, Erdogan H, Ucar M, Sogut Sirmak MK. Erdosteine prevents doxorubicin-induced cardiotoxicity in rats. *Pharmacological Research* 2003; **48**:377-382.
61. Feleszko W, Mlynarczuk I, Balkowiec-Iskra EZ, Czajka A, Switaj T, Stoklosa T, et al. Lovastatin potentiates antitumor activity and attenuates cardiotoxicity of doxorubicin in three tumor models in mice. *Clinical Cancer Research: An Official Journal Of The American Association For Cancer Research* 2000; **6**:2044-2052.
62. Shimpo K, Nagatsu T, Yamada K, Sato T, Niimi H, Shamoto M, et al. Ascorbic acid and adriamycin toxicity. *The American Journal of Clinical Nutrition* 1991; **54**:1298S-1301S.

63. Wahab MH, Akoul ES, Abdel Aziz AA. Modulatory effects of melatonin and vitamin E on doxorubicin-induced cardiotoxicity in Ehrlich ascites carcinoma-bearing mice. *Tumori* 2000; **86**:157-162.
64. Kurbacher C, Wagner U, Kolster B, Andreotti P, Krebs D, Bruckner H. Ascorbic acid (vitamin C) improves the antineoplastic activity of doxorubicin, cisplatin, and paclitaxel in human breast carcinoma cells in vitro. *Cancer Letters* 1996; **103**:183-189.
65. Alberts DS, Peng YM, Moon TE. alpha-Tocopherol pretreatment increases adriamycin bone marrow toxicity. *Biomedicine Express* 1978; **29**:189-191.
66. Husken B, de Jong J, Beekman B, Onderwater RC, van der Vijgh WJ, Bast A. Modulation of the in vitro cardiotoxicity of doxorubicin by flavonoids. *Cancer Chemotherapy And Pharmacology* 1995; **37**:55-62.
67. Breed JGS, Zimmerman ANE, Dormans JAMA, Pinedo HM. Failure of the antioxidant vitamin E to protect against adriamycin-induced cardiotoxicity in the rabbit. *Cancer Research* 1980; **40**:2033-2038.
68. Herman EH, Ferrans VJ, Myers CE, Van Vleet JF. Comparison of the effectiveness of (+/-)-1,2-bis(3,5-dioxopiperaziny-1-yl)propane (ICRF-187) and N-acetylcysteine in preventing chronic doxorubicin cardiotoxicity in beagles. *Cancer Research* 1985; **45**:276-281.
69. Myers C, Bonow R, Palmeri S, Jenkins J, Corden B, Locker G, et al. A randomized controlled trial assessing the prevention of doxorubicin cardiomyopathy by N-acetylcysteine. *Seminars In Oncology* 1983; **10**:53-55.

70. Pearlman M, Jendiroba D, Pagliaro L, Keyhani A, Liu BJ, Freireich E. Dexrazoxane in combination with anthracyclines lead to a synergistic cytotoxic response in acute myelogenous leukemia cell lines. *Leukemia Research* 2003; **27**:617-626.
71. Tebbi CK, London WB, Friedman D, Villaluna D, De Alarcon PA, Constine LS, et al. Dexrazoxane-associated risk for acute myeloid leukemia/myelodysplastic syndrome and other secondary malignancies in pediatric Hodgkin's disease. *Journal of Clinical Oncology* 2007; **25**:493-500.
72. Spencer CM, Goa KL. Amifostine. A review of its pharmacodynamic and pharmacokinetic properties, and therapeutic potential as a radioprotector and cytotoxic chemoprotector. *Drugs* 1995; **50**:1001-1031.
73. Treskes M, Van der Vijgh WJ. WR2721 as a modulator of cisplatin- and carboplatin-induced side effects in comparison with other chemoprotective agents: a molecular approach. *Cancer Chemotherapy And Pharmacology* 1993; **33**:93-106.
74. Herman EH, Zhang J, Chadwick DP, Ferrans VJ. Comparison of the protective effects of amifostine and dexrazoxane against the toxicity of doxorubicin in spontaneously hypertensive rats. *Cancer Chemotherapy And Pharmacology* 2000; **45**:329-334.
75. Hirschel-Scholz S, Caverzasio J, Bonjour JP. Inhibition of parathyroid hormone secretion and parathyroid hormone-independent diminution of tubular calcium reabsorption by WR-2721, a unique hypocalcemic agent. *The Journal of Clinical Investigation* 1985; **76**:1851-1856.

76. Glover D, Riley L, Carmichael K, Spar B, Glick J, Kligerman MM, et al. Hypocalcemia and inhibition of parathyroid hormone secretion after administration of WR-2721 (a radioprotective and chemoprotective agent). *The New England Journal Of Medicine* 1983; **309**:1137-1141.
77. May SW, Pollock SH. Selenium-Based Antihypertensives: Rationale and Potential. *Drugs* 1998; **56**:959-964.
78. May SW, Herman HH, Roberts SF, Ciccarello MC. Ascorbate depletion as a consequence of product recycling during dopamine .beta.-monooxygenase catalyzed selenoxidation. *Biochemistry* 1987; **26**:1626-1633.
79. Ursini F, Bindoli A. The role of selenium peroxidases in the protection against oxidative damage of membranes. *Chemistry And Physics Of Lipids* 1987; **44**:255-276.
80. Stadtman TC. Selenocysteine. *Annu Rev Biochem* 1996; **65**:83-100.
81. Clark L, Combs GJ, Turnbull B, Slate E, Chalker D, Chow J, et al. Effects of selenium supplementation for cancer prevention in patients with carcinoma of the skin. A randomized controlled trial. Nutritional Prevention of Cancer Study Group. *JAMA* 1996; **276**:1957-1963.
82. Li HJ, Stampfer MJ, Giovannucci EL, Morris JS, Willett WC, Gaziano JM, et al. A prospective study of plasma selenium levels and prostate cancer risk. *Journal of the National Cancer Institute* 2004; **96**:696-703.
83. Clark LC, Dalkin B, Krongrad A, Combs GF, Jr., Turnbull BW, Slate EH, et al. Decreased incidence of prostate cancer with selenium supplementation: results of

- a double-blind cancer prevention trial. *British Journal of Urology* 1998; **81**:730-734.
84. Subramaniam S, Shyama S, Jagadeesan M, Shyamala Devi CS. Oxidant and antioxidant levels in the erythrocytes of breast cancer patients treated with CMF. *Medical Science Research* 1993; **21**:79.
85. Jiang C, Jiang W, Ip C, Ganther H, Lu J. Selenium-induced inhibition of angiogenesis in mammary cancer at chemopreventive levels of intake. *Molecular Carcinogenesis* 1999; **26**:213-225.
86. Sundstrom H, Korpela H, Viinikka L, Kauppila A. Serum selenium and glutathione peroxidase, and plasma lipid peroxides in uterine, ovarian or vulvar cancer, and their responses to antioxidants in patients with ovarian cancer. *Cancer Letters* 1984; **24**:1-10.
87. Prasad KN, Cole WC, Kochupillai V, Kumar A. High doses of multiple antioxidant vitamins: essential ingredients in improving the efficacy of standard cancer therapy. *Journal of the American College of Nutrition* 1999; **18**:13-25.
88. Ames BN, Shigenaga MK, Hagen TM. Oxidants, Antioxidants, and the Degenerative Diseases of Aging. *Proceedings of the National Academy of Sciences of the United States of America* 1993; **90**:7915-7922.
89. Knight JA. Review: Free radicals, antioxidants, and the immune system. *Annals Of Clinical And Laboratory Science* 2000; **30**:145-158.
90. Arnold RD, Mager DE, Slack JE, Straubinger RM. Effect of repetitive administration of Doxorubicin-containing liposomes on plasma pharmacokinetics

- and drug biodistribution in a rat brain tumor model. *Clinical Cancer Research* 2005; **11**:8856-8865.
91. Siegal T, Horowitz A, Gabizon A. Doxorubicin encapsulated in sterically stabilized liposomes for the treatment of a brain tumor model: biodistribution and therapeutic efficacy. *Journal of Neurosurgery* 1995; **83**:1029-1037.
 92. Gabizon A, Shiota R, Papahadjopoulos D. Pharmacokinetics and tissue distribution of doxorubicin encapsulated in stable liposomes with long circulation times. *Journal of the National Cancer Institute* 1989; **81**:1484-1488.
 93. Sharma US, Sharma A, Chau RI, Straubinger RM. Liposome-mediated therapy of intracranial brain tumors in a rat model. *Pharmaceutical Research* 1997; **14**:992-998.
 94. Straubinger RM, Arnold RD, Zhou R, Mazurchuk R, Slack JE. *Antivascular and Antitumor Activities of Liposome-associated Drugs*. 2004: IAR.
 95. Fielding RM. Liposomal drug delivery. Advantages and limitations from a clinical pharmacokinetic and therapeutic perspective. *Clinical Pharmacokinetics* 1991; **21**:155-164.
 96. Drummond DC, Meyer O, Hong K, Kirpotin DB, Papahadjopoulos D. Optimizing liposomes for delivery of chemotherapeutic agents to solid tumors. *Pharmacological Reviews* 1999; **51**:691-743.
 97. Papahadjopoulos D, Nir S, Oki S. Permeability properties of phospholipid membranes: effect of cholesterol and temperature. *Biochimica Et Biophysica Acta* 1972; **266**:561-583.

98. Immordino ML, Dosio F, Cattell L. Stealth liposomes: review of the basic science, rationale, and clinical applications, existing and potential. *International Journal of Nanomedicine* 2006; **1**:297-315.
99. Gert S, Daan JAC. Liposomes: quo vadis? *Pharmaceutical Science & Technology Today* 1998; **1**:19-31.
100. Maeda H. The enhanced permeability and retention (EPR) effect in tumor vasculature: the key role of tumor-selective macromolecular drug targeting. *Advanced Enzyme Regulation* 2001; **41**:189-207.
101. Bergers G, Benjamin LE. Tumorigenesis and the angiogenic switch. *Nature Review Cancer* 2003; **3**:401-410.
102. Brown DM, *Drug delivery systems in cancer therapy / edited by Dennis M. Brown*. Cancer drug discovery and development. 2004: Totowa, N.J. : Humana Press, c2004.
103. Brannon-Peppas L, Blanchette JO. Nanoparticle and targeted systems for cancer therapy. *Advanced Drug Delivery Reviews* 2004; **56**:1649-1659.
104. Maeda H, Sawa T, Konno T. Mechanism of tumor-targeted delivery of macromolecular drugs, including the EPR effect in solid tumor and clinical overview of the prototype polymeric drug SMANCS. *Journal of Controlled Release* 2001; **74**:47-61.

Abbreviations

BT-474	human breast carcinoma cell
CAT	catalase
DNR	daunorubicin
DOX	doxorubicin
EDTA	ethylenediaminetetraacetic acid
EPI	epirubicin
EPR	enhanced permeability and retention
ESI	electrospray ionization
FDA	food and drug administration
GSHPx	glutathione peroxidase
HPLC-MS/MS	high-performance liquid chromatography – tandem mass spectrometry
MRM	multiple reaction monitoring
PAESe	phenyl-2-aminoethyl selenide
PAESeO	phenyl-2-aminoethyl selenoxide
PEG	polyethylene glycol
PC-3	human prostate carcinoma
PK	pharmacokinetic
RES	reticular endothelial system
ROS	reactive oxygen species

SOD	superoxide dismutase
SSL	sterically stabilized liposomes
SSL-PAESe	sterically stabilized PAESe liposomes
TBHP	<i>tert</i> -butylhydroperoxide

CHAPTER 2

**THE CARDIOPROTECTIVE AND ANTITUMOR EFFECTS OF THE
ANTIOXIDANT PHENYLAMINOETHYL SELENIDE: IN VITRO HUMAN
PROSTATE AND BREAST CANCER CELLS AND IN VIVO XENOGRAFT
MODEL OF HUMAN PROSTATE CANCER**

Jeong Yeon Kang, Leah J. Costyn, Tamas Nagy, Elizabeth A. Cowan, Charlie D. Oldham, Sheldon W. May, Robert D. Arnold. 2011. *Archives of Biochemistry and Biophysics*, 515:112-119.

Reprinted here with permission of the publisher

Abstract

Anthracyclines are potent anticancer agents, but their clinical use is limited by dose-limiting cardiotoxicity mediated by free radical generation. The objectives of this study were to evaluate the activity of phenylaminoethyl selenides (PAESe), novel antioxidants, to reduce doxorubicin (DOX)-induced cardiotoxicity. The effect of PAESe on the growth of human prostate carcinoma (PC-3) and breast carcinoma (BT-474) cells *in vitro* alone and in combination with clinically used anticancer agents DOX, vincristine and a known oxidant, *tert*-butylhydroperoxide (TBHP) was determined by 3-(4,5-Dimethylthiazol-2-yl)-2,5-diphenyltetrazolium-bromide (MTT) and sulforhodamine B (SRB) staining. Results showed that up to 1 μ M and 10 μ M PAESe did not alter the growth of PC-3 and BT-474 cells, respectively. Concomitant use of PAESe decreased the oxidative mediated cytotoxicity of TBHP in a dose-dependent manner, whereas PAESe had limited to no effect on vincristine or DOX activity. Also, intracellular reactive oxygen species (ROS) were determined by quantifying the oxidation of cell-permeant indicator. Further PAESe reduced the formation of intracellular ROS from TBHP and DOX in a dose-dependent manner. In addition, the effect of PAESe on antitumor activity of DOX was determined in a xenograft tumor model of human prostate cancer implanted in nude mice. PAESe did not significantly alter the antitumor activity of DOX. Interestingly, PAESe alone appeared to decrease tumor volume relative to saline treated controls. There were no significant differences in tumor volume of PAESe alone or in combination relative to DOX alone. DOX treatment significantly decreased mice body weight, whereas

concomitant administration of PAESe with DOX was similar to control. Histological changes of myocardium were also examined to evaluate the effect of PAESe on the cardiotoxicity mediated by DOX. Results showed that PAESe decreased the neutrophil and macrophage infiltration observed following DOX treatment. This suggests that PAESe can be used in combination with DOX to preserve its antitumor activity, but decreases its non-target toxicity.

1. Introduction

Cancer is the second leading cause of death in the United States in 2012. Among several cancers, prostate and breast cancers are most commonly diagnosed types of cancer among men and women in 2012 [1]. Anthracyclines such as doxorubicin (DOX) and daunorubicin are widely used anticancer agents that are highly effective in the treatment of several solid tumors, acute leukemia, and non-Hodgkin's lymphomas [2-4]. However, their clinical use is limited by severe dose-limiting cardiotoxicity such as cardiomyopathy and congestive heart failure [2]. DOX treatment has been known to dysregulate blood pressure and flow rate as well as decrease contractility of heart [5, 6]. In addition, DOX toxicity has been shown to cause myofibrillar loss, sarcoplasmic reticulum disruption, mitochondria swelling and lesions [6, 7]. These characteristics eventually lead to myocardial dysfunction and can progress to heart failure.

The risk of developing anthracycline-mediated cardiomyopathy rises rapidly above a cumulative dose of 550 mg/m^2 body surface area [2]. However, cardiotoxicity has been observed after a single dose of DOX at 240 mg/m^2 [8]. A retrospective analysis of three phase III clinical trials showed that congestive heart failure occurred with total

cumulative DOX doses of 300 mg/m² or less [9]. Also, myocardial dysfunction has been recognized years after treatment [10]. To reduce the potential for cardiotoxicity and resultant heart failure, current recommendations suggest that the total cumulative dose of anthracycline is not exceeded 550 mg/m².

Although there are several hypotheses to explain DOX toxicity [11-16], the cardiotoxicity is believed to result primarily from reactive free radicals produced during the intracellular metabolism of DOX [17-19]. Reactive free radicals such as superoxide anion (O₂^{•-}), hydroxyl radical (OH[•]), and peroxynitrite (ONOO⁻) are capable of non-specific oxidation of macromolecules including cellular components and membranes, ultimately leading to cellular damage and death [20].

The metabolism of quinone-containing compounds like DOX could lead to free radical generation in a microsomal NADPH-oxidase system [21]. Due to the presence of quinone moiety in the tetracyclic aglycone molecule, DOX can form many free radicals by cycling from a quinone to semiquinone then back to quinone, leading the production of O₂^{•-} from oxygen molecule [2]. Also, DOX has been reported to increase the peroxidation of polyunsaturated fatty acids within membranes as well as free oxygen radical activity through generation of O₂^{•-} [16, 17].

Antioxidants have been shown to be effective against the cardiac toxicity of DOX [22]. Many of the studies have been carried out to apply antioxidant to protect the heart from DOX-induced oxidative damage [22-25]. The concomitant administration of antioxidants, *e.g.*, vitamin C, α -tocopherol (vitamin E), has been studied using *in vivo* model systems and assessed clinically [26-29].

Phenylaminoethyl selenide (PAESe) is a novel antioxidant that was developed to treat cardiovascular disease [30-33]. PAESe has been shown to exhibit potent antioxidant activity, reacting rapidly with many metabolic oxidants such as peroxide, ONOO⁻, and hydroperoxides. The selenoxide product generated from this antioxidant activity PAESe is then readily recycled back to the selenide form by cellular reductants such as ascorbate and glutathione, with no complex side reactions [30, 34-39]. Metabolic oxidants are known to react readily with DNA, resulting in base modification and induction of double- and single-strand breaks [34, 40]. It has been demonstrated that GSH-mediated redox cycling of PAESe results in protection of DNA against oxidant-induced damage [34].

The present study was performed to determine the cardioprotective effect of PAESe on anthracycline-induced cardiotoxicity through antioxidant effects while preserving the anticancer activity of DOX in *in vitro* and *in vivo* models of human cancer.

2. Materials and Methods

2.1. Chemicals and Reagents

Vincristine was obtained from Calbiochem (La Jolla, CA). RPMI 1640 media and F-12K Nutrient Mixture (Kaighn's Mod.) were purchased from Mediatech (Manassas, VA). CM-H₂DCFDA (5-(and-6)-chloromethyl-2',7'-dichlorodihydrofluorescein diacetate acetyl ester) was purchased from Invitrogen (Carlsbad, CA). Doxorubicin hydrochloride, *tert*-butylhydroperoxide (TBHP) and 3-(4,5-Dimethylthiazol-2-yl)-2,5-diphenyltetrazolium bromide (MTT) were obtained from Sigma-Aldrich Inc (St. Louis, MO). Acetic acid, dimethyl sulfoxide (DMSO), sulforhodamine B (SRB), trichloroacetic

acid (TCA), tris(hydroxymethyl)aminomethane (TRIS), Fetal bovine serum (FBS) and trypsin (0.25% w/v) were purchased from Thermo Fisher Scientific Inc. (Rockford, IL).

2.2. Cell lines

Androgen-independent human prostate epithelial cells (PC-3) were obtained from American Type Culture Collection (ATCC) (Rockville, MD) and were cultured in F-12K media supplemented with 10% (v/v) FBS in a humidified cell culture chamber (NuAire Inc. Plymouth, MN) at 37°C, 5% CO₂. Cells were passaged when they reached approximately 80-90% confluency.

Human breast cancer cell line (BT-474) was obtained from American Type Culture Collection (ATCC) (Rockville, MD) and maintained in RPMI 1640 media supplemented with 10% (v/v) FBS and penicillin (100 U/mL)/streptomycin (100 µg/ml) in a humidified cell culture chamber (NuAire Inc. Plymouth, MN) at 37°C, 5% CO₂. Cells were passaged when they reached approximately 70-80% confluency.

2.3. Growth inhibition effect of PAESE alone and in combination with known cytotoxic agents

2.3.1. Cytotoxicity of PAESE

The cytotoxicity of PAESE on PC-3 and BT-474 growth inhibition was determined at 24, 48 and 72 hr. PC-3 cells were seeded at 2×10^3 cells/well in 96 well plates with F-12K media supplemented with 10% (v/v) FBS and penicillin (100 U/mL)/streptomycin (100 µg/ml). BT-474 cells (5×10^3 cells/well) were plated in 96 wells

with RPMI 1640 media supplemented with 10% (v/v) FBS and penicillin (100 U/mL)/streptomycin (100 µg/ml). Plates were incubated for 24 hr prior to media change and replacement with serum supplemented media containing PAESe (0.04 to 10,000 nM). Plates were then incubated at 37°C, 5% CO₂ for an additional 24, 48 or 72 hr. Three studies (n=3) were performed with 5 replicates at each concentration of PAESe. The growth inhibition effect was assessed at each time point by mitochondrial enzymatic assay (MTT) and a protein binding assay (SRB), described below.

2.3.2. Growth inhibition effect of PAESe in combination with DOX/Vincristine/TBHP

The effect of PAESe on the cytotoxic effects of conventional anticancer agents, such as DOX (topoisomerase II antagonist and known to cause free radical mediated cardiotoxicity) and vincristine (tubulin binding drug), and a known oxidant TBHP were determined. Cells were seeded as described above in cytotoxicity of PAESe. After 24 hr seeding, the media was withdrawn and replaced with serial dilutions of PAESe (100 to 10,000 nM) and DOX (100, 500 nM) or vincristine (5 to 25 nM) or TBHP (3 to 3,000 µM) for PC-3 cells to a final volume of 200 µL. For BT-474 cells, the media was replaced with serial concentrations of PAESe (100 to 1,000 nM) in combination with DOX (100 to 1,000 nM) or vincristine (1 to 50 nM) or TBHP (0.3 to 300 µM) to a final volume of 200 µL. Three studies (n=3) were performed with 5 replicates for each concentration of PAESe. MTT and SRB assays were performed after 72 hr incubation time to determine cytotoxic effects.

2.3.3. Assessment of cell growth and viability

The cytotoxic effects of PAESE and/or DOX, vincristine, TBHP were tested using conventional MTT and SRB staining. MTT and SRB staining were performed as described previously [41, 42]. Briefly, 10 μ L of MTT reagent were added to each well and plates were placed at 37°C, 5% CO₂ for 2 hr. The resultant insoluble formazans were dissolved in 200 μ L DMSO and absorbance was measured at 550 nm using Synergy H/T multi-mode microplate reader (BioTek Instruments, Inc., Winooski, VT). SRB staining was performed by fixing viable cells with 10% (w/v) TCA for 1 hr at 4°C. Fixed cells were stained with SRB dye for 5 min, and excess SRB was removed by washing plates with 1% (v/v) acetic acid. The absorbance of cellular protein-bound dye extracted by 10 mM TRIS buffer (pH 7.5) was determined at 490 nm using a Synergy H/T multi-mode microplate reader. Mean \pm standard error of the mean (SEM) were calculated and described as percent (%) of control.

2.4. ROS generation

Intracellular ROS formation was determined by quantifying the oxidation of a non-fluorescent marker to its fluorescent product (DCF, 2',7'-dichlorofluorescein). Cell-permeant indicator CM-H₂DCFDA is known to detect several ROS such as H₂O₂, OH[•], ONOO⁻ and ROO[•]. Briefly, cells (2×10^5) were plated in 96 wells and incubated for 24 hr in 37°C at 5% CO₂ condition. CM-H₂DCFDA was dissolved in DMSO to make a concentrated stock solution and added to each well to a final working concentration of 5 μ M. After incubating cells at 37°C for 30 min, the loading media was replaced with prewarmed serum free media, and incubated at 37°C for 10 min to allow the

deacetylation and oxidation of the dye. Cells were treated with different concentration of PAESe (0 to 1000 nM) and DOX (0 to 500 nM) or TBHP (0 to 300 μ M), and were incubated at 37°C in darkness. Cells in the absence of drugs were used as controls. After 2 hr, media was aspirated and 0.5% Triton X-100 (pH 7.4) in 0.01 M Tris-HCl (200 μ L) was added to each wells for 5 min to detach the cells. Fluorescence intensity of the cell lysates (100 μ L) was measured with a FLUOstar OPTIMA plate reader (BMG Labtech, Offenburg, Germany) at an excitation wavelength of 485 nm and an emission wavelength of 520 nm.

2.5. Tumor growth inhibition effect of PAESe

2.5.1. Animal model

Nude (NCr) mice (body weight, approx. 25 g) at 6-8 weeks of age were obtained from Taconic Farms, Inc., (Germantown, NY). Mice were maintained according to an approved Institutional Animal Care and Use Committee (IACUC) protocol at the University of Georgia and the U.S. Public Health Service (PHS) Policy on Humane Care and Use of Laboratory Animals, updated 1996. Mice were kept in pathogen-free cages in a light and temperature-controlled isolated room and provided with standard rodent chow and sterile water *ad libitum* during the experimental periods. PC-3 cell suspension in serum free media (1×10^7 cells/mL) was mixed with ice-cold Matrigel (BD Biosciences, Franklin Lakes, NJ) in 1:1 (v/v), and 100 μ L of the mixture was injected subcutaneously into the flank to establish tumor xenograft. Tumor growth and body weight were monitored every other day. When tumor volume reached approximately 200 mm³, DOX

and PAESe treatments were initiated. Tumor volume was assessed using digital calipers as described previously where the volume was the product of largest dimension and (smallest dimension)² [43]. Mice were observed every other day until 1 week after the last injection for their general appearance as well as the treatment-mediated toxicities such as weight change, blood stool, and reduced activity.

2.5.2. Effect of PAESe on antitumor activity of DOX

Mice were divided into four groups, control, DOX (DOX treated), PAESe (PAESe treated), and DOX+PAESe (DOX + PAESe treated), n = 5-8 animals/group. A 100 to 150 μ L of DOX and PAESe were administered weekly by tail vein injections (each containing 5 mg/kg DOX, and 10 mg/kg PAESe) in five injections to animals for a total cumulative dose of 25 mg/kg body weight for DOX, and 50 mg/kg body weight for PAESe. Control animals were injected with the vehicle alone (saline-control) following the same dosing schedule. Two weeks after the last injection, mice were sacrificed by cervical dislocation under isoflurane anesthesia. The heart and tumor were excised rapidly, and stored in formalin solution at 4°C until paraffin embedding. The heart tissues were used for histological evidence of cardiotoxicity. Tumor volume and body weight (Mean \pm SEM) for each group was plotted by time versus normalized tumor volume and body weight to day 0 treatment.

2.6. Histological examination

For histological evaluation, mice hearts were fixed in formalin solution (10%, v/v) for 24 hr, bisected longitudinally and embedded in paraffin. Serial sections were

collected and stained with hematoxylin and eosin (H&E). Stained hearts were examined under a Nikon AZ100 stereo-fluorescent microscope mounted with a Nikon *DS-Qi1Mc color* camera. NIS-Elements image analysis software was used for processing. Micrographs were analyzed and captured by pathologist who was blinded.

2.7. Statistical analysis

Data from *in vitro* and *in vivo* studies were analyzed using one-way ANOVA followed by a post-hoc analysis (Bonferroni corrected t-test). A p -value ≤ 0.05 was regarded as statistically significant.

3. Results

3.1. Growth inhibition effect of PAESe and in combination with known cytotoxic agents

3.1.1. Cytotoxicity of PAESe

The cytotoxic effects of PAESe on prostate (PC-3) and breast (BT-474) cancer cells were assessed by measurement of MTT and SRB absorbance after 24, 48 and 72 hr. PAESe did not significantly inhibit *in vitro* growth of PC-3 cells at 0.1 to 1,000 nM (Fig 2-1) and BT-474 cells at 0.04 to 10,000 nM (Fig 2-2), although some growth inhibition was observed at drug concentrations above 10 μ M at 72 hr (Fig 2-1A).

3.1.2. Growth inhibition effect of PAESe in combination with DOX/Vincristine/TBHP

The growth inhibition activity of PAESe in combination with DOX, vincristine and TBHP was determined in PC-3 and BT-474 cells. TBHP or vincristine was co-treated with PAESe instead of DOX to compare the effect of PAESe on the cytotoxicity of DOX by their discerned mechanism of actions. After 24 hr seeding, PAESe and DOX or vincristine or TBHP were added into the each well, and then MTT and SRB assay were performed after 72 hr exposure.

The cytotoxic activity of vincristine on PC-3 (Fig 2-3) and BT-474 (Fig 2-4) cells was not altered by the presence of PAESe, as expected. TBHP, which is well-known potent oxidizing agent, was used to determine the antioxidant activity of PAESe. TBHP exerted oxidative-mediated cytotoxicity on PC-3 (Fig 2-5) and BT-474 (Fig 2-6) cells when used alone. However, PAESe decreased significantly ($p < 0.05$) this cytotoxic effect of TBHP on both cells in dose-dependent manner, as expected (Fig 2-5, 2-6). Interestingly, PAESe had limited effect on DOX to decrease MTT and SRB staining of PC-3 (Fig 2-7) and BT-474 (Fig 2-8) cells when used in combination.

3.2. ROS generation

We next detected the effect of PAESe on DOX-mediated generation of intracellular oxidants using cell-permeant indicator, CM-H₂DCFDA to quantify production of free radicals. Preliminary studies suggested that ROS generation was maximal at 1 to 2 hr, but not detectable at 24 hr when cells were exposed to TBHP and/or PAESe, relative to control. In PC-3 cells, an increase in ROS was observed with increasing concentration of both DOX and TBHP, as expected (Table 2-1). However, free

radical generation after exposure to TBHP and DOX were decreased significantly ($p < 0.05$) in the presence of PAESe in a dose-dependent manner. PAESe reduced free radicals generated from TBHP and DOX in a dose-dependent manner up to 300 μM and 500 nM, respectively. As seen in Table 2-2, the production of free radicals on BT-474 cells was increased with increasing concentrations of DOX and TBHP. However, PAESe decreased significantly ($p < 0.05$) free radicals generated by DOX and TBHP in a concentration-dependent manner.

3.3. Effect of PAESe on antitumor activity of DOX

The effect of PAESe on antitumor activity of DOX was determined in an *in vivo* xenograft tumor model of human prostate cancer in NCr (*nu/nu*) nude mice. After 32 days treatment, the DOX group (5 mg/kg/week) had smaller tumor volumes ($223\% \pm 55$) compared to controls ($473\% \pm 188$) (Figure 2-9A). As seen in DOX+PAESe group, PAESe did not alter significantly the antitumor activity of DOX ($256\% \pm 65$), which corresponded with *in vitro* results (section 3.1). Interestingly, PAESe alone decreased tumor volume ($196\% \pm 77$) relative to saline treated controls. Significant ($p < 0.05$) differences in tumor volumes, compared to control animals, were first observed 24 days after initiating. However, there were no significant differences in the tumor volume of animals treated with PAESe alone or in combination relative to free DOX. Mice body weight was decreased significantly ($p < 0.05$) in DOX group ($-8.62\% \pm 4.06$) (Figure 2-9B). However, no significant differences in animal weights were observed between DOX+PAESe ($0.22\% \pm 3.13$) and control ($7.12\% \pm 1.25$) groups.

3.4. Histological examination

Histopathological examination showed treatment-mediated differences between control and treatment groups. Micrograph of the myocardium of the left ventricular wall of control (Figure 2-10A) and PAESE group (Figure 2-10B) mice showed a histologically normal appearance. The myocardium was intact and faint outlines of cross striation. On the other hand, cardiotoxicity was observed in the DOX group (Figure 2-10C), *i.e.*, four minute inflammatory foci in 8 longitudinal sections. There was also a disruption and fragmentation of the myofibers accompanied by a small focus of inflammatory infiltrate composed of small numbers of neutrophils (Neu) and macrophages (Mac). In DOX+PAESE group (Figure 2-10D), one minute inflammatory foci in 8 longitudinal sections was observed, indicating that there was a reduction of myocardial damage compared to the DOX treatment group. There was also disruption and fragmentation of the myofibers accompanied by a small focus of inflammatory infiltrate composed of macrophages (Mac).

4. Discussion

DOX is one of the most effective anthracyclines to treat a variety of cancers including leukemia, lymphomas, as well as a number of solid tumors. However, DOX treatment is limited by cumulative dose-dependent myocardial damage that can be fatal. There are several proposed mechanisms for anthracycline-mediated cardiotoxicity including free radical formation, oxidative damage to membrane lipids and cellular components, inhibition of DNA synthesis, release of vasoactive substances such as histamine and catecholamine, increased intracellular Ca^{2+} concentration, changes in

cardiac β -adrenergic receptors, and lower glutathione peroxidase activities in the heart [11, 14, 17, 44-46]. Among them, the primary cause of myocardial damage has been correlated to the formation of free oxygen radicals [23, 47].

The heart is a particularly vulnerable organ to free radical damage induced by DOX due to several reasons; 1) there are limited antioxidants in the heart, 2) cardiolipin, which is a phospholipid in the cardiomyocyte, has a high affinity to the DOX, and 3) oxidative metabolism is highly activated so that the reaction with free radical is enhanced [23]. Cardiac mitochondria are known as the primary target of free radical damage [48, 49]. Altered mitochondrial function can affect energetic production, leading to contractile failure of the heart [50, 51].

Free radicals are also known to damage cells by breaking DNA strands as well as changing the oxidative state of nucleic acids, proteins, and lipids [52]. These oxygen-derived toxic species can be detoxified by antioxidant enzymes such as superoxide dismutase, catalase, and selenium-dependent glutathione peroxidase under normal physiological conditions. However, DOX metabolism could interrupt this balance with high free radical formation and oxidative stress so that lipid peroxidation is induced and cellular homeostasis is changed [34, 53-55]. Evidence suggests that DOX treatment reduces selenium-dependent glutathione peroxidase in myocardial cells [50], resulting in an increase in the formation of free radicals and a decrease in the ability to detoxify them. The quinone group on the tetracycline ring of DOX is responsible for the oxidation–reduction processes. An electron is transferred from the quinone moiety yielding a semiquinone form catalyzed by either NADPH-cytochrome c-reductase or *b*₅-reductase.

The semiquinone moiety can be recycled back to the quinone form by oxidization with molecular oxygen to $O_2^{\cdot-}$ [56-59].

Among several reactive free radicals derived from DOX, $O_2^{\cdot-}$ is believed primarily responsible for inducing cardiac dysfunction mediated by lipid peroxidation [17, 56, 60, 61]. It has been shown that malondialdehyde, which is a product of lipid peroxidation, was increased in the hearts and cardiac microsomes of mice treated with DOX [17, 62]. This $O_2^{\cdot-}$ is then converted into H_2O_2 and O_2 by superoxide dismutase. Another important species that leads to the oxidative damage to cardiomyocytes is $ONOO^-$ [63, 64]; it is known to target cardiomyocytes mitochondria primarily [65]. $ONOO^-$ reacts readily with DNA to induce double- and single-strand damage and base modifications [34, 40]. Also, evidence suggests that nitric oxide (NO^{\cdot}) may also play an important role in cardiac dysfunction. Nitric oxide regulates contractility and blood flow in the heart [66], however, excessive nitric oxides can induce cardiomyocyte oxidative damage, leading to cardiomyopathy and congestive heart failure [64, 67, 68]. Synthesis of nitric oxide in the presence of $O_2^{\cdot-}$ is known to induce the formation of $ONOO^-$ [69]. In addition, H_2O_2 , which is reduced to OH^{\cdot} in the presence of Fe^{2+} , and OH^{\cdot} is known to initiate free radical-mediated chain reactions that result in myocardial damage and lipid peroxidation by removing hydrogen atoms from unsaturated fatty acids [70]. The use of antioxidants may be a favorable approach to reduce the cardiotoxicity of anthracyclines, thereby improving clinical utility of these promising chemotherapeutic agents. Many studies have explored the use of antioxidants in diminishing DOX-induced cardiotoxicity [22, 23].

PAESe was developed as a potent antioxidant to treat cardiovascular disease. It has been shown that selenium redox cycling increases the free radical scavenging effects of PAESe against oxidant-induced DNA damage [34]. In this redox cycling process, the selenoxide-form of PAESe is produced when this selenide reduces cellular oxidants such as peroxide or ONOO⁻, and the selenoxide is then recycled back to PAESe by cellular reductants such as ascorbate and glutathione.

DOX is one of the standard adjuvant chemotherapeutics used to treat women with early-stage invasive breast cancer. A number of clinical trials showed that chemotherapy containing anthracyclines, like DOX, prolongs survival time over non-anthracycline chemotherapy regimens [71], and this advantage on survival was significant for women with HER-2 positive, not negative breast cancer [72]. Based on these results, we determined the effect of PAESe on antitumor activity of DOX using *in vitro* BT-474 breast cancer cell that overexpress HER-2.

PC-3 cells were also broadly utilized to determine the therapeutic effect of DOX due to its high sensitivity to DOX [73, 74]. Moreover, PC-3 cell was chosen for *in vivo* evaluation to induce cardiotoxicity. PC-3 cell allows for long-term treatment of DOX since it is slower growing primary tumor [75].

Up to 1 μ M PAESe was found to have little to no cytotoxic effects to PC-3 cells after 72 hr exposure. Similarly, the growth of BT-474 cells was not altered by PAESe up to 10 μ M. We then examined whether there would be an effect of PAESe on the antitumor activity of DOX. In this combination study, 100 to 1000 nM for DOX were chosen based on the clinically relevant cytostatic concentration (*i.e.*, 1–100 % peak plasma concentration) that was represented by 10–1000 nM [76]. We found that PAESe

did not affect the antitumor activity with DOX in PC-3 as well as BT-474 cells both at non-toxic and at cytotoxic concentrations. The cytotoxicity of DOX has been correlated with antagonism of topoisomerase-2 rather than free radical generation, whereas cardiotoxicity has known to be more related with free radical formation as mentioned above [18]. PAESe did not alter the antitumor activity of vincristine, known to inhibit growth via tubulin polymerization [77]. However, the oxidant-mediated cytotoxicity of TBHP was decreased significantly ($p < 0.05$) in the presence of PAESe in a dose-dependent manner. These data suggest that PAESe may be useful in combination with DOX to preserve DOX's antitumor activity, but decrease the toxicity of its ROS on cardiomyocytes.

These results were further supported by the extent of ROS generation study which was estimated by CM-H₂DCFDA, a membrane permeable non-fluorescent reduced derivative of DCF. The acetate groups of CM-H₂DCFDA are removed by esterase cleavage intracellularly, followed by oxidation that can be determined using a fluorescence microplate reader or visualized by fluorescence microscopy. CM-H₂DCFDA can detect several ROS including ONOO⁻, H₂O₂, OH[•] and peroxy radical. The results showed clearly that ROS generation after DOX exposure was suppressed significantly in the presence of PAESe on PC-3 and BT-474 cells, although DOX at 500 nM on BT-474 cells appeared to require more PAESe over 1000 nM to decrease significantly free radicals. These results suggest that PAESe might be used in combination with DOX to decrease the cytotoxicity related to the ROS generation without altering its antitumor activity.

We then examined whether *in vitro* results in which PAESe decreased ROS generation without altering the antitumor effects of DOX could be related to *in vivo* treatment. In a human prostate xerograph (PC-3) mouse model, concomitant administration of PAESe did not alter the antitumor activity of DOX as compared to DOX alone. These results are in agreement with our *in vitro* data showing PAESe did not alter the cytotoxic effect of DOX.

However, it is noteworthy that PAESe alone appears to have some antitumor effects. The unexpected anticancer activity of PAESe might be associated with altering *in vivo* immune function. Antioxidants have been shown to enhance not only the activity of several immune cells such as lymphocytes, macrophage and mononuclear cells but also the cytotoxicity of natural killer cells, which are known to destroy tumors in a non-specific fashion [78]. Also, immune function has known to be increased by up-regulation of the interleukin-2 receptors expression as well as the responsiveness of T cell to interleukin-2 through antioxidant activity. Unlike *in vitro* studies, tumor cells could be more vulnerable to the activity of chemotherapeutic agents in an *in vivo* system because of the immune-enhancing effect of PAESe to increase the cytotoxic activity of a variety of immune cells as demonstrated in animal and human studies [78]. This is a possible explanation for the increase in antitumor activity of PAESe alone, but further studies are needed to elucidate this activity.

Histological examinations supported the hypothesis that PAESe can reduce DOX-mediated cardiotoxicity. Myocardium of mice treated with PAESe alone was intact and normal similar to the control. Cardiac damages such as disrupted myocardial fibers,

immune cell infiltration, and inflammation [64] were decreased in the group treated DOX with PAESe relative to the one treated with DOX alone.

In conclusion, we demonstrated that PAESe did not alter DOX antitumor activity and limited DOX-mediated cardiotoxicity and weight loss. These effects are believed to be related to its potent antioxidant activity, as assessed by *in vitro* growth inhibition assays, alteration in ROS generation, *in vivo* tumor growth inhibition, and histopathological examination. Future studies are needed to determine optimal exposure-response profile of PAESe and to examine its effect on the immune system *in vivo*. Also, further examination is required to elucidate whether PAESe itself has antitumor activity. Nevertheless, the benefit of this study is worthy because this is the first to demonstrate the ability of PAESe to reduce DOX-induced cardiotoxicity and weight loss, without altering its antitumor activity, suggesting that concomitant administration of PAESe could improve the clinical utility of DOX.

Table 2-1. Free radical scavenging effects of PAESE on TBHP and DOX in PC-3 cells

TBHP			
PAESE	0 μ M	30 μ M	300 μ M
0 nM	100	121 \pm 7	193 \pm 13
100 nM	103 \pm 5	111 \pm 5	150 \pm 10*
1000 nM	101 \pm 3	102 \pm 4	142 \pm 7*

DOX			
PAESE	0 nM	100 nM	500 nM
0 nM	100	142 \pm 9	184 \pm 11
50 nM	105 \pm 5	118 \pm 5*	156 \pm 8*
500 nM	91 \pm 2	113 \pm 5*	142 \pm 9*

Mean \pm SEM, * $p \leq 0.05$ vs. controls, n=5 x 3 studies.

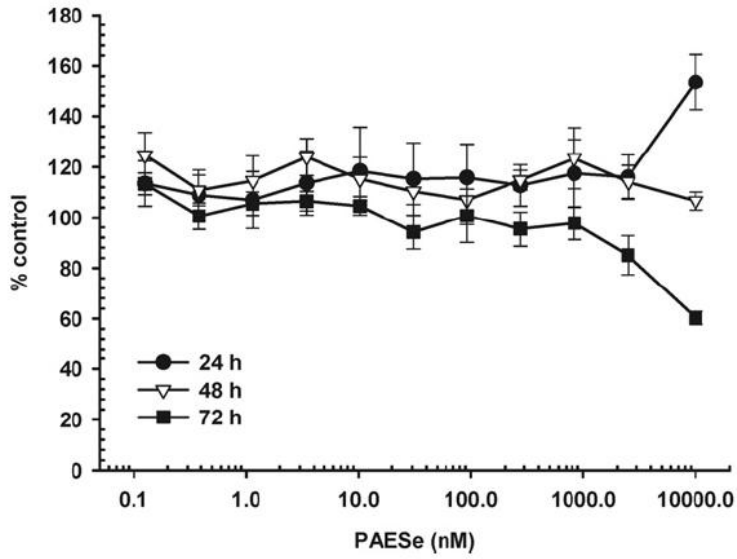
Table 2-2. Free radical scavenging effects of PAESe on TBHP and DOX in BT-474 cells

TBHP			
PAESe	0 μ M	30 μ M	300 μ M
0 nM	100	110 \pm 7	193 \pm 13
100 nM	96 \pm 3	111 \pm 5	150 \pm 10*
1000 nM	95 \pm 4	102 \pm 4	142 \pm 7*

DOX			
PAESe	0 nM	100 nM	500 nM
0 nM	100	151 \pm 4	177 \pm 6
50 nM	116 \pm 4	142 \pm 5	177 \pm 9
500 nM	114 \pm 3	127 \pm 5*	160 \pm 6

Mean \pm SEM, * $p \leq 0.05$ vs. controls, n=5 x 3 studies.

(A)



(B)

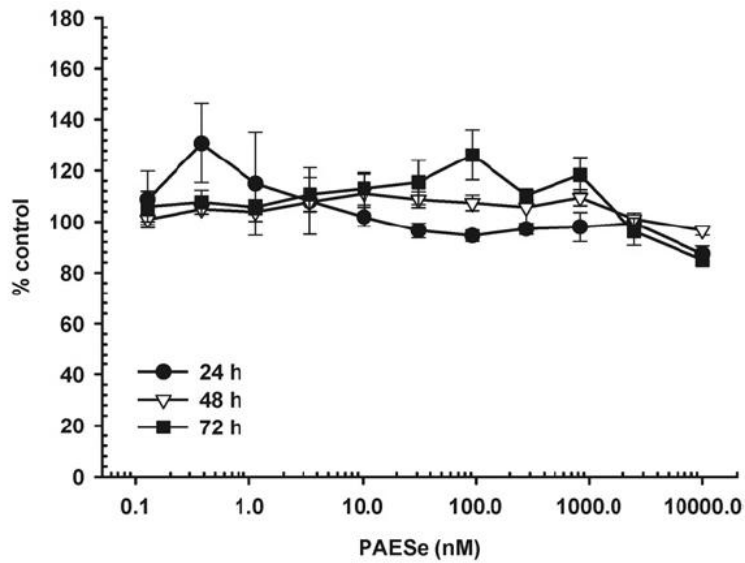


Figure 2-1. Effect of PAESE on the growth of PC-3 cells *in vitro*. PC-3 cells were treated with PAESE (0.1–10,000 nM) for 24, 48 and 72 hr prior to analysis cytotoxicity using MTT (A) and SRB (B) staining. Data are presented as means \pm SEM of three independent studies (n = 5).

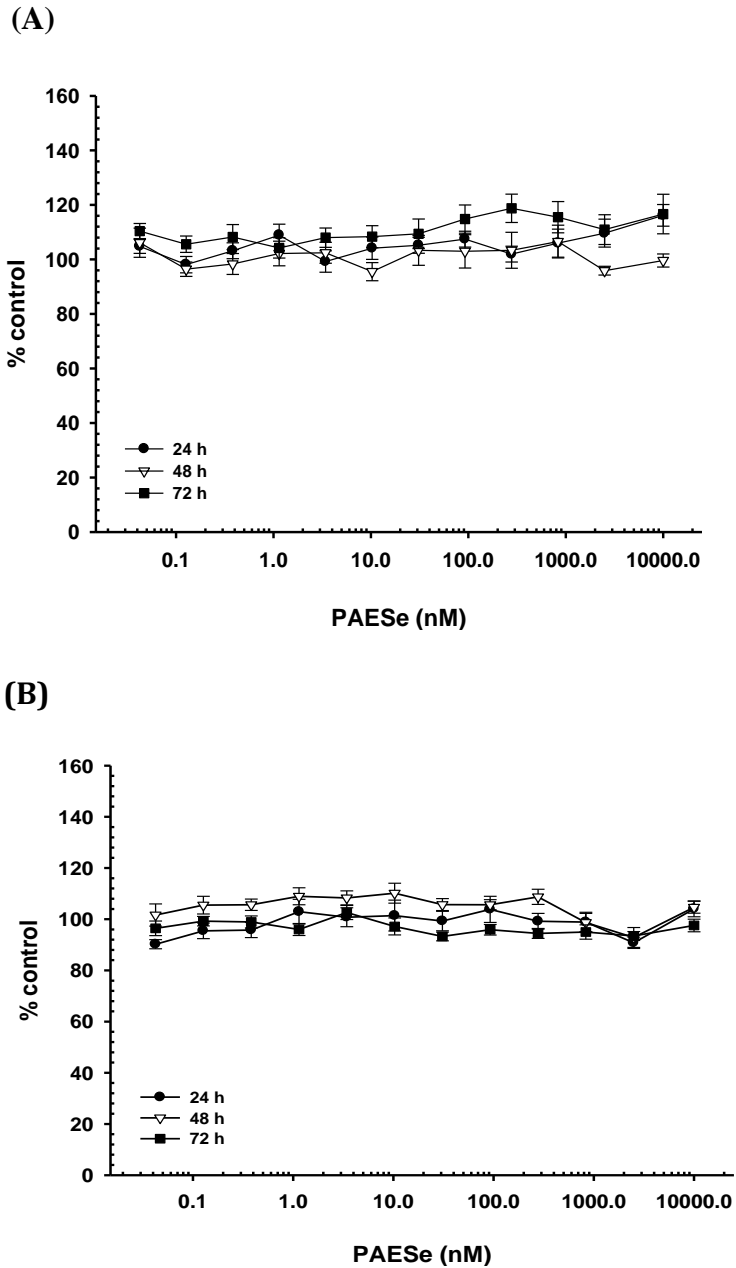
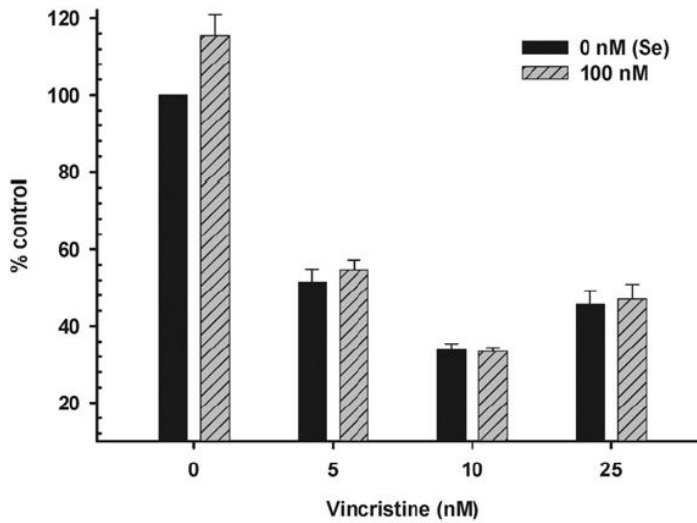


Figure 2-2. Growth inhibition of PAESE on the growth of BT-474 cells *in vitro*. PAESE (0.04 to 10,000 nM) were treated to BT-474 cells for 24, 48, and 72 hr followed by analysis using MTT (A) and SRB (B) staining. Data are presented as the Mean \pm SEM of three independent studies (n=5)

(A)



(B)

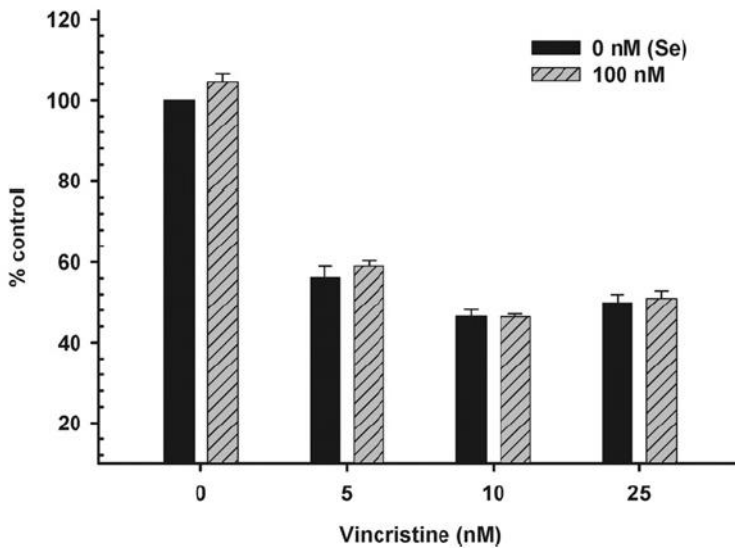


Figure 2-3. Effect of PAESe on the growth inhibition of vincristine in PC-3 cells. The effect of PAESe (100 nM) on the cytotoxic activity of vincristine (5–25 nM) was determined by MTT (A) and SRB (B) staining after 72 hr incubation. Data are presented as means \pm SEM of three independent studies (n = 5).

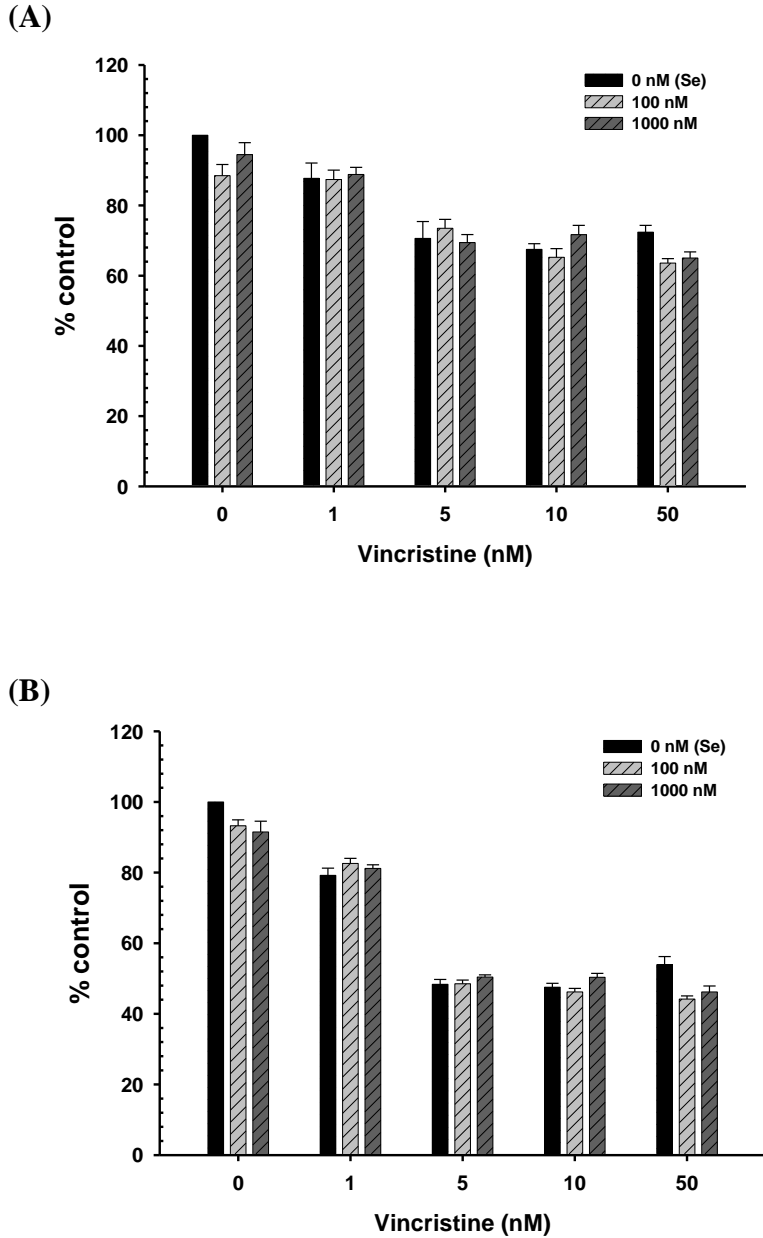
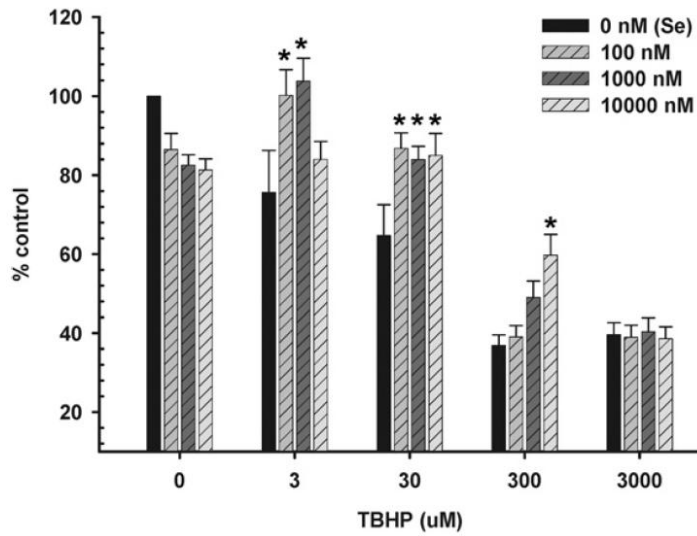


Figure 2-4. Growth inhibitory effect of PAESE in combination with Vincristine on BT-474 cells by (A) MTT and (B) SRB The effect of PAESE (100 and 1000 nM) on growth inhibition of vincristine (1 to 50 nM) was determined by MTT (A) and SRB (B) assay after 72 hr incubation. Data are presented as means \pm SEM of three independent studies (n = 5)

(A)



(B)

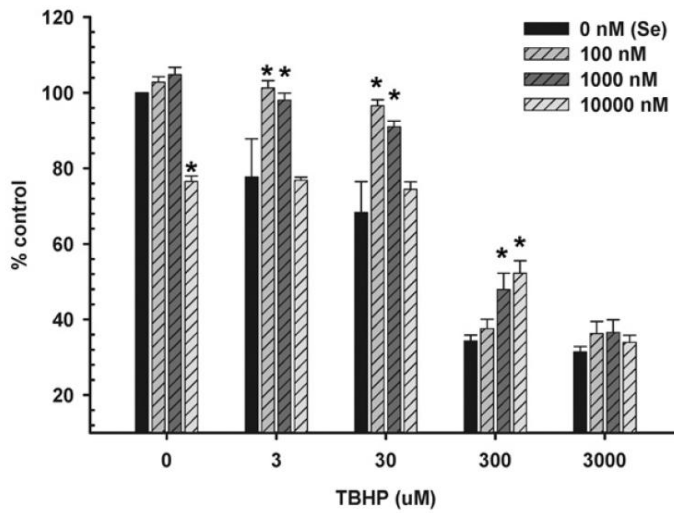


Figure 2-5. Effect of PAESe on the growth inhibition of TBHP in PC-3 cells. The effect of PAESe (100–10,000 nM) on the cytotoxic activity of TBHP (3–3000 μ M) was determined by MTT (A) and SRB (B) staining after 72 hr incubation. Data are presented as means \pm SEM of three independent studies ($n = 5$). An asterisk indicates a significant (p -value <0.05) difference compared to control, 0 nM (Se).

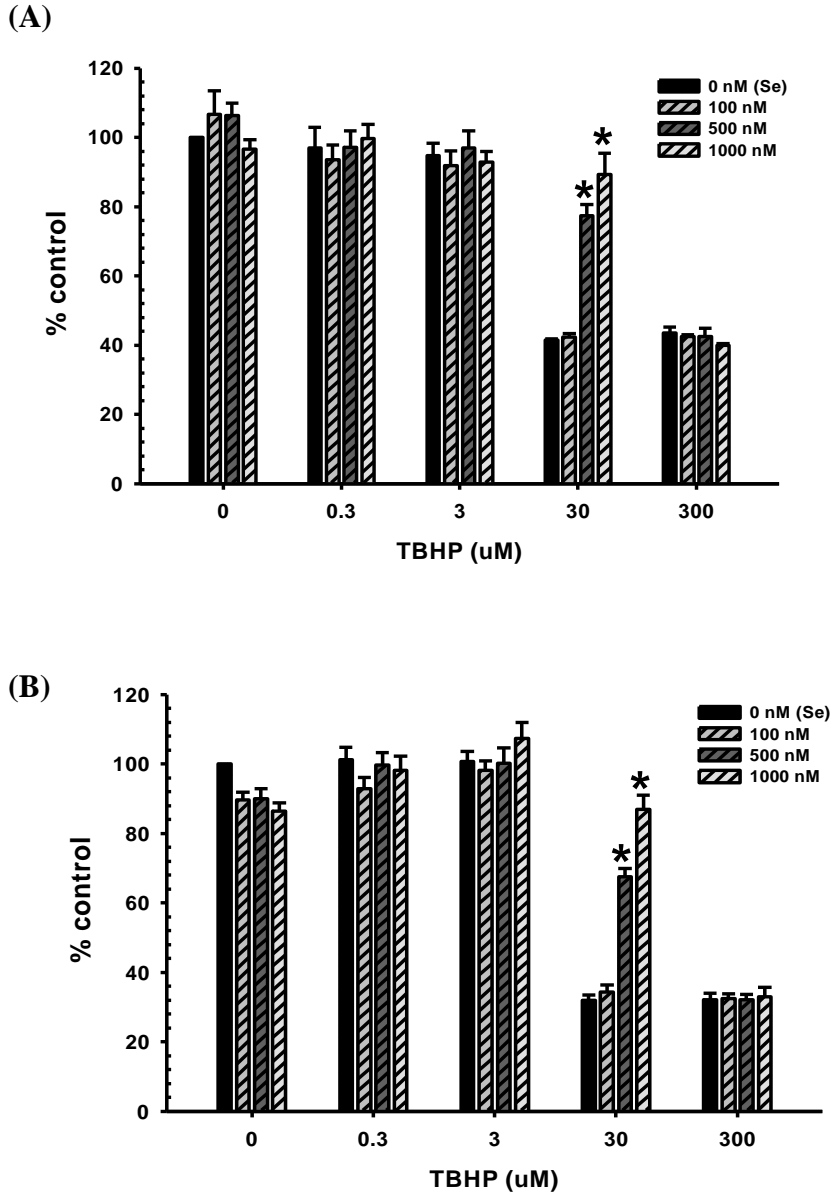


Figure 2-6. Growth inhibitory effect of PAESe in combination with TBHP on BT-474 cells by (A) MTT and (B) SRB TBHP (0.3 to 300 μ M), as positive control, was co-treated with PAESe (100 and 1000 nM) to BT-474 cells to determine the effect of PAESe on the cytotoxicity of TBHP by MTT (A) and SRB (B) assay after 72 hr incubation. Data are presented as means \pm SEM of three independent studies (n = 5). An asterisk indicates a significant ($p < 0.05$) difference compared to control, 0 nM (Se).

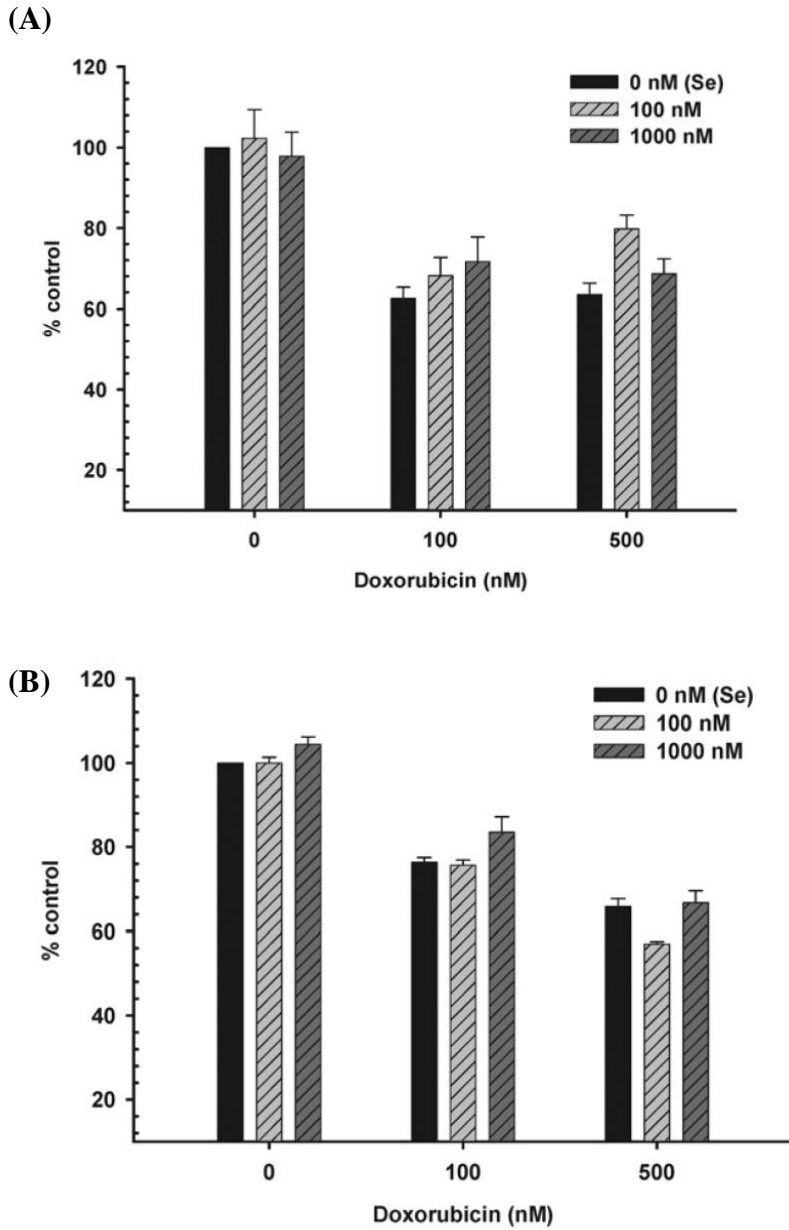


Figure 2-7. Effect of PAESE on the growth inhibition of DOX in PC-3 cells. The effect of PAESE (100 and 1000 nM) on the cytotoxic activity of DOX (100 and 500 nM) was determined by MTT (A) and SRB (B) staining after 72 hr incubation. Data are presented as means \pm SEM of three independent studies (n = 5).

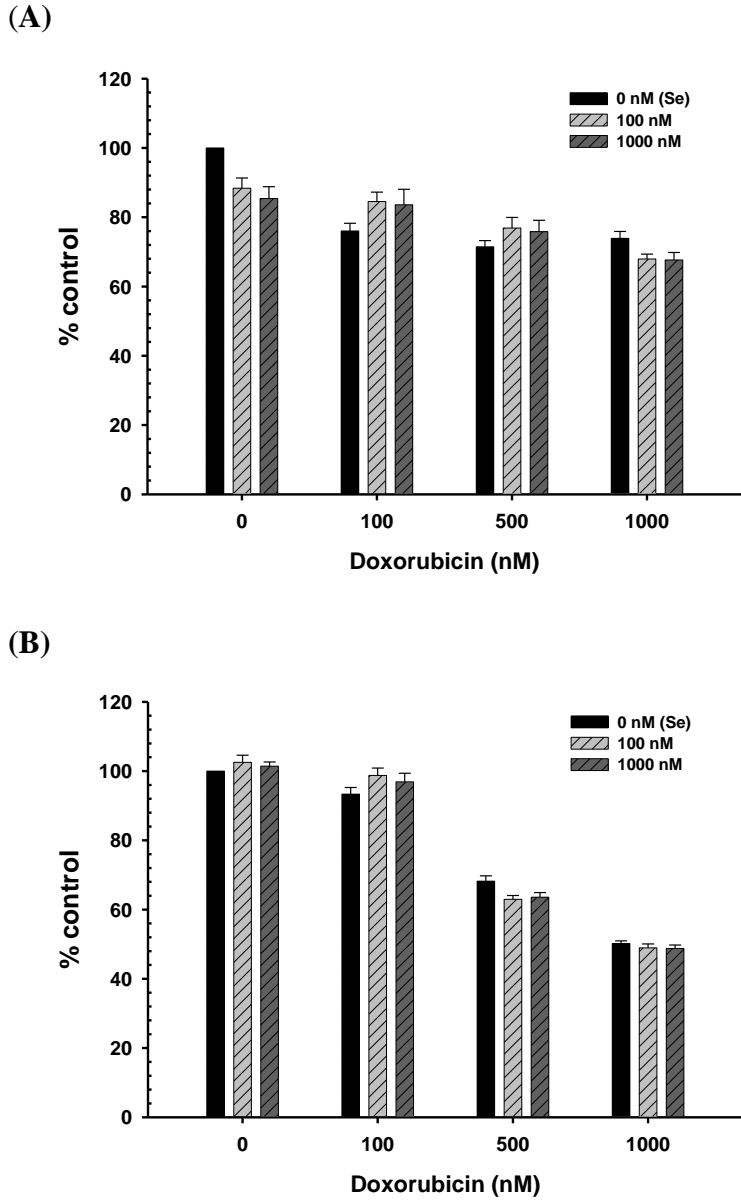
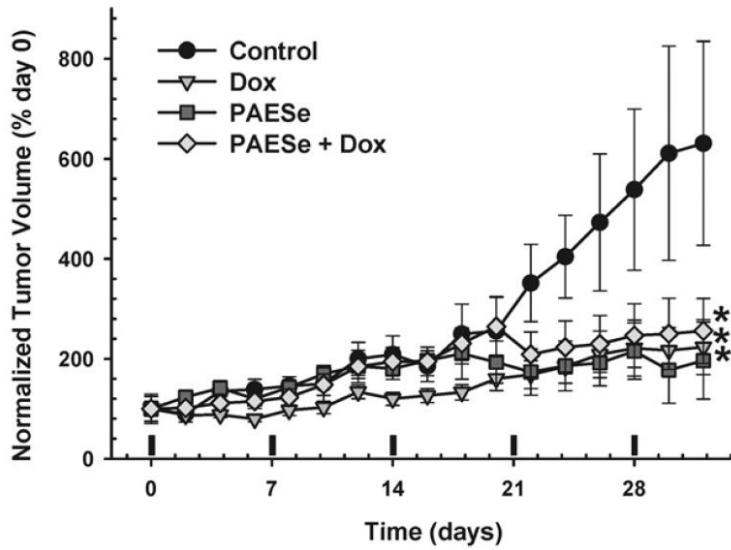


Figure 2-8. Growth inhibitory effect of PAESE in combination with DOX on BT-474 cells by (A) MTT and (B) SRB The effect of PAESE (100 and 1000 nM) on growth inhibition of DOX (100 and 1000 nM) was determined by MTT (A) and SRB (B) staining after 72 hr incubation. Data are presented as means \pm SEM of three independent studies (n = 5)

(A)



(B)

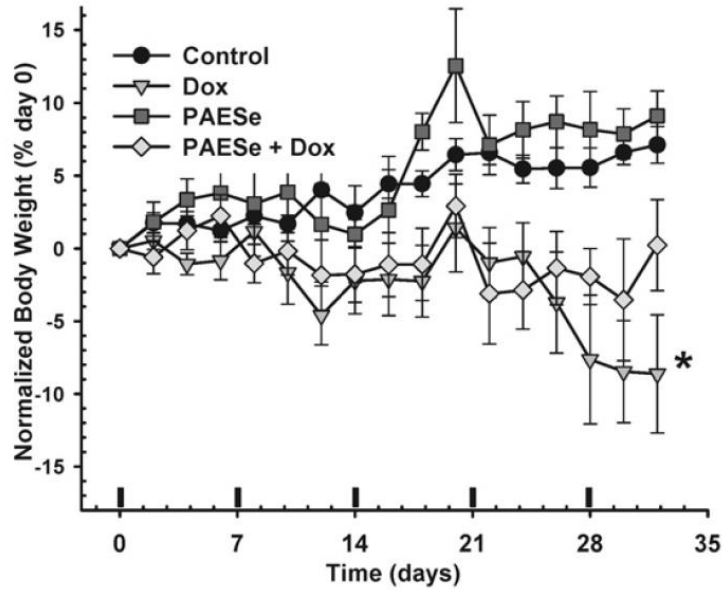


Figure 2-9. Effect of PAESe on antitumor activity of DOX in a PC-3 xenograft model. The effect DOX, PAESe, DOX + PAESe, and vehicle-control on tumor growth (A) and body weight (B) in a tumor xenograft model of human (PC-3) prostate cancer was determined. Treatment, 5 mg/kg/week for DOX and 10 mg/kg/week for PAESe was

administered by tail vein injection weekly (black bars) after tumors reached 200 mm³. Tumor volume and body weight were monitored every other day, data are presented as means \pm SEM (n = 5–8) and were normalized to average tumor volume or body weight on day 0. An asterisk indicates a significant ($p < 0.05$) difference compared to control.

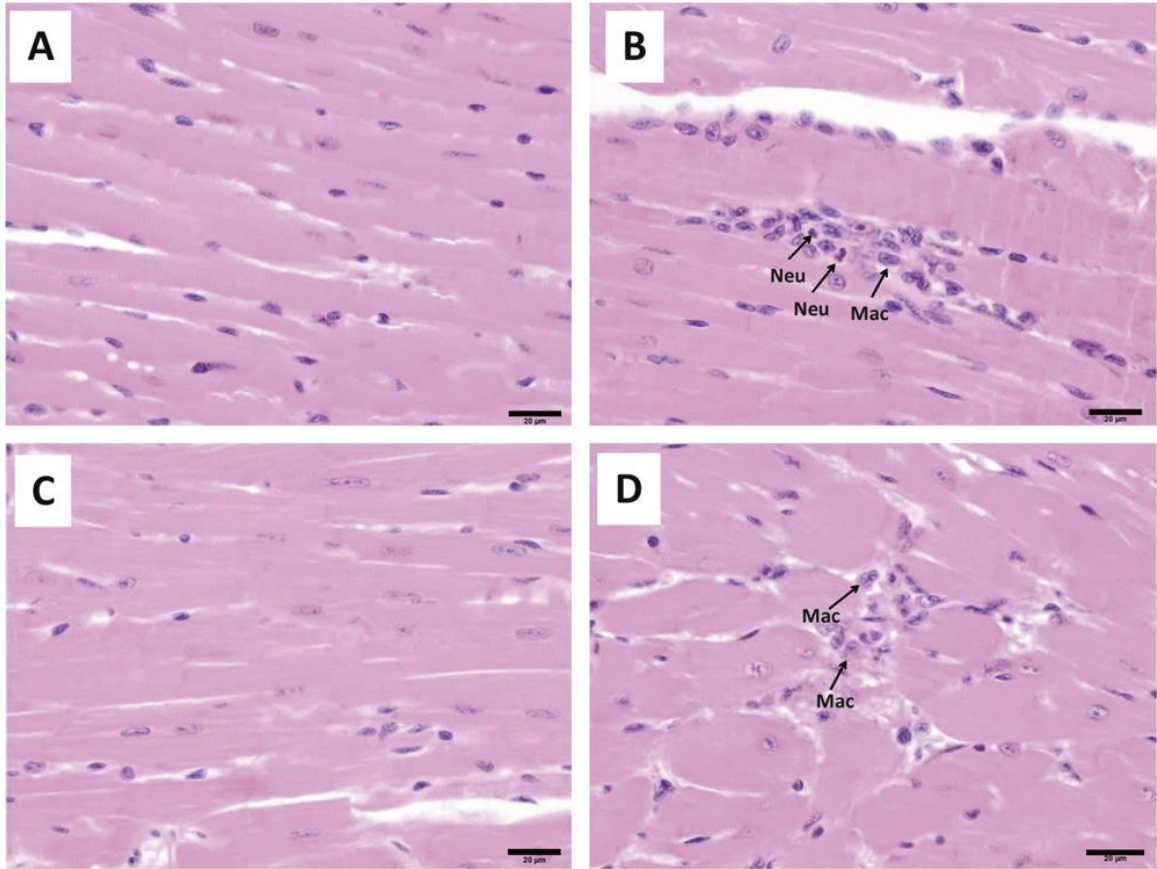


Figure 2-10. Histological examination of heart. Two weeks after the last treatment, hearts of (A) control, (B) DOX, (C) PAESe and (D) DOX+PAESe group were excised, fixed, and processed for histological examination. Micrographs of the myocardium sections stained with H&E at high magnification ($400\times$, scale bars = $20\ \mu\text{m}$) were captured.

References

1. Siegel R, DeSantis C, Virgo K, Stein K, Mariotto A, Smith T, et al. Cancer treatment and survivorship statistics, 2012. *CA: A Cancer Journal For Clinicians* 2012; **62**:220-241.
2. Hande KR. Clinical applications of anticancer drugs targeted to topoisomerase II. *Biochimica et Biophysica Acta (BBA) - Gene Structure and Expression* 1998; **1400**:173-184.
3. Plosker GL. Epirubicin: A review of its pharmacodynamic and pharmacokinetic properties, and therapeutic use in cancer chemotherapy. *Drugs* 1993; **45**:788.
4. Bronchud MH, Howell A, Crowther D, Hopwood P, Souza L, Dexter TM. The use of granulocyte colony-stimulating factor to increase the intensity of treatment with doxorubicin in patients with advanced breast and ovarian cancer. *Br J Cancer* 1989; **60**:121-125.
5. Singal PK, Deally CMR, Weinberg LE. Subcellular effects of adriamycin in the heart: A concise review. *Journal of Molecular and Cellular Cardiology* 1987; **19**:817-828.
6. Cassidy SC, Chan DP, Rowland DG, Allen HD. Effects of Doxorubicin on Diastolic Function, Contractile Reserve, and Ventricular–Vascular Coupling in Piglets. *Pediatric Cardiology* 1998; **19**:450-457.

7. Saeki K, Obi I, Ogiku N, Shigekawa M, Imagawa T, Matsumoto T. Doxorubicin directly binds to the cardiac-type ryanodine receptor. *Life Sciences* 2002; **70**:2377-2389.
8. Billingham ME, Mason JW, Bristow MR, Daniels JR. Anthracycline cardiomyopathy monitored by morphologic changes. *Cancer treatment reports* 1978; **62**:865-872.
9. Swain SM, Whaley FS, Ewer MS. Congestive heart failure in patients treated with doxorubicin. *Cancer* 2003; **97**:2869-2879.
10. Freter CE. Doxorubicin cardiac toxicity manifesting seven years after treatment. Case report and review. *The American journal of medicine* 1986; **80**:483.
11. Bristow MR, Sageman WS, Scott RH, Billingham ME, Bowden RE, Kernoff RS, et al. Acute and Chronic Cardiovascular Effects of Doxorubicin in the Dog: The Cardiovascular Pharmacology of Drug-Induced Histamine Release. *Journal of Cardiovascular Pharmacology* 1980; **2**:487-516.
12. Tong J. Myocardial adrenergic changes at two stages of heart failure due to adriamycin treatment in rats. *American journal of physiology. Heart and circulatory physiology* 1991; **29**:H909.
13. Gosalvez M, van Rossum GDV, Blanco MF. Inhibition of Sodium-Potassium-activated Adenosine 5'-Triphosphatase and Ion Transport by Adriamycin. *Cancer Research* 1979; **39**:257-261.
14. Singal PK, Pierce GN. Adriamycin stimulates low-affinity Ca²⁺ binding and lipid peroxidation but depresses myocardial function. *American Journal of Physiology - Heart and Circulatory Physiology* 1986; **250**:H419-H425.

15. Olson HM. Electrolyte and morphologic alterations of myocardium in adriamycin-treated rabbits. *The American journal of pathology* 1974; **77**:439.
16. Doroshow JH. Effect of Anthracycline Antibiotics on Oxygen Radical Formation in Rat Heart. *Cancer Research* 1983; **43**:460-472.
17. Myers C, McGuire W, Liss R, Ifrim I, Grotzinger K, Young R. Adriamycin: the role of lipid peroxidation in cardiac toxicity and tumor response. *Science* 1977; **197**:165-167.
18. Keizer HG, Pinedo HM, Schuurhuis GJ, Joenje H. Doxorubicin (adriamycin): A critical review of free radical-dependent mechanisms of cytotoxicity. *Pharmacology & Therapeutics* 1990; **47**:219-231.
19. Olson RD, Boerth RC, Gerber JG, Nies AS. Mechanism of adriamycin cardiotoxicity: Evidence for oxidative stress. *Life Sciences* 1981; **29**:1393-1401.
20. Chance B, Sies H, Boveris A. Hydroperoxide metabolism in mammalian organs. *Physiological Reviews* 1979; **59**:527-605.
21. Handa K, Sato S. Generation of free radicals of quinone group-containing anti-cancer chemicals in NADPH-microsome system as evidenced by initiation of sulfite oxidation. *Gann* 1975; **66**:43-47.
22. Siveski-Iliskovic N, Hill M, Chow DA, Singal PK. Probucol Protects Against Adriamycin Cardiomyopathy Without Interfering With Its Antitumor Effect. *Circulation* 1995; **91**:10-15.
23. Quiles JL, Huertas JsR, Battino M, Mataix JRamirez-Tortosa MC. Antioxidant nutrients and adriamycin toxicity. *Toxicology* 2002; **180**:79-95.

24. Yagmurca M, Fadillioglu E, Erdogan H, Ucar M, Sogut S, Irmak MK. Erdosteine prevents doxorubicin-induced cardiotoxicity in rats. *Pharmacological Research* 2003; **48**:377-382.
25. Van Vleet JF. Cardiac disease induced by chronic adriamycin administration in dogs and an evaluation of vitamin E and selenium as cardioprotectants. *The American journal of pathology* 1980; **99**:13.
26. Shimpo K, Nagatsu T, Yamada K, Sato T, Niimi H, Shamoto M, et al. Ascorbic acid and adriamycin toxicity. *The American Journal of Clinical Nutrition* 1991; **54**:1298S-1301S.
27. Sadzuka Y, Sugiyama T, Shimoi K, Kinane N, Hirota S. Protective effect of flavonoids on doxorubicin-induced cardiotoxicity. *Toxicology Letters* 1997; **92**:1-7.
28. Legha SS, Wang Y-M, Mackay B, Ewer M, Hortobagyi GN, Benjamin RS, et al. Clinical and Pharmacologic investigation of the effects of α -tocopherol on adriamycin cardiotoxicity. *Annals of the New York Academy of Sciences* 1982; **393**:411-417.
29. Wahab MH, Akoul ES, Abdel Aziz AA. Modulatory effects of melatonin and vitamin E on doxorubicin-induced cardiotoxicity in Ehrlich ascites carcinoma-bearing mice. *Tumori* 2000; **86**:157-162.
30. May SW, Pollock SH. Selenium-Based Antihypertensives: Rationale and Potential. *Drugs* 1998; **56**:959-964.
31. May SW, Wang L, Gill-Woznichak MM, Browner RF, Ogonowski AA, Smith JB, et al. An Orally Active Selenium-Based Antihypertensive Agent with Restricted

- CNS Permeability. *Journal of Pharmacology and Experimental Therapeutics* 1997; **283**:470-477.
32. May SW. Selenium-based drug design: rationale and therapeutic potential. *Expert Opinion on Investigational Drugs* 1999; **8**:1017-1030.
33. May SW. Selenium-based pharmacological agents: an update. *Expert Opinion on Investigational Drugs* 2002; **11**:1261-1269.
34. De Silva V, Woznichak MM, Burns KL, Grant KB, May SW. Selenium Redox Cycling in the Protective Effects of Organoselenides against Oxidant-Induced DNA Damage. *Journal of the American Chemical Society* 2004; **126**:2409-2413.
35. May SW, Herman HH, Roberts SF, Ciccarello MC. Ascorbate depletion as a consequence of product recycling during dopamine .beta.-monooxygenase catalyzed selenoxidation. *Biochemistry* 1987; **26**:1626-1633.
36. Overcast JD, Ensley AE, Buccafusco CJ, Cundy C, Broadnax RA, He S, et al. Evaluation of Cardiovascular Parameters of a Selenium-Based Antihypertensive Using Pulsed Doppler Ultrasound. *Journal of Cardiovascular Pharmacology* 2001; **38**:337-346.
37. Pollock SH, Herman HH, Fowler LC, Edwards AS, Evans CO, May SW. Demonstration of the antihypertensive activity of phenyl-2-aminoethyl selenide. *Journal of Pharmacology and Experimental Therapeutics* 1988; **246**:227-234.
38. Woznichak MM, Overcast JD, Robertson K, Neumann HM, May SW. Reaction of Phenylaminoethyl Selenides with Peroxynitrite and Hydrogen Peroxide. *Archives of Biochemistry and Biophysics* 2000; **379**:314-320.

39. Cowan EA, Oldham CD, May SW. Identification of a thioselenurane intermediate in the reaction between phenylaminoalkyl selenoxides and glutathione. *Archives of Biochemistry and Biophysics* 2011; **506**:201-207.
40. Henle ES, Linn S. Formation, Prevention, and Repair of DNA Damage by Iron/Hydrogen Peroxide. *Journal of Biological Chemistry* 1997; **272**:19095-19098.
41. Mosmann T. Rapid colorimetric assay for cellular growth and survival: Application to proliferation and cytotoxicity assays. *Journal of Immunological Methods* 1983; **65**:55-63.
42. Skehan P, Storeng R, Scudiero D, Monks A, McMahon J, Vistica D, et al. New Colorimetric Cytotoxicity Assay for Anticancer-Drug Screening. *Journal of the National Cancer Institute* 1990; **82**:1107-1112.
43. Davol PA, Frackelton AR. Targeting human prostatic carcinoma through basic fibroblast growth factor receptors in an animal model: Characterizing and circumventing mechanisms of tumor resistance. *The Prostate* 1999; **40**:178-191.
44. Gewirtz DA. A critical evaluation of the mechanisms of action proposed for the antitumor effects of the anthracycline antibiotics adriamycin and daunorubicin. *Biochemical Pharmacology* 1999; **57**:727-741.
45. Fujita N, Hiroe M, Ohta Y, Horie T, Hosoda S. Chronic Effects of Metoprolol on Myocardial [beta]-Adrenergic Receptors in Doxorubicin-Induced Cardiac Damage in Rats. *Journal of Cardiovascular Pharmacology* 1991; **17**:656-661.

46. Revis NW, Marusic N. Glutathione peroxidase activity and selenium concentration in the hearts of doxorubicin-treated rabbits. *Journal of Molecular and Cellular Cardiology* 1978; **10**:945-948.
47. Iliskovic N, Hasinoff BB, Malisza KL, Li T, Danelisen I, Singal PK. Mechanisms of beneficial effects of probucol in adriamycin cardiomyopathy. *Molecular and Cellular Biochemistry* 1999; **196**:43-49.
48. Papadopoulou LC, Theophilidis G, Thomopoulos GN, Tsiftoglou AS. Structural and functional impairment of mitochondria in adriamycin-induced cardiomyopathy in mice: suppression of cytochrome c oxidase II gene expression. *Biochemical Pharmacology* 1999; **57**:481-489.
49. Gille L, Nohl H. Analyses of the Molecular Mechanism of Adriamycin-Induced Cardiotoxicity. *Free Radical Biology and Medicine* 1997; **23**:775-782.
50. Doroshov JH, Locker GY, Myers CE. Enzymatic Defenses of the Mouse Heart Against Reactive Oxygen Metabolites: ALTERATIONS PRODUCED BY DOXORUBICIN. *The Journal of Clinical Investigation* 1980; **65**:128-135.
51. Santos DL, Moreno AJM, Leino RL, Froberg MK, Wallace KB. Carvedilol Protects against Doxorubicin-Induced Mitochondrial Cardiomyopathy. *Toxicology and Applied Pharmacology* 2002; **185**:218-227.
52. Wallace KB. Doxorubicin-induced cardiac mitochondrionopathy. *Pharmacology & Toxicology* 2003; **93**:105-115.
53. Zhou S, Palmeira CM, Wallace KB. Doxorubicin-induced persistent oxidative stress to cardiac myocytes. *Toxicology Letters* 2001; **121**:151-157.

54. Olson RD, Mushlin PS. Doxorubicin cardiotoxicity: analysis of prevailing hypotheses. *The FASEB Journal: Official Publication Of The Federation Of American Societies For Experimental Biology* 1990; **4**:3076-3086.
55. Yu T-W, Anderson D. Reactive oxygen species-induced DNA damage and its modification: A chemical investigation. *Mutation Research/Fundamental and Molecular Mechanisms of Mutagenesis* 1997; **379**:201-210.
56. Kalyanaraman B, Perez-Reyes E, Mason RP. Spin-trapping and direct electron spin resonance investigations of the redox metabolism of quinone anticancer drugs. *Biochimica et Biophysica Acta (BBA) - General Subjects* 1980; **630**:119-130.
57. Minotti G. Paradoxical inhibition of cardiac lipid peroxidation in cancer patients treated with doxorubicin. Pharmacologic and molecular reappraisal of anthracycline cardiotoxicity. *The Journal of Clinical Investigation* 1996; **98**:650.
58. Venditti P, Balestrieri M, De Leo T, Di Meo S. Free radical involvement in doxorubicin-induced electrophysiological alterations in rat papillary muscle fibres. *Cardiovascular Research* 1998; **38**:695-702.
59. Sarvazyan NA, Askari A, Huang WH. Effects of doxorubicin on cardiomyocytes with reduced level of superoxide dismutase. *Life Sciences* 1995; **57**:1003-1010.
60. Yen HC. The protective role of manganese superoxide dismutase against adriamycin-induced acute cardiac toxicity in transgenic mice. *The Journal of Clinical Investigation* 1996; **98**:1253.

61. Doroshow JH, Davies KJ. Redox cycling of anthracyclines by cardiac mitochondria. II. Formation of superoxide anion, hydrogen peroxide, and hydroxyl radical. *Journal of Biological Chemistry* 1986; **261**:3068-3074.
62. Mimnaugh EG, Gram TE, Trush MA. Stimulation of mouse heart and liver microsomal lipid peroxidation by anthracycline anticancer drugs: characterization and effects of reactive oxygen scavengers. *Journal of Pharmacology and Experimental Therapeutics* 1983; **226**:806-816.
63. Vasquez-Vivar J, Martasek P, Hogg N, Masters BSS, Pritchard KAKalyanaraman B. Endothelial Nitric Oxide Synthase-Dependent Superoxide Generation from Adriamycin. *Biochemistry* 1997; **36**:11293-11297.
64. Weinstein DM, Mihm MJ, Bauer JA. Cardiac Peroxynitrite Formation and Left Ventricular Dysfunction following Doxorubicin Treatment in Mice. *Journal of Pharmacology and Experimental Therapeutics* 2000; **294**:396-401.
65. Mihm MJ, Yu F, Weinstein DM, Reiser PJ, Bauer JA. Intracellular distribution of peroxynitrite during doxorubicin cardiomyopathy: evidence for selective impairment of myofibrillar creatine kinase. *British Journal of Pharmacology* 2002; **135**:581-588.
66. Varin R, Mulder P, Richard V, Tamion F, Devaux C, Henry J-P, et al. Exercise Improves Flow-Mediated Vasodilatation of Skeletal Muscle Arteries in Rats With Chronic Heart Failure : Role of Nitric Oxide, Prostanoids, and Oxidant Stress. *Circulation* 1999; **99**:2951-2957.

67. Adams V, Jiang H, Yu J, Mbius-Winkler S, Fiehn E, Linke A, et al. Apoptosis in skeletal myocytes of patients with chronic heart failure is associated with exercise intolerance. *Journal of the American College of Cardiology* 1999; **33**:959-965.
68. Vejstrup NG, Bouloumie A, Boesgaard Sr, Andersen CB, Nielsen-Kudsk JE, Mortensen SA, et al. Inducible Nitric Oxide Synthase (iNOS) in the Human Heart: Expression and Localization in Congestive Heart Failure. *Journal of Molecular and Cellular Cardiology* 1998; **30**:1215-1223.
69. Cai L, Klein JB, Kang YJ. Metallothionein Inhibits Peroxynitrite-induced DNA and Lipoprotein Damage. *Journal of Biological Chemistry* 2000; **275**:38957-38960.
70. Rajagopalan S, Politi PM, Sinha BK, Myers CE. Adriamycin-induced Free Radical Formation in the Perfused Rat Heart: Implications for Cardiotoxicity. *Cancer Research* 1988; **48**:4766-4769.
71. (EBCTCG) EBCTCG. Effects of chemotherapy and hormonal therapy for early breast cancer on recurrence and 15-year survival: an overview of the randomised trials. *Lancet* 2005; **365**:1687-1717.
72. Gennari A, Sormani MP, Pronzato P, Puntoni M, Colozza M, Pfeffer U, et al. HER2 Status and Efficacy of Adjuvant Anthracyclines in Early Breast Cancer: A Pooled Analysis of Randomized Trials. *Journal of the National Cancer Institute* 2008; **100**:14-20.
73. Liu X, Chen Z, Chua CC, Ma Y-S, Youngberg GA, Hamdy R, et al. Melatonin as an effective protector against doxorubicin-induced cardiotoxicity. *American journal of physiology. Heart and circulatory physiology* 2002; **283**:H254-H263.

74. Polin L, Valeriote F, White K, Panchapor C, Pugh S, Knight J, et al. Treatment of human prostate tumors PC-3 and TSU-PR1 with standard and investigational agents in SCID mice. *Investigational New Drugs* 1997; **15**:99-108.
75. Kim SJ, Uehara H, Karashima T, McCarty M, Shih N, Fidler IJ. Expression of Interleukin-8 Correlates with Angiogenesis, Tumorigenicity, and Metastasis of Human Prostate Cancer Cells Implanted Orthotopically in Nude Mice. *Neoplasia* 2001; **3**:33.
76. Kurbacher CM, Wagner U, Kolster B, Andreotti PE, Krebs D, Bruckner HW. Ascorbic acid (vitamin C) improves the antineoplastic activity of doxorubicin, cisplatin, and paclitaxel in human breast carcinoma cells in vitro. *Cancer Letters* 1996; **103**:183-189.
77. John A., Hadfield SD, Nicholas Hirst and Alan T. McGown. Tubulin and microtubules as targets for anticancer drugs. *Progress in Cell Cycle Research* 2003; **5**:309-325.
78. Patrick L. Selenium Biochemistry and Cancer: A Review of the Literature. *Alternative Medicine Review* 2004; **9**:239-258.

Abbreviations

BT-474	human breast carcinoma cell
CM-H ₂ DCFDA	5-(and-6)-chloromethyl-2',7'-dichlorodihydrofluorescein diacetate acetyl ester
DCF	2',7'-dichlorofluorescein
DMSO	dimethyl sulfoxide
DOX	doxorubicin
FBS	fetal bovine serum
H ₂ O ₂	hydrogen peroxide
MTT	3-(4,5-Dimethylthiazol-2-yl)-2,5-diphenyltetrazolium bromide
NADPH	reduced nicotinamide adenine dinucleotide phosphate
O ₂ ^{•-}	superoxide anion
OH [•]	hydroxyl radical
ONOO ⁻	peroxynitrite anion
PAESe	phenyl-2-aminoethyl selenide
PC-3	androgen-independent human prostate cancer epithelial cells
ROO [•]	peroxyl radical
ROS	reactive oxygen species
SEM	standard error of the mean
SRB	sulforhodamine B
TBHP	<i>tert</i> -butylhydroperoxide

TCA	trichloroacetic acid
TRIS	tris(hydroxymethyl)aminomethane

CHAPTER 3

QUANTIFICATION OF LIPOSOMAL PHENYLAMINOETHYL SELENIDES BY

HIGH PERFORMANCE LIQUID CHROMATOGRAPHY-TANDEM MASS

SPECTROMETRY AND PHARMACOKINETIC IN RATS

Jeong Yeon Kang, Ibrahim Aljuffali, Charlie D. Oldham, Sheldon W. May, Robert D. Arnold. To be submitted to *Journal of Chromatography B*

Abstract

Novel selenium-based therapeutic agent, phenyl-2-aminoethyl selenide (PAESe), has a protective effect against anthracycline-induced cardiotoxicity as well as antihypertensive activity mediated by its scavenging effect of reactive oxygen species. A simple and selective analytical method was developed and validated using high-performance liquid chromatography - tandem mass spectrometry (HPLC-MS/MS) with electrospray ionization in multiple reaction monitoring mode for the quantification of PAESe in rat plasma. A lower limit of quantification was 50 nM. The accuracy and precision of the response were within the acceptable range ($\pm 15\%$) of the theoretical concentration for intra-day and inter-day assay. This assay was used to determine the pharmacokinetics of free PAESe and a newly developed PAESe liposome (SSL-PAESe) formulation. The circulation half-life and exposure (area under the drug concentration time profile, AUC) of PAESe were increased significantly ($p < 0.05$) in animals dosed with SSL-PAESe (101 hr) compared to free PAESe (8.78 min). This correlated with decreases in the rate of elimination and total systemic clearance after administration of SSL-PAESe relative to free PAESe ($p < 0.05$). These results suggest that PAESe can be encapsulated stably in SSL and used to control the PAESe exposure compared to free drug administration. In conclusion, we developed a sensitive and selective HPLC-MS/MS assay and used this assay to determine the pharmacokinetics of free- and SSL-PAESe. These data suggest that encapsulation of PAESe in SSL provides a broaden potential of PAESe as a clinical therapeutic agent. Furthermore, this assay will serve as basis for examining tissue/tumor

distribution to optimizing dosing schedules and gain mechanistic insights into PAESE cardioprotective and antitumor activity.

1. Introduction

Doxorubicin (DOX) is a potent anticancer agent used to treat a variety of cancers including acute leukemia, non-Hodgkin's lymphomas, breast, ovarian and lung cancer [1]. However, the clinical usage of DOX is limited by myocardial damage induced by generation of reactive free radicals such as superoxide anion, hydroxyl radical, and peroxynitrite [2]. A variety of antioxidants and scavenging agents have been evaluated with the goal to reduce DOX-induced oxidative damage in order to alleviate DOX-mediated cardiotoxicity. Currently two agents, *i.e.*, Dexrazoxane (Zinecard[®]) and Amifostine (Ethyl[®]) have been approved by FDA as chemoprotectants. However, they have been shown to reduce the activity of the primary chemotherapeutic agent or have off-target toxicities that have generally limited their usefulness [3, 4].

Phenyl-2-aminoethyl selenide (PAESE, Fig 3-1B) was shown to exert a potent antioxidant activity by reacting with metabolic oxidants such as peroxide, peroxynitrite anion, and hydroperoxides using redox recycling [5-8]. Previously, we demonstrated that PAESE decreased doxorubicin-induced free radical generation and cardiotoxicity using *in vitro* cell culture and *in vivo* mouse models (**Chapter 2**) [9]. PAESE had limited to little to no effect on growth inhibitory or cytotoxic *in vitro* antitumor activity of DOX on prostate cancer cells, *in vitro*. PAESE also decreased the formation of intracellular reactive oxygen species from DOX. However, we observed PAESE has the antitumor activity in a mouse xenograft model of human prostate cancer (PC-3) [9]. We suggested

that PAESe reduced cardiotoxicity when used in combination with DOX and unexpectedly exhibited *in vivo* antitumor activity, however the mechanism is not clear.

Here, a sensitive and selective high-performance liquid chromatography – tandem mass spectrometry (HPLC-MS/MS) method was developed and applied to determine the pharmacokinetic (PK) properties of PAESe in rat plasma. High-performance liquid chromatography (HPLC) has been commonly used with ultraviolet (UV) and fluorescence detector (FLD) methods for quantifying drugs and metabolites in biological samples. However, it has been reported that analytical method based on HPLC-UV or FLD were not sensitive enough to detect low level of analytes in the matrix [10]. Mass spectrometry (MS) is currently regarded as a rapid and effective method for the analysis of drugs in complex biological matrix. It has excellent sensitivity and specificity, especially tandem mass spectrometry (MS/MS), since the analyte is ionized by their inherent mass and charge [11, 12]. In addition, it is known that MS/MS detection can reduce interferences effectively from endogenous components as well as can simplify sample extraction [13, 14]. This sensitive analytical assay is also preferred for *in vivo* PK studies in animal models because the limited amount of plasma sample is required.

In this study, we developed long circulating PAESe liposome (SSL-PAESe) and investigated the effect of encapsulation of PAESe to alter its disposition (*i.e.* increase circulation half-life and increase systemic drug exposure, AUC) based on our previous study that showed *in vivo* antitumor activity of PAESe. Encapsulation in SSL is well known to change the PK properties of compounds radically by pegylation; pegylated liposomal doxorubicin has been approved as clinical products in the U.S. (Doxil[®]) and Canada (Caelyx[®]) in virtue of the enhanced anticancer activity and diminished

cardiotoxicity [15-17].

The objective of the study was to develop a nanoparticulate drug carrier and evaluate PK properties of free and encapsulated PAESe. In order to achieve this objective, we developed and validated a highly selective and robust HPLC-MS/MS assay with electrospray ionization (ESI) in multiple reaction monitoring (MRM) mode.

2. Experiments

2.1. Materials and reagents

Analytical grade methanol (MeOH), acetonitrile (ACN), formic acid, chloroform and sucrose were purchased from Thermo Fisher Scientific Inc. (Rockford, IL). Water was obtained from a Milli-Q system (Millipore Corp., Billerica, MA). 1,2-distearoyl-sn-glycero-3-phosphatidylcholine (DSPC) and 1,2-distearoyl-sn-glycero-3-phosphoethanolamine-N-[poly(ethyleneglycol) 2000] (DSPE-PEG) were obtained from Avanti Polar Lipids Inc. (Alabaster, AL). Cholesterol was obtained from Sigma-Aldrich (St. Louis, MO) and recrystallized from MeOH before use. Heparin sodium for injection USP (5,000 units/mL) was obtained from Elkin-Sinn, Inc. (Cherry Hill, NJ). All other chemicals and solvents were analytical grade and purchased from Sigma-Aldrich (St. Louis, MO).

2.2. HPLC-MS/MS

The mobile phase was MeOH:0.2 % formic acid (50:50, v/v), and was vacuum filtered using a 0.45 μm nylon filter (Millipore Corp., Billerica, MA) prior to use. FPAESe (4-fluoro-phenyl-2-aminoethyl selenide) was used as internal standard (I.S.).

HPLC-MS/MS separation was performed on an HPLC Agilent 1100 Series, which consists of a degasser, a binary pump, an auto-sampler, and a thermostated column compartment, coupled with Agilent XCT Ultra Plus ion-trap mass spectrometer with an ESI interface (Agilent Technologies, Inc., Santa Clara, CA). The separation was performed on a Zorbax Eclipse Plus C18 column (100 × 4.6 mm, 3.5 μm, Agilent Technologies) equipped with a Phenomenex Security Guard C18 guard column (4.0 x 3.0 mm) and the column temperature was maintained at 20 °C. An additional in-line filter (Mac-Mod Analytical, Inc., Chadds Ford, PA) was connected before the guard column. The temperature of auto-sampler was set at 20 °C and the injection volume was 20 μL. The flow rate of mobile phase was 0.25 mL/min and the mobile phase was isocratic. Total analysis time was 5 minutes. The analytes were introduced from column to the MS through an ESI source. Nitrogen was used as a desolvation gas, and helium was introduced into the trap as the collision gas. Desolvation gas was set at 350 °C with a flow rate of 9.0 L/min and nebulizer pressure of 40.0 psi. Capillary, exit and skimmer voltages for MS were optimized to acquire highest sensitivity of compounds. The HPLC–MS/MS system was controlled, and data analysis was performed using software provided by manufacture (Agilent, ChemStation, Santa Clara, CA).

2.3. Preparation of Calibration Standard Solutions and Quality Control Samples

PAESe and the FPAESe (I.S.) were weighted using a Cahn C-33 microbalance (Orion research, Inc., Beverly, MA). Individually weighed compounds were transferred to volumetric flasks and dissolved in a mobile phase to prepare stock solutions of 100 μM. The stock solution of PAESe was then diluted with a mobile phase to give final

concentrations of 10, 8, 5, 2, 1, 0.8, 0.5, 0.25, and 0.1 μM in pooled blank rat plasma for calibration standards. The FPAESe stock solution was used to prepare the I.S. in mobile phase at a final concentration of 400 nM. Quality control (QC) samples were prepared by dilution of a PAESe stock solution into MeOH at 0.3 μM (low), 1.5 μM (medium) and 3 μM (high). All standard and QC samples were prepared freshly for each analysis.

2.4. Sample Preparation

A 50 μL plasma sample thawed to equilibrate in room temperature was transferred into a 1.5 mL polypropylene centrifuge tube. A 200 μL ACN was added to the plasma to achieve a final plasma/organic solvent (v/v) ratio of 20%, and vortexed to precipitate sample plasma proteins. A 10 μL volume of freshly prepared I.S. solution was spiked into the plasma to achieve a final concentration of 400 nM FPAESe. The mixture was cooled in an ice water bath for 1 hr, then centrifuged at $10,000 \times g$ for 10 min at 4°C . The deproteinized supernatant was transferred to a new 1.5 mL polypropylene centrifuge tube and dried with a stream of filtered nitrogen. Dried residues were reconstituted with 100 μL of mobile phase and vortex-mixed. Reconstituted samples were transferred into low volume glass vial inserts for HPLC-MS/MS analysis.

2.5. Method Validation

2.5.1. Specificity and selectivity

The specificity and selectivity of method was determined based on the retention time of each chromatogram and MRM response of drug-free plasma and plasma spiked

with PAESe and I.S. The response of blank plasma was also monitored in the selected MRM mode for PAESe and I.S. to test the presence of endogenous substance that might interfere with the signal for PAESe or I.S. Carryover contamination caused by “cross-talk” was monitored between the scans for mass transition of PAESe and the I.S. The response for the plasma sample spiked with PAESe was monitored while operating MRM condition for the I.S. and vice versa.

2.5.2. Lower limit of quantification (LLOQ) and linearity

Lower limit of quantification (LLOQ) for PAESe was determined by analyzing blank rat plasma spiked with PAESe standard solution. LLOQ was determined based on the following criteria: *i*) an accuracy and a coefficient of variation (CV) of the response were within $\pm 20\%$ of the theoretical concentration and *ii*) the response was at least 5 times higher than the baseline noise ($S/N > 5$). Calibration standard curves for PAESe were generated over the range from 0.1 to 10 μM by plotting the ratio of the peak area of analytes to the I.S. versus the theoretical concentration.

2.5.3. Accuracy and precision

The accuracy and precision of method were determined using triplicates of three different QC concentrations. Accuracy is defined as the average percent error of actual concentration to the theoretical concentration of each QC sample, and precision is expressed by the percent CV within a single concentration. Intra-day accuracy and precision were evaluated by analyzing triplicate QC samples prepared at three different concentrations independently within 24 hr. Inter-day accuracy and precision were

determined by analyzing triplicate QC samples prepared at three different concentrations each day over 3 or more separate days within a 7 day period.

2.5.4. Stability

To investigate stability, PAESe solution at two different concentrations (0.5, 1.0 μM) were selected and stored under various time- and temperature-dependent conditions. The samples in triplicates were kept at room temperature or $-20^{\circ}\text{C}/-80^{\circ}\text{C}$ for room temperature stability or freezer stability, respectively for 4 weeks. For freeze-thaw stability, the samples stored at -20°C were thawed at room temperature for 24 hr, and were then refrozen at -20°C in triplicate for 3 cycles. Samples were then analyzed as described above. Stability was determined by comparing the calculated value of each sample with theoretical concentration of freshly prepared samples; a percent change and CV greater than $\pm 10\%$ was considered as a significant degradation.

2.6. Preparation of PAESe liposomes

Sterically stabilized PAESe liposomes (SSL-PAESe) were formulated by thin-film hydration method and remote loading procedure that is based on the induction of the uptake of charged drugs into preformed liposomes using combined pH and electrochemical gradients [15, 16, 18]. Briefly, SSL-PAESe was prepared with DSPC:Cholesterol:DSPE-PEG (9:5:1 mole %) in 250 mM ammonium sulfate (pH 5.0), followed by passing through double stacked $0.08\ \mu\text{m}$ polycarbonate filters (GE water & Process Tech., Boulder, CO) in a thermobarrel high-pressure extruder (Northern Lipids, Vancouver, British Columbia, Canada) six to eight times at $60\ ^{\circ}\text{C}$. Extraliposomal

ammonium sulfate was eliminated by dialysis overnight in isotonic, 10% (w/v) sucrose solution at 4 °C. PAESE solution in 10% (w/v) sucrose was warmed at 65°C, and was then mixed with the preformed liposomes for 1 hr at 65 °C with occasional vortexing. Extraliposomal drugs were separated by membrane dialysis and the SSL-PAESE was filtered through 0.2 µm syringe filters (VWR International LLC, Radnor, PA) for sterilization. SSL-PAESE formulations were stored at 4 °C protected from light until use.

Encapsulation efficiency was determined by comparing the drug:lipid ratio after drug loading to the ratio before drug loading based on the concentration of PAESE and phospholipid. The concentration of PAESE was determined by absorbance at 260 nm using a spectrophotometer (Synergy HT Multi-Mode Microplate Reader, BioTek Instruments Inc., Winooski, VT). The phospholipid concentration was measured by an inorganic phosphate assay following acid hydrolysis [19]. Mean particle diameter of SSL-PAESE was determined using a submicron particle sizer (Nicomp model 380 dynamic light scattering, Santa Barbara, CA). Data were evaluated by volume-weighted analysis. A mean diameter of 80-110 nM was measured from final formulation. The final concentration of PAESE was typically 1.5 mg/mL with > 80 % encapsulation efficiency at a drug:lipid ratio of 0.2:1.0 (mol:mol).

2.7. Plasma pharmacokinetics

Male Fischer 344 rats (160 – 200 g, Harlan Sprague–Dawley, Indianapolis, IN) were anesthetized with 90 mg/kg ketamine and 9 mg/kg xylazine by intramuscular injection. The jugular vein was cannulated with polyurethane tubing (Micro-Renathane, Braintree Scientific, INC., Braintree, MA), and was positioned subcutaneously and the

tubing exteriorized through a scapular incision. The cannula was flushed with 50-100 mL heparinized (50 units/mL) saline to prevent the clotting of blood. Three days after surgery, free PAESE was prepared by dissolving in normal saline (0.90% w/v) and sterilized by passing through 0.2 μ m syringe filter, and SSL-PAESE was prepared as described above. Free PAESE or SSL-PAESE was quantified immediately prior to administration, as describe above. Drug was administered intravenously (*i.v.*) to the rats *via* a tail vein injection at a dose of 10 or 5 mg/kg, PAESE or SSL-PAESE. Blood samples (100-200 μ L) were collected by jugular cannula at -10, 2, 5, 10, 15, 20, 30, 45 min, 1, 2, 4 hr for free PAESE group and -10, 2, 5, 15, 30, 45, 1, 2, 4, 6, 8, 12, 24, 48, 120 hr for SSL-PAESE group after the injection by a staggered sampling to minimize excessive blood loss. The cannula was flushed with 100 mL heparinized (5 units/mL) saline after sampling. Blood samples were transferred into heparinized 1.5 mL polypropylene centrifuge tubes and cooled on ice immediately. Plasma was separated from blood by centrifugation at 10,000 \times g for 10 min at 4 $^{\circ}$ C followed by snap-frozen in liquid nitrogen, and stored at -80 $^{\circ}$ C until analysis. Animals were maintained in a light- and temperature-controlled room and were provided a standard rat chow diet and water *ad libitum*. All procedures regarding animal handling, care, and surgery followed a protocol approved by the Institutional Animal Care and Use Committee (IACUC) of the University of Georgia according to the US Public Health Service (PHS) Policy on Human Care and Use of Laboratory Animals, updated 2002.

2.8. Pharmacokinetic analysis

2.8.1. Noncompartmental analysis

A noncompartmental analysis was performed to generate initial estimates of PK parameters including terminal elimination rate (k), half-life ($t_{1/2}$), apparent volume of distribution (V), total systemic clearance (CL), area under the plasma concentration-time curve (AUC), and maximum plasma concentration (C_{\max}) using the nonlinear regression analysis program (WinNonlin version 4.1, Pharsight Corp., Mountain View, CA). Parameter estimates from data for animals treated with each formulation were compared using student t-test. Results were considered significantly different at $p < 0.05$.

2.8.2. Pharmacokinetic modeling

PK model was developed to predict the parameters and their precision after SSL-PAESE administration. Both naïve pooled data and naïve averaged data approaches were used to plot data. The goodness-of-fit was assessed by analyzing residuals, accuracy, precision, confidence intervals, correlation between parameters, condition number, and objective criteria (Akaike information criteria, Schwarz criteria, sum of squares, and estimator criterion value) to estimate the parameters as well as select the best-fit model using WinNonlin [20].

3. Results

3.1. HPLC-MS/MS Conditions

The composition of the mobile phase was optimized with an isocratic mixture of MeOH:0.2 % formic acid (50:50, v/v) to maximize sensitivity and minimize analytical time. The signal for PAESe and I.S. was monitored in positive mode and ESI mode due to its strong intensity and high mass response. FPAESe (Fig 3-1A) was selected as the I.S. due to its structural similarity to PAESe. Parameters for fragmentation were optimized by direct infusion of a standard solution in mobile phase into the ionization source coupled with MS to obtain the maximum signal intensity of the product ions. For both PAESe and I.S., the optimal capillary voltage and capillary exit voltage were 4000 V and 100 V, respectively, with a skimmer voltage of 40 V.

3.2. Validation of HPLC–MS/MS Method

3.2.1. *Specificity and selectivity*

Quantification was performed in MRM mode to monitor specific ion transitions for selective detection of the analytes of interest. Fig 3-2 and 3-3 showed the representative total ion chromatogram and product ion chromatogram of plasma sample spiked with PAESe (300 ng/mL) and FPAESe (300 ng/mL) to demonstrate the specificity and selectivity of the proposed method. Unique precursor/product ion-pairs were identified by strong intensity at m/z 184.0 \rightarrow 154.7 for PAESe and m/z 204.0 \rightarrow 174.7 for I.S. Since $[M+H]^+$ of PAESe and I.S. had the most intense signal at m/z 184.0 and

m/z 204.0 respectively, they were selected as the precursor ion. The product ion peaks for PAESe and I.S. were observed at m/z 154.7 and 174.7, respectively, as shown in Fig. 3-3. The retention time was 3.6 min for both PAESe and FPAESe; total chromatographic run time was 5.0 min. Neither endogenous interference nor cross-talk between the responses were found around the retention times of PAESe and I.S. in the blank plasma. Table 3-1 summarizes the fragmentation parameters for PAESe and FPAESe.

3.2.2. Lower limit of quantitation (LLOQ) and linearity

LLOQ is defined as the lowest concentration analyzed with acceptable signal to noise ratio (>5), accuracy ($\pm 20\%$ nominal value) and precision ($<\pm 20\%$). LLOQ of 50 nM was determined experimentally for PAESe with 80.8% of inter-day accuracy, and 18.2% of precision respectively, which was sufficient for the purpose of the PK study. Linearity was determined over the concentration range of 50 nM to 10 μM . Calibration curves were generated by plotting the corresponding peak area to the nine standard concentrations at 0.05, 0.1, 0.25, 0.5, 0.8, 1, 2, 5, 8, 10 μM using a weighing scheme of the inverse of the variance ($1/x^2$). The response showed a good linearity over the concentration range with correlation coefficient (r^2) of 0.995 or better.

3.2.3. Accuracy and precision

Accuracy and precision of the method were determined at three QC standard concentrations at 0.3, 1.5, and 3.0 μM in triplicates for validation. Concentrations of QC were calculated from each calibration standard curve. The accuracy is calculated by comparing the average of calculated concentrations to their theoretical concentrations (%)

of nominal) and the precision by the percent CV. Intra- and inter-day accuracy and precision of the method were acceptable with $\pm 15\%$ of their theoretical concentration with weighing scheme of the inverse of the variance ($1/x^2$) (Table 3-2). The accuracy for intra-day and inter-day was determined to be within the range of 1.0–6.7% and 2.0–4.1% of their theoretical concentrations, respectively. The precision was found to be less than 14% CV for all QC samples in both intra-day and inter-day assay.

3.2.4. Stability

Stability of PAESe was tested under various time- and temperature-dependent storage conditions. No significant degradation was found in all samples in given conditions with deviation within $\pm 10\%$ of the theoretical concentrations in 4 weeks storage (Table 3-3). These results demonstrated that PAESe were considered stable at room temperature as well as $-20^\circ\text{C}/-80^\circ\text{C}$ with three cycles of freeze–thaw process during at least 4 weeks.

3.3. Plasma pharmacokinetics

The validated analytical HPLC-MS/MS method was applied to determine the PK properties of PAESe in free and encapsulated form after *i.v.* administration to the rat. PAESe was administered to rats at a dose of 10 mg/kg for free PAESe and 5 mg/kg for SSL-PAESe, and blood was collected from the jugular cannula over the next 4 hr for free PAESe and 120 hr for SSL-PAESe due to PK differences between the two formulations.

The plasma drug concentration–time profile after a single dose of free PAESe and SSL-PAESe was shown in Fig 3-4. Data were presented as means \pm standard deviation of

two independent studies (n = 4 for free PAESe; n=6 for SSL-PAESe). The LLOQ of the method (50 nM) was low enough to determine PAESe up to 120 hr after SSL-PAESe administration. A two-compartment PK model was chosen to provide the best-fit of the data in Fig 3-4 using WinNonlin. The representative PK parameters estimated by two-compartment model are listed in Table 3-4.

Results showed that free PAESe was eliminated rapidly after *i.v.* administration with alpha distribution half-life ($\alpha_{1/2}$) of 1.96 min and beta elimination half-life ($\beta_{1/2}$) of 8.78 min. A large apparent volume of distribution for free PAESe group (3.16 L/kg) indicates that PAESe is extensively distributed to tissues, and may be released over a prolonged time [15, 21, 22]. However, the PK properties of PAESe were dramatically changed when encapsulating PAESe in SSL compared with free PAESe. The circulation half-life was significantly increased in the animals dosed with SSL-PAESe (101 hr) compared to free drugs (8.78 min) ($p < 0.05$). There were also significant decrease in total systemic CL (-99.3 %), and increase in AUC (6,787 %) in animals receiving SSL-PAESe compared to free PAESe ($p < 0.05$). The peak concentration (C_{max}) was also increased after SSL-PAESe administration.

4. Discussion

PAESe exhibits antihypertensive activity mediated by a scavenging effect in regard to dopamine- β -monooxygenase dependent ascorbate depletion [7, 8, 23]. Recently, we have demonstrated that PAESe exhibits a protective effect against anthracycline-induced cardiotoxicity *in vitro* cell culture as well as *in vivo* antitumor activity (**Chapter 2**) [9]. Here, we developed and validated a HPLC–MS/MS method for the quantification

of PAESe in rat plasma for the purpose of conducting PK studies and to aid in developing a greater understanding of its antitumor and chemoprotective effects. A tandem mass spectrometer with MRM condition was used to improve sensitivity and specificity in assay by selecting compound-specific ion-pairs based on their inherent mass and charge.

The ESI-MS parameters were optimized based on the signal response of analytes after direct infusion of PAESe solution in mobile phase or blank plasma into the ionization source. Parameters include capillary voltage, skimmer voltage, capillary exit voltage, octopole radio frequency, octopole direct current, trap drive and lens voltages. These parameters have an important role in sensitivity by affecting ion formation and migration [24]. Optimization of the parameters was performed in a certain sequence in accordance with the recommendation of manufacturer. The optimal value was fixed before the following parameter was optimized.

The interference caused by co-eluting compounds also had a significant impact on the sensitivity by affecting ionization efficiency. Interference peaks by co-eluting compounds or endogenous substances in plasma were not examined in this method. Contamination by carryover of analytes (cross-talk) was also monitored since it causes a fallacious quantification of analyte of interest that is analyzed by HPLC-ESI-MS [25]. Cross-talk is usually generated by incomplete removal of ions with similar or identical mass in the other precursor-product ion channel in which the product ions of the first mass transition scan are not cleared completely before the second mass transition begins, which remains the artifacts in the whole mass transition. No cross-talk was identified with this method.

The ratio of organic solvent is one of the important factors for protein precipitation for improving sensitivity in sample preparation [16]. Protein precipitation with 100% ACN shortened the processing time and increased the method sensitivity. However, this may be associated with PAESe poor solubility in polar aprotic solvents like ACN vs. polar protic solvents like MeOH. In addition, ACN was applied to samples over 30 seconds while vortex mixing because some of the analyte can be trapped in the precipitates from rapid precipitation process by producing a lump of the precipitate, resulting in the decreased sensitivity and increased variability in the sample preparation.

This HPLC-MS/MS analytical method was used to quantify PAESe in small volume plasma samples (30-100 μ L) of animals administered free- or PAESe encapsulated in long-circulating type liposomes. Previous research demonstrated that α -methylated derivative of PAESe (MePAESe) administered by *i.v.* to rats was cleared rapidly from the blood with $\alpha_{t1/2}$ of 20 sec and $\beta_{t1/2}$ of 63 min [8], which can limit the exposure and therapeutic efficacy of compounds. Thus, we developed a long-circulating type liposome and encapsulated PAESe with the goal of increasing its systemic exposure.

Nanoparticulate drug carriers are known to alter drug disposition such as circulation half-life, tissue/tumor distribution, and rate/extent of drug release, which are responsible for the increased therapeutic efficacy and reduced toxicity in animal models [15, 18, 26, 27]. Sterically stabilized liposome (SSL) is one type of nanoparticulate drug carrier that has long-circulating properties through a surface coating with hydrophilic polymer like polyethylene glycol (PEG) that reduces interaction with plasma components by steric hindrance effect [28]. SSL formulation prevents not only opsonization and rapid clearance of compound by reticular-endothelial system but also decreases the rate of

drug-carrier distribution to primary organs of clearance (*i.e.*, liver, lung, spleen), leading to their reduced elimination [15, 29]. Encapsulation of drug into SSL can promote the accumulation of drug in tissues by increasing circulation time as well as by reducing drug elimination rate and clearance of drug [30, 31]. The more drugs can reach the desirable tissue in SSL because the most of the drug can be remained inside the SSL in the body and released slowly from the liposomes during an extended duration of circulation [15]. Moreover, biodistribution pattern can be controlled to prevent drug accumulation in tissue that are sensitive and undesirable to be delivered by encapsulating in SSL [29]. Even though some pharmacological effects such as cardioprotective effect against anthracycline or antihypertensive effect have been already identified in free form of PAESe, it will be necessary to determine the effect of encapsulated form that can be manifested by increasing availability through the enhanced exposure of compound.

The effect of drug:lipid ratio on the encapsulation efficiency was evaluated by determining the encapsulation efficiency of various formulations with using serial concentrations of PAESe. Encapsulation efficiency of SSL-PAESe was decreased with increasing drug:lipid ratio (Fig. 3-5) since the excess of drug solution might cause the instability of liposome formulation and pH gradient in mixture of liposome and drug solution. In order to administer the corresponding amount of PAESe in encapsulated form with free form to animal, the drug:lipid ratio of 2:1 was used even though the ratio of 0.2:1 has maximal encapsulation efficiency (>80%).

The PK properties of free PAESe and SSL-PAESe were determined to evaluate the effect of liposomal formulation on disposition of PAESe. The analytical method developed in this study was linear over the concentration range for this *in vivo* PK study.

There were significant differences in the observed plasma PK profile and parameters between free- and SSL-PAESe administration groups (Fig. 3-4, Table 3-4). Whereas free PAESe was cleared rapidly, PAESe was observed in the plasma for a prolonged period when administered with SSL-PAESe in animal. The rate of elimination and clearance of PAESe were also decreased significantly in SSL-PAESe group. PAESe was detected in rat plasma with 42 ng/mL at 120 hr after administration of SSL-PAESe, while PAESe was not able to be detected at 1 hr after administration of free PAESe. Although the free fraction of PAESe was not determined explicitly, based on rapid clearance of free PAESe, it is supportive that PAESe was stably entrapped within the SSL. This is similar to other drugs that are rapidly cleared when compared to those remote loaded into SSL formulations [15, 26]. This result is even more striking because the noticeable PK differences were observed between two formulations although the dose of SSL-PAESe (5 mg/kg) was the half of dose of free PAESe (10 mg/kg). SSL-PAESe was formulated for the dose of 5 mg/kg since it corresponds to the maximal allowed amount for injection to rat. These results demonstrate that PAESe encapsulation in SSL increases the exposure of PAESe with the decreased amount of PAESe.

These characteristics of SSL are associated with not only the increased efficacy but also the reduced toxicity of encapsulated compound [32]. It was shown that cardiotoxicity of doxorubicin could be reduced when administered in SSL formulation because doxorubicin was less converted to doxorubicinol, which is a metabolite known as one of the major causes of cardiomyopathy [33, 34]. Indeed, a previous study has reported that selenium-containing metabolites were identified in brain tissue after administration of MePAESe [8]. Encapsulation of PAESe into SSL may control

penetration of PAESe into the central nervous system by decrease in production of its metabolites, which prevent brain accumulation and undesirable side effects like neurotoxicity. Nevertheless, it is necessary to identify the efficacy of encapsulated PAESe in SSL to further evaluate its potential as a chemoprotectant and antitumor agent.

In conclusion, an HPLC-MS/MS analytical method with ESI was developed and validated for the quantification of PAESe in rat plasma. Small volume plasma samples (50 μ L) and simple preparation and extraction were used to quantify, LLOQ of 50 nM, PAESe over desired concentration and time frame. Encapsulated PAESe into SSL increased the exposure of PAESe – thus circulation half-life and alter *in vivo* biodisposition. The reliable and effective method developed in this study was successfully applied to determine PK properties of PAESe in plasma after administration of free or long-circulating liposomal formulation to rats. Clearly, PK results showed the circulation half-life of PAESe was significantly increased in encapsulated PAESe relative to free PAESe, which suggest encapsulation in SSL can extend a potential of PAESe as a pharmacological agent by its enhanced exposure and availability by long-circulating property of SSL. This analytical method could be used to advance development of formulation and establish the mechanism behind the antitumor effect of PAESe.

Table 3-1. MRM parameters for PAESe and FPAESe (I.S.)

	PAESe	FPAESe*
Precursor ion (<i>m/z</i>)	184.0	204.0
Product ion (<i>m/z</i>)	154.7	174.7
Width (<i>m/z</i>)	2.0	2.0
Cutoff mass	50	55
Retention Time (min)	3.6	3.6

*Internal standard

Table 3-2. Intra-day and Inter-day accuracy and precision for PAESe

QC control (μM)	Intra-day assay		Inter-day assay	
	Accuracy (%)	Precision (CV%)	Accuracy (%)	Precision (CV%)
0.3	101	14.0	102	14.9
1.5	103	8.5	95.9	14.4
3.0	93.3	10.4	95.9	9.8

Table 3-3. Stability of PAESe for 4 weeks

Theoretical conc. (μM)	Measured conc. (μM) (CV%)			
	Room temp.	Freeze-thaw	Freezer (-20°C)	Freezer (-80°C)
0.5	0.492 (13.4)	0.498 (10.7)	0.510 (4.64)	0.552 (N/A)
1.0	1.02 (6.83)	1.07 (3.43)	1.07 (6.08)	1.109 (N/A)

Table 3-4. Model-predicted pharmacokinetic parameters for free PAESE and SSL-PAESE

Variables	Free PAESE Mean (CV %)	SSL-PAESE Mean (CV %)
Dose (mg/kg)	10	5
C _{max} (µg/mL)	3.16 (38.2)	9.97 (40.8)
α _{t1/2} (hr)	0.0326 (31.0)	0.0201 (19.5)
β _{t1/2} (hr)	0.146 (13.3)	101 (30.2)
AUC (µg • hr/mL)	0.196 (17.8)	13.5 (26.3)
V (L/kg)	3.16 (38.2)	0.502 (40.8)
CL (L/hr/kg)	51.2 (17.8)	0.371 (26.3)

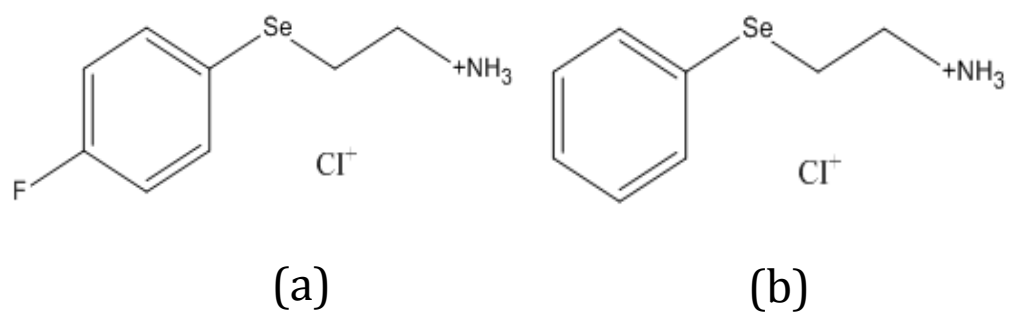


Figure 3-1. Chemical structures of phenylaminoalkyl selenide (a) 4-fluoro-phenyl-2-aminoethyl selenide (FPAESE), the internal standard (I.S.) and (b) phenyl-2-aminoethyl selenide (PAESE).

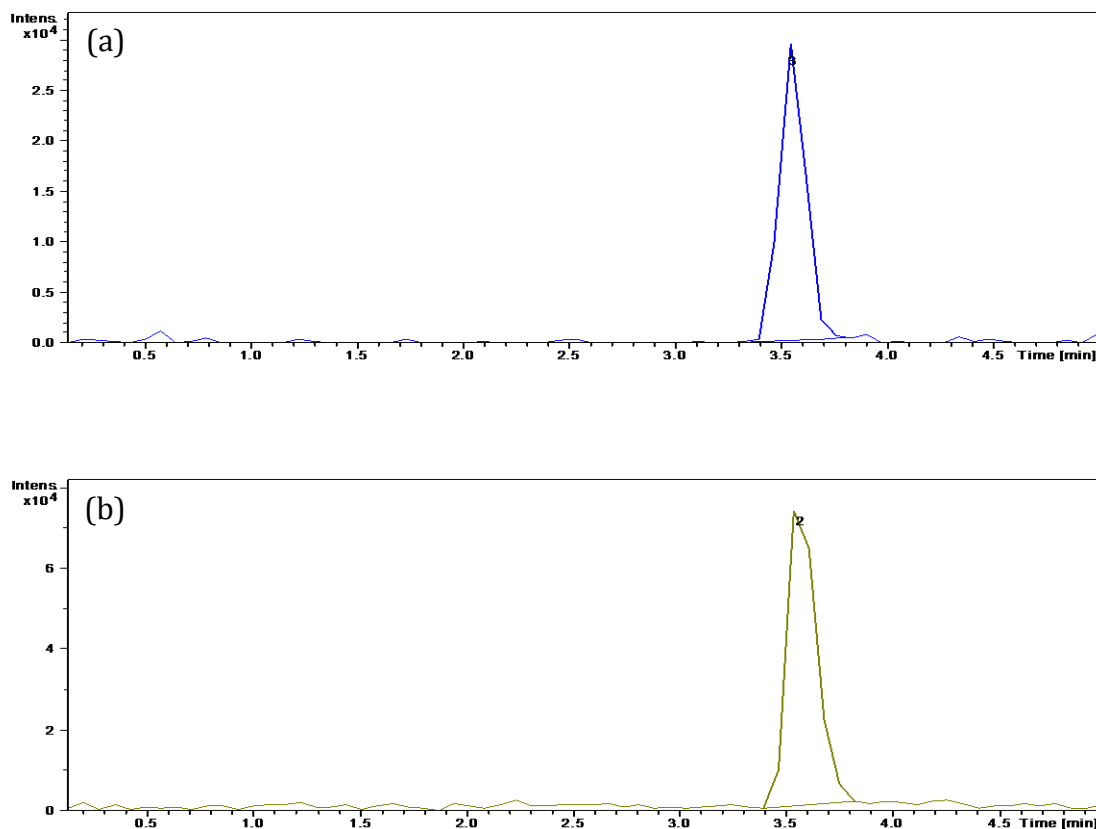


Figure 3-2. Total ion chromatogram (a) PAESe; (b) FPAESe (I.S.) Blank rat plasma spiked with PAESe or FPAESe of 300 ng/mL was deproteinated with ACN to remove plasma protein. The mixture was cooled on ice for 1 hr, and then was centrifuged at $10,000 \times g$ for 10 min at 4°C. The supernatant transferred into new tubes was evaporated with a stream of dry nitrogen, followed by reconstitution with mobile phase to inject into the HPLC-MS/MS system for analysis. The retention time was 3.6 min for both PAESe and FPAESe.

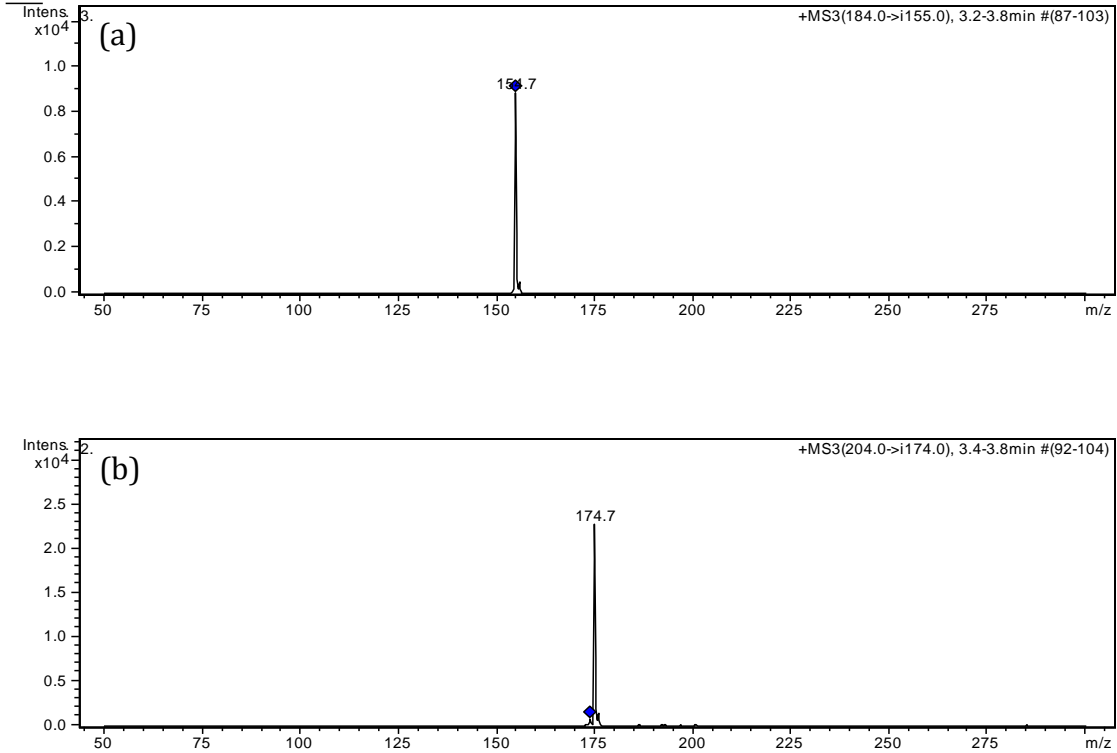


Figure 3-3. Product ion chromatogram (a) PAESe; (b) FPAESe (I.S.) Blank rat plasma spiked with PAESe or FPAESe of 300 ng/mL was prepared as described in Fig. 3-2. MRM mode was applied to monitor specific ion transitions of PAESe and I.S. The maximum signal was detected as the precursor ions at m/z 184.0 and m/z 204.0 for $[M+H]^+$ of PAESe and I.S., respectively. The most intense signal was determined at m/z 184.0 \rightarrow 154.7 for PAESe and m/z 204.0 \rightarrow 174.7 for I.S. as precursor/product ion-pairs.

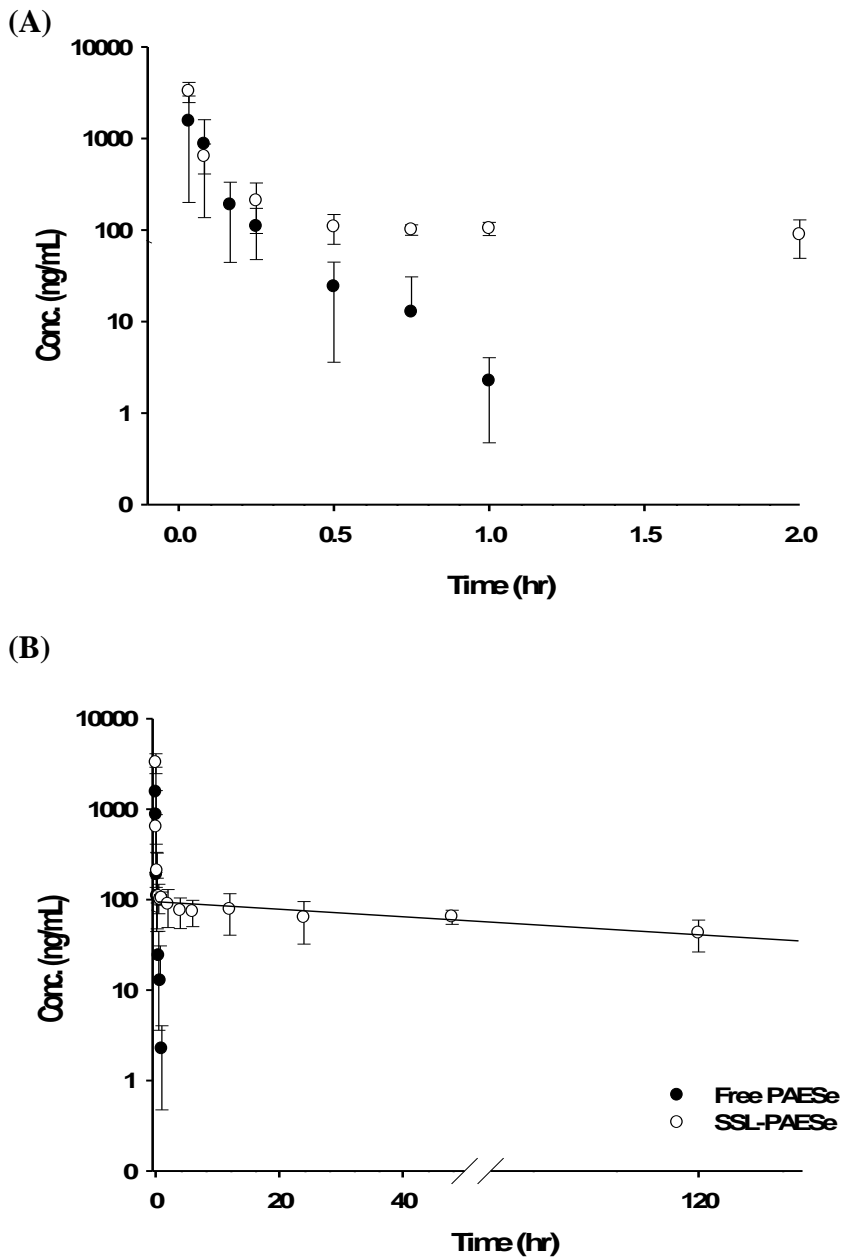


Figure 3-4. Mean plasma concentration-time profile after *i.v.* administration of free PAESe (10 mg/kg) and SSL-PAESe (5 mg/kg) Free PAESe (10 mg/kg) or SSL-PAESe (5 mg/kg) was intravenously administered by tail vein to the cannulated rats. Blood samples (100-200 μ L) were collected by jugular cannula. Plasma separated from blood by

centrifugation at $10,000 \times g$ for 10 min at 4 °C was analyzed by HPLC-MS/MS. Data were presented as means \pm standard deviation of two independent studies (n = 4 for free PAESe; n=6 for SSL-PAESe).

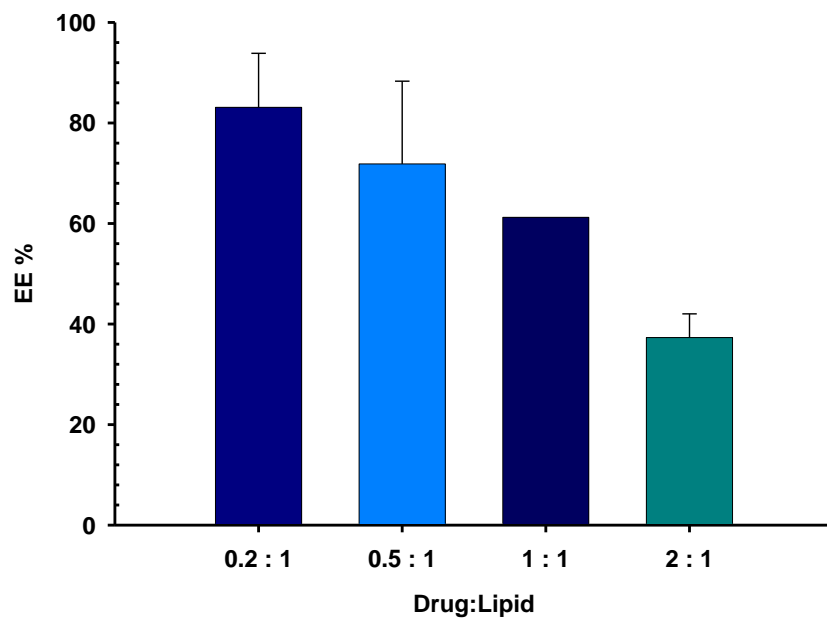


Figure 3-5. Encapsulation efficiency according to the drug:lipid ratio The effect of drug:lipid ratio on the encapsulation efficiency of SSL-PAESe.

Reference

1. Hande KR. Clinical applications of anticancer drugs targeted to topoisomerase II. *Biochimica et Biophysica Acta (BBA) - Gene Structure and Expression* 1998; **1400**:173-184.
2. Jose LQ, Jesus RH, Maurizio B, Jose M, Ramirez-Tortosa MC. Antioxidant nutrients and adriamycin toxicity. *Toxicology*; **180**:79-95.
3. Pearlman M, Jendiroba D, Pagliaro L, Keyhani A, Liu B, Freireich EJ. Dexrazoxane in combination with anthracyclines lead to a synergistic cytotoxic response in acute myelogenous leukemia cell lines. *Leukemia Research* 2003; **27**:617-626.
4. Herman EH, Zhang J, Chadwick DP, Ferrans VJ. Comparison of the protective effects of amifostine and dexrazoxane against the toxicity of doxorubicin in spontaneously hypertensive rats. *Cancer Chemotherapy and Pharmacology* 2000; **45**:329-334.
5. May SW. Selenium-based drug design: rationale and therapeutic potential. *Expert Opinion on Investigational Drugs* 1999; **8**:1017-1030.
6. May SW. Selenium-based pharmacological agents: an update. *Expert Opinion on Investigational Drugs* 2002; **11**:1261-1269.
7. May SW, Pollock SH. Selenium-Based Antihypertensives: Rationale and Potential. *Drugs* 1998; **56**:959-964.

8. May SW, Wang L, Gill-Woznichak MM, Browner RF, Ogonowski AA, Smith JB, et al. An Orally Active Selenium-Based Antihypertensive Agent with Restricted CNS Permeability. *Journal of Pharmacology and Experimental Therapeutics* 1997; **283**:470-477.
9. Kang JY, Costyn LJ, Nagy T, Cowan EA, Oldham CD, May SW, et al. The antioxidant phenylaminoethyl selenide reduces doxorubicin-induced cardiotoxicity in a xenograft model of human prostate cancer. *Archives of Biochemistry and Biophysics* 2011; **515**:112-119.
10. Jin M-C, OuYang X-K, Chen X-h. High-performance liquid chromatography coupled with electrospray ionization tandem mass spectrometry for the determination of flocoumafen and brodifacoum in whole blood. *Journal of Applied Toxicology* 2007; **27**:18-24.
11. Darbre PD, Aljarrah A, Miller WR, Coldham NG, Sauer MJ, Pope GS. Concentrations of parabens in human breast tumours. *Journal of Applied Toxicology* 2004; **24**:5-13.
12. Maurer HH. Advances in analytical toxicology: the current role of liquid chromatography-mass spectrometry in drug quantification in blood and oral fluid. *Analytical & Bioanalytical Chemistry* 2005; **381**:110-118.
13. Jiao J, Carella AJ, Steeno GS, Darrington RT. Optimization of triple quadrupole mass spectrometer for quantitation of trace degradants of pharmaceutical compounds. *International Journal of Mass Spectrometry* 2002; **216**:209-218.
14. Zhong D, Shi X, Sun L, Chen X. Determination of three major components of bitespiramycin and their major active metabolites in rat plasma by liquid

- chromatography-ion trap mass spectrometry. *Journal of Chromatography B* 2003; **791**:45-53.
15. Arnold RD, Mager DE, Slack JE, Straubinger RM. Effect of repetitive administration of Doxorubicin-containing liposomes on plasma pharmacokinetics and drug biodistribution in a rat brain tumor model. *Clinical Cancer Research* 2005; **11**:8856-8865.
 16. Arnold RD, Slack JE, Straubinger RM. Quantification of Doxorubicin and metabolites in rat plasma and small volume tissue samples by liquid chromatography/electrospray tandem mass spectroscopy. *Journal of Chromatography B* 2004; **808**:141-152.
 17. Guodong Z, Yahya A, Brian SC, Robert DA. Synthesis of lipids for development of multifunctional lipid-based drug-carriers. *Bioorganic & Medicinal Chemistry Letters* 2011; **21**:6370-6375.
 18. Siegal T, Horowitz A, Gabizon A. Doxorubicin encapsulated in sterically stabilized liposomes for the treatment of a brain tumor model: biodistribution and therapeutic efficacy. *Journal of Neurosurgery* 1995; **83**:1029-1037.
 19. Bartlett GR, *Phosphorous assay in column chromatography*. 1959, J. Biol.Chem. p. 466-468.
 20. Gabrielsson J, Weiner D. Pharmacokinetic Pharmacodynamic Data Analysis: Concepts and Applications. *Swedish Academy of Pharmaceutical Sciences* 2006:438-463.

21. MacKichan JJ, *Influence of protein binding and use of unbound (free) drug concentrations*, in *Applied Pharmacokinetics*. 1992, Applied Therapeutics: Vancouver, Washington. p. 1-48.
22. McNamara PJ, Levy G, Gibaldi M. Effect of plasma protein and tissue binding on the time course of drug concentration in plasma. *Journal of Pharmacokinetics and Biopharmaceutics* 1979; **7**:195-206.
23. May SW, Herman HH, Roberts SF, Ciccarello MC. Ascorbate depletion as a consequence of product recycling during dopamine β -monooxygenase catalyzed selenoxidation. *Biochemistry* 1987; **26**:1626-1633.
24. Kruve A, Herodes K, Leito I. Optimization of electrospray interface and quadrupole ion trap mass spectrometer parameters in pesticide liquid chromatography/electrospray ionization mass spectrometry analysis. *Rapid Communications In Mass Spectrometry* 2010; **24**:919-926.
25. Hughes NC, Wong EYK, Fan J, Bajaj N. Determination of carryover and contamination for mass spectrometry-based chromatographic assays. *The AAPS Journal* 2007; **9**:E353-E360.
26. Gabizon A, Shiota R, Papahadjopoulos D. Pharmacokinetics and tissue distribution of doxorubicin encapsulated in stable liposomes with long circulation times. *Journal of the National Cancer Institute* 1989; **81**:1484-1488.
27. Sharma US, Sharma A, Chau RI, Straubinger RM. Liposome-mediated therapy of intracranial brain tumors in a rat model. *Pharmaceutical Research* 1997; **14**:992-998.

28. Immordino ML, Dosio F, Cattell L. Stealth liposomes: review of the basic science, rationale, and clinical applications, existing and potential. *International Journal of Nanomedicine* 2006; **1**:297-315.
29. Gert S, Daan JAC. Liposomes: quo vadis? *Pharmaceutical Science & Technology Today* 1998; **1**:19-31.
30. Drummond DC, Noble CO, Hayes ME, Park JW, Kirpotin DB. Pharmacokinetics and in vivo drug release rates in liposomal nanocarrier development. *Journal of Pharmaceutical Sciences* 2008; **97**:4696-4740.
31. Gates C, Pinney RJ. Amphotericin B and its delivery by liposomal and lipid formulations. *Journal of Clinical Pharmacy and Therapeutics* 1993; **18**:147-153.
32. Gabizon AA. Pegylated liposomal doxorubicin: metamorphosis of an old drug into a new form of chemotherapy. *Cancer Investigation* 2001; **19**:424-436.
33. Gabizon A, Shmeeda H, Barenholz Y. Pharmacokinetics of Pegylated Liposomal Doxorubicin: Review of Animal and Human Studies. *Clinical Pharmacokinetics* 2003; **42**:419-436.
34. Ranson MR, Cheeseman S, White S, Margison J. Caelyx (stealth liposomal doxorubicin) in the treatment of advanced breast cancer. *Critical Reviews in Oncology and Hematology* 2001; **37**:115-120.

Abbreviations

ACN	acetonitrile
AUC	area under the plasma drug concentration-time curve
$\alpha_{t1/2}$	alpha distribution half-life
$\beta_{t1/2}$	beta elimination half-life
CL	total systemic clearance
C_{max}	maximum plasma concentration
CV	coefficient of variation
DSPC	1,2-distearoyl-sn-glycero-3-phosphatidylcholine
DSPE-PEG	1,2-distearoyl-sn-glycero-3-phosphoethanolamine-N-[poly(ethylene glycol) 2000)
ESI	electrospray ionization
FPAESe	4-fluoro-phenyl-2-aminoethyl selenide
HPLC	high performance liquid chromatography
I.S.	internal standard
k	terminal elimination rate
LLOQ	lower limit of quantification
MeOH	methanol
MRM	multiple reaction monitoring
MS	mass spectrometry
MS/MS	tandem mass spectrometry

m/z	mass to charge
PAESe	phenyl-2-aminoethyl selenide
PK	pharmacokinetic
QC	quality control
SSL	sterically stabilized liposomes
SSL-PAESe	sterically stabilized PAESe liposomes
$t_{1/2}$	half-life
V	apparent volume of distribution

CHAPTER 4

CARDIOPROTECTION AND ANTITUMOR ACTIVITY OF

PHENYLAMINOETHYL SELENIDES ENCAPSULATED IN LIPOSOMES

Jeong Yeon Kang, Leah J. Costyn, Tamas Nagy, Charlie D. Oldham, Sheldon W. May, Robert D. Arnold. To be submitted to *Journal of Clinical Cancer Research*

Abstract

Anthracyclines are highly effective anticancer agents, but their clinical use is limited by dose-limiting cardiotoxicity mediated by free radical generation. This study evaluated the antitumor and cardioprotective effect of encapsulated PAESe (SSL-PAESe) using a tumor (PC-3) xenograft mouse model of human prostate cancer in nude mice. Differences in tumor volume and histological changes in the heart following H&E staining were examined. Surprisingly, PAESe encapsulated in long circulating liposome and administered at ½ the dose of free drug had greater *in vivo* antitumor activity compared to free PAESe. Tumor volume of DOX+PAESe, SSL-PAESe and DOX+SSL-PAESe groups was decreased significantly ($p < 0.05$) compared to controls. Body weight of PAESe and SSL-PAESe groups were greater than other groups. Survival time of SSL-PAESe and DOX+SSL-PAESe groups were significantly ($p < 0.05$) longer than control and free DOX treatment groups. No evidence of cardiotoxicity was observed in groups treated with PAESe, DOX+PAESe, SSL-PAESe, and DOX+SSL-PAESe. This effect is believed to be associated with the increased circulation time following encapsulation, however the molecular mechanism underlying the antitumor activity is still not known. Further, the protective effect of PAESe on cardiomyocytes following long-term DOX treatment was determined in nude mice by histological examination following H&E staining of the heart and quantification of the necrotic index. Results showed PAESe decreased evidence of DOX-induced cardiomyopathy, such as disruption and fragmentation of myofibers after long-term exposure of DOX. These data suggest that

PAESe can be used in combination with DOX to decrease cardiotoxicity associated with free radical generation, even after long-term exposure of DOX.

1. Introduction

Doxorubicin (DOX) is one of the most widely used anthracyclines and is efficacious against several cancers, *i.e.*, breast, ovarian, acute leukemia and non-Hodgkin's lymphomas [1]. However, its clinical usage has been hampered by dose-limiting cardiotoxicities, such as cardiomyopathy and congestive heart failure (CHF) [1]. Clinically, cardiomyopathy can be observed after single treatment at 240 mg/m² body surface area, and cardiotoxicity, leading to CHF and death, is known to increase at cumulative doses above 550 mg/m² [2].

The primary cause of DOX-mediated cardiotoxicity is believed to be associated with generation of reactive free radicals from DOX and its metabolites during its intracellular metabolism [3]. Reactive free radicals including superoxide anion (O₂^{•-}), hydroxyl radical (OH[•]) and peroxynitrite (ONOO⁻) are produced from the metabolic cycling between a quinone and semiquinone form of DOX in a microsomal NADPH-oxidase system [4, 5]. Cardiomyocyte is prone to oxidative damage by free radicals from DOX due to unique features of the hearts such as a limited number of antioxidants and the high affinity of myocardial phospholipid to DOX [3].

The concomitant administration of antioxidants to prevent cardiotoxicity by inhibiting the production or facilitating the removal of free radicals has been explored. For example, vitamins (vitamin C, E), flavonoids (7-monohydroxyethylrutoside; monoHER) and lipid lowering drugs (statins) have been explored as chemoprotectants in

preclinical and clinical studies [6-8]. Some antioxidants, such as dexrazoxane (Zinecard[®]) and amifostine (Ethyol[®]), were approved by the U.S. Food and Drug Administration (FDA) to decrease free radicals mediated toxicity of chemotherapeutics such as DOX and cisplatin. However, concerns related to insufficient cardioprotection or undesirable side effects, such as acute myeloid leukemia and myelosuppression induced by synergic effect with primary antitumor agents, have been reported [9, 10].

Phenyl-2-aminoethyl selenide (PAESe) is a selenium-based antioxidant that has showed promise for treating cardiovascular disease, such as hypertension [11-14]. PAESe is known to provide a protective effect against oxidant-induced DNA damage through its redox cycling process [15]. Throughout this redox cycling, PAESe is converted to the oxidized PAESe (PAESeO) by rapid reactions with many metabolic oxidants such as peroxide, peroxy nitrite anion, and hydroperoxides, which are known to cause base modifications and induction of double- and single-strand breaks, (Fig 1-2) [15, 16]. The resultant oxidized form is then recycled back easily to the reduced form (PAESe) by ascorbate and glutathione without complex side reactions [13, 15, 17-19].

Previously, we demonstrated PAESe had a protective effect against DOX-induced cardiotoxicity by its antioxidant effect as well as an antitumor activity using *in vitro* cell culture and an *in vivo* mouse model of human prostate (PC-3) cancer (**Chapter 2**) [20]. The *in vitro* antitumor, *i.e.*, growth inhibitory effects, of DOX was not altered by PAESe (up to 10 μ M) on PC-3 prostate cancer cells whereas the generation of intracellular reactive free radicals from DOX was decreased in the presence of PAESe in a dose-dependent manner. Most interestingly, PAESe appeared to exert antitumor activity in the *in vivo* prostate tumor xenograft mouse model in the absence of DOX [20].

Recently we encapsulated PAESE in sterically stabilized liposomes (SSL) and evaluated their effect on the pharmacokinetics of PAESE (**Chapter 3**). Animals administered SSL-PAESE had significantly ($p < 0.05$) greater circulation times and exposures than free PAESE treatment groups. This corresponded to a significant ($p < 0.05$) decrease in the elimination rate and clearance of SSL-PAESE compared to free drug. We hypothesized that this long-circulating PAESE liposome would have improved antitumor efficacy and cardioprotectant properties, as well as reduce undesirable toxicity [21-24].

In this study, the effect of SSL-PAESE on antitumor activity and survival was determined *in vivo* using an established human prostate (PC-3) tumor xenograft model in athymic NCr (*nu/nu*) nude mice. We also determined the cardioprotective effect of PAESE against chronic cardiotoxicity, which is more commonly recognized and clinically the most important form.

2. Materials and Methods

2.1. Chemicals and Reagents

PAESE was synthesized, purified and fully characterized as described previously [17]. F-12K Nutrient Mixture (Kaighn's Mod.) was obtained from Mediatech (Manassas, VA). Doxorubicin hydrochloride was purchased from Sigma-Aldrich Inc (St. Louis, MO). Chloroform and sucrose were obtained from Thermo Fisher Scientific Inc. (Rockford, IL). Lipids, 1,2-distearoyl-sn-glycero-3-phosphatidylcholine (DSPC) and 1,2-distearoyl-sn-glycero-3-phosphoethanolamine-N-[poly(ethylene glycol) 2000] (DSPE-PEG) were

purchased from Avanti Polar Lipids Inc. (Alabaster, AL). Cholesterol was purchased from Sigma-Aldrich (St. Louis, MO) and recrystallized from methanol ($\times 3$) before use.

2.2. Tumor growth inhibition effect of PAESe and SSL-PAESe

2.2.1. Cell culture and tumor xenograft animals

Human prostate adenocarcinoma (PC-3) obtained from American Type Culture Collection (ATCC) (Rockville, MD) was maintained in F-12K media supplemented with 10% (v/v) FBS and 100 U/mL penicillin in a humidified cell culture chamber at 37°C, 5% CO₂. Cells were subcultured when reached approximately 80-90% confluency.

Athymic, NCr (*nu/nu*), mice at 6-8 weeks with body weight of ~ 25 g were used for the study. A PC-3 cell-Matrigel mixture was prepared by mixing ice-cold Matrigel (BD Biosciences, Franklin Lakes, NJ) and PC-3 cell suspension in serum free media (1×10^7 cells/mL) at a 1:1 (v/v) ratio, as described previously [20]. A 100 μ L volume of the mixture was then injected subcutaneously into the flank to develop tumor xenograft. Mice were maintained and handled as described above.

2.2.2. Preparation of SSL-PAESe

Sterically stabilized PAESe liposomes (SSL-PAESe) were formulated with DSPC:Cholesterol:DSPE-PEG (9:5:1 mole %) by thin-film hydration method and remote loading procedure that is based on the combined pH and electrochemical gradients so as to induce encapsulating charged drugs into preformed liposomes, as previously described [21, 25]. Briefly, lipid components hydrated with 250 mM ammonium sulfate (pH 5.0)

were passed through stacked 0.08 μm polycarbonate filters (GE water & Process Tech., Boulder, CO) in a thermobarrel high-pressure extruder (Northern Lipids, Vancouver, British Columbia, Canada) six to eight times at 60 °C. Excessive ammonium sulfate was removed by dialysis in 10% (w/v) sucrose solution at 4 °C overnight. PAESE solution in 10% (w/v) sucrose was then mixed with the preformed liposomes for 1 hr at 65 °C with occasional vortexing. Uncapsulated PAESE was removed by dialysis and the SSL-PAESE was passed through 0.2 μm syringe filters (VWR International LLC, Radnor, PA) for sterilization. The final SSL-PAESE formulations were stored at 4 °C protected from light until use. Concentration of PAESE was determined using a spectrophotometer (Synergy HT Multi-Mode Microplate Reader, BioTek Instruments Inc., Winooski, VT) at 260 nm absorbance. Mean particle diameter of final SSL-PAESE formulation was 80-110 nm when measuring using a submicron particle sizer (Nicomp model 380 dynamic light scattering, Santa Barbara, CA). Particle size data was analyzed using volume-weighted function. Encapsulation efficiencies was over 80% with drug/lipid ratio of 0.2:1.0 (mol:mol). The final concentration of PAESE was typically 1.5 mg/mL.

2.2.3. Effect of SSL-PAESE on a xenograft model of human prostate cancer

Treatment was initiated at 2 weeks after inoculation of tumor cells when tumor volume reached approximately 200 mm^3 . PAESE solution in a normal saline (0.90%, w/v) was sterilized using 0.2 μm syringe filter to make free PAESE formulation. SSL-PAESE was prepared as described above. Mice were randomized to divide into 6 groups: DOX, PAESE, DOX+PAESE, SSL-PAESE, DOX+SSL-PAESE, and control, n = 7-10 animals/cohort. Drugs (100 to 150 μL) were administered to the animals weekly for 4

weeks (a total of 5 treatments) by tail vein injection a dose of 5 mg/kg for DOX, 10 mg/kg for PAESe, 5+10 mg/kg DOX+PAESe, 5 mg/kg SSL-PAESe, 5+5 mg/kg DOX+SSL-PAESe. Control groups were treated with normal saline following the same dosing schedule. Tumor growth and body weight were measured every 3 days. Tumor volume was assessed by the following formula: (largest dimension) \times (smallest dimension)² \times 0.5 using digital calipers [26]. Mice were monitored every day for survival and signs of treatment-mediated toxicity such as blood stool and reduced activity. Mice were sacrificed if weight loss exceeded 20% relative to control, ulceration of sc-tumor or if obvious signs of toxicity such as infection and lethargy were observed, as described above. For any animal that was euthanized, death was considered to have happened on the following day. After sacrificing mice by CO₂, the hearts were excised and stored in formalin solution for histological evaluation.

2.3. Protective effect of PAESe on cardiotoxicity induced by long-term exposure of DOX

Athymic, NCr (*nu/nu*), mice obtained from Taconic Farms, Inc., (Germantown, NY) and were used at 6-8 weeks with body weight of ~ 25 g. Randomized animals were treated with individually with DOX (5 mg/kg) or DOX (5 mg/kg) + PAESe (10 mg/kg) or normal saline as control *via* intravenous (*i.v.*) tail vein injections weekly for 4 weeks (total of 5 treatments). After a 4 week drug holiday, the same treatments were repeated for an additional 3 weeks. Total experiment period was 12 weeks. Body weight was measured every 3 days. Animals were sacrificed if weight loss exceeded 20% of their initial body weight normalized to control or if sc-tumor ulceration or obvious signs of

toxicity such as infection or lethargy were observed [27]. Two weeks after the last treatment, mice were sacrificed by CO₂ euthanasia followed by exsanguination. Hearts were collected and stored in a formalin solution for preparation for histological evaluation by H&E staining, as described below. Necrotic index was assessed by the number of necrotic foci to the total number of section examined of the heart stained by H&E [28]. All sections were analyzed by a pathologist blinded to sample identity.

Mice were maintained in pathogen-free cages in a light and temperature-controlled isolated room and provided with standard rodent chow and sterile water *ad libitum* during the experimental periods. All procedures regarding animal handling, care, and surgery followed a protocol approved by the Institutional Animal Care and Use Committee (IACUC) of the University of Georgia and the U.S. Public Health Service (PHS) Policy on Humane Care and Use of Laboratory Animals, updated 2002.

2.4. Histological examination

Histological changes in heart tissues were examined, following staining with hematoxylin and eosin (H&E), for evidence of anthracycline-mediated cardiotoxicity, as reported previously [20]. Briefly, hearts fixed in formalin solutions (10%, v/v) were bisected longitudinally followed by paraffin embedding. Serial sections were collected and stained with H&E. A total of four sections from each heart were examined using a Nikon AZ100 stereo-fluorescent microscope mounted with a Nikon *DS-Qi1Mc color* camera, and then analyzed by NIS-Elements image analysis software. The necrotic index was calculated by the number of necrotic foci of the total number of sections examined of

the heart stained by H&E. Micrographs were examined microscopically and evaluated by a pathologist who was initially blinded to their identity.

2.5. Statistical analysis

Data were analyzed using one-way ANOVA followed by a post-hoc analysis (Bonferroni corrected t-test), Sigma Stat (v3.1, Systat Software Inc., San Jose, CA). Survival data were analyzed by plotting percent survival using Kaplan–Meier survival curve. A p value ≤ 0.05 was regarded as statistically significant.

3. Results

3.1. Effect of PAESe and SSL-PAESe on a xenograft model of human prostate cancer

Tumor volume and body weight were measured during 8 weeks after the treatment was initiated. Tumor growth inhibitory effect was observed in the entire treatment group relative to control by day 33 after initiating treatment (Fig 4-1A). Indeed, tumor volumes were significantly decreased in DOX+PAESe, SSL-PAESe, and DOX+SSL-PAESe groups compared to control around 1 week after the last treatment. The antitumor activity of DOX was not significantly altered when coadministered with PAESe (DOX+PAESe; 229% \pm 20) or SSL-PAESe (DOX+SSL-PAESe; 199% \pm 41) relative to free DOX (337% \pm 46). Further, tumor volume in DOX+PAESe, DOX+SSL-PAESe as well as SSL-PAESe group (309% \pm 63) was significantly decreased compared

to saline treated control ($786\% \pm 234$) at day 33. It was remarkable because the half dose (5 mg/kg) was used in SSL-PAESe group compared to PAESe (10 mg/kg).

Body weight among all of the treatment groups was not significantly different initially, as shown in Fig 4-1B. However, body weight of PAESe ($25\% \pm 2$) and SSL-PAESe ($25\% \pm 2$) groups was significantly higher than DOX ($5\% \pm 5$) and DOX+PAESe ($3\% \pm 6$) groups from day 51 even though DOX and DOX+PAESe appeared not to affect body weight at this time. No significant loss in body weight was observed between control ($12\% \pm 4$) and DOX+SSL-PAESe ($11\% \pm 5$) group.

The survival time of SSL-PAESe and DOX+SSL-PAESe group was significantly increased compared to animals receiving saline and DOX, as shown in Fig 4-2. The median survival for saline treated control (day 55) and DOX group (day 58) was not significantly different (Table 4-1). This result suggests that DOX might shorten the lifespan of animals by its toxicity as control groups were deceased by their tumor burden even though the tumor volume of DOX group was decreased significantly compared to control group. However, coadministration of DOX with PAESe (day 75) or SSL-PAESe (day 72) did extend survival relative to DOX group (day 58) while tumor volume of these 2 groups was not significantly different relative to that of DOX group (Fig 4-1A). No significant difference was observed in the median survival among the groups receiving DOX+PAESe (day 75), DOX+SSL-PAESe (day 72), and PAESe (day 71). Notably, a significant increase was observed in survival time for the animals receiving SSL-PAESe compared to control and DOX group. The median survival for SSL-PAESe group was 62% and 53% higher than controls and DOX groups, respectively (Table 4-1).

3.2. Protective effect of PAESE on cardiotoxicity induced by long-term exposure of DOX

Athymic, NCr (*nu/nu*), mice (~ 25 g) were treated with 5 mg/kg of DOX or 5+10 mg/kg of DOX + PAESE or normal saline as control *via* intravenous (*i.v.*) tail vein injections weekly for 4 weeks. After a 4 week drug holiday, the same treatments were repeated for an additional 3 weeks. Two weeks after the last treatment, mice were sacrificed, and hearts were collected and stored for histological evaluation by H&E staining. Body weight was measured every 3 days. No significant differences were observed in body weight in all of the experimental groups (Fig 4-3). Histological alteration was examined to determine the cardioprotective effect of PAESE at 12th week after the treatment was initiated. Significant difference was observed in the degree of cardiac tissue destruction between control (Fig 4-4A) and DOX alone (Fig 4-4C) groups. In all of the DOX (4/4) treated group, the evidence of anthracycline mediated cardiomyopathy was observed in the myocardium of the left ventricle wall with Grade 1 using a modification of the Jaenke method [29]. Disruption and fragmentation of the myocardial fibers were observed accompanied with inflammatory infiltrate foci composed of neutrophils and macrophages in each longitudinal section. In contrast, intact myocardium with faint outlines of cross striation was observed in all of the DOX+PAESE (0/3) treated group (Fig 4-4B), which was not significantly different from the control group (Fig 4-4A). The cardioprotective effects of PAESE were also supported by differences in necrotic index, as shown in Table 4-2. Necrotic index values of all of the DOX treatment groups were increased compared to the control and DOX+PAESE treated

groups, which were zero. These results demonstrate that PAESe has a protective effect against cardiomyopathy induced by long-term DOX treatment.

4. Discussion

Anthracyclines such as DOX (Adriamycin[®]) and Daunorubicin (Cerubidine[®]) are well-established antitumor agents that are highly effective in the treatment of various types of cancers including breast, ovarian, lung cancer, acute leukemia, and non-Hodgkin's lymphomas [1]. However, their therapeutic potential is limited by severe dose-dependent cardiotoxicity that frequently leads to cardiomyopathy and congestive heart failure [1].

There are several hypotheses to explain the observed anthracycline-induced myocardial damage. DOX is believed to inhibit selectively the expression of cardiac muscle genes such as alpha-actin, troponin I, and myosin light chain 2, as well as the muscle-specific M isoform of creatine kinase [30]. DOX is also believed to stimulate the release of intracellular calcium as well as vasoactive substances such as catecholamine and histamine that induce myocardial damages [31, 32]. The activity of β -adrenergic receptors or antioxidant enzymes in cardiac myocyte has also been found altered following treatment with DOX [33, 34]. Among them, reactive free radicals generated from DOX are generally accepted as the primary cause of its cardiotoxicity [3-5, 35-37].

The quinone moiety on the tetracycline ring of DOX is responsible for free radicals formation. Electron transfer from quinone to semiquinone group of DOX is catalyzed by NADPH-cytochrome c-reductase or b₅-reductase. Superoxide anion is then generated by oxidation of molecular oxygen when semiquinone form converts to the

quinone form [37, 38]. Due to this intracellular metabolism, DOX continues to generate various reactive free radicals such as hydrogen peroxide (H_2O_2), hydroxyl radical (OH^\bullet), and peroxynitrite ($ONOO^-$) [4, 39]. These free radicals induce oxidative injury in cellular components such as myofibrillar loss and sarcoplasmic reticulum disruption as well as lipid membrane peroxidation by disrupting oxidative balance and cellular homeostasis [15, 40-42]. Cumulative damage is hypothesized to cause myocardial dysfunction, such as blood pressure dysregulation and impaired heart contractility, which progress to heart failure [43]. Moreover, the heart is susceptible to direct damage by free radicals from DOX because the concentration of antioxidants is limited in the heart, whereas the myocardial phospholipid, cardiolipin, has a high affinity to DOX [3].

In this regard, antioxidants or scavenging agents have been explored to offer a cardioprotective effect against DOX. The protective effects of well-known antioxidants, such as vitamin C or α -tocopherol, to mitigate DOX induced cardiotoxicity have been investigated using *in vivo* mouse and guinea pig models [6, 7]. Two antioxidants approved by the U.S. FDA, *i.e.*, dexrazoxane and amifostine, are used to reduce free radicals generated from antineoplastic agents such as DOX and cisplatin. However, their usage is restricted due to the risk of interfering or synergizing the antitumor activity of primary chemotherapeutic agents. Dexrazoxane caused myelosuppression and can lead to acute myeloid leukemia and myelodysplastic syndrome [9, 44]. Amifostine has been reported to have insufficient activity to not only protect cardiotoxicity but also alter mortality of DOX *in vivo* rat model [10].

Phenyl-2-aminoethyl selenide (PAESe) is a novel selenium-based antioxidant that was developed to treat cardiovascular disease [11-14]. PAESe exhibits potent antioxidant

activity by selenium redox cycling. PAESe can be converted to phenyl-2-aminoethyl selenoxide (PAESeO) by reacting rapidly with many metabolic oxidants, and PAESeO is then recycled back readily to PAESe in the presence of ascorbate and glutathione without complex side reactions [13, 15, 17-19]. This redox cycling of PAESe confers a protective effect against oxidant-induced DNA damage because metabolic oxidants such as peroxide, peroxyxynitrite anion, and hydroperoxides are known to react readily with DNA, resulting in base modifications and induction of double- and single-strand breaks [15, 16].

In our previous study using a tumor xenograft mouse model, PAESe did not alter the antitumor activity of DOX. We believe this is due to the fact the antitumor activity of DOX has been associated with antagonism of topoisomerase II of DOX rather than formation of reactive free radicals, as mentioned above. Interestingly, PAESe showed evidence of direct antitumor effect relative to controls. This is in agreement with an earlier study (**Chapter 2**), where PAESe reduced PC-3 tumor growth relative to controls and was not significantly different than DOX treatment. This observation was unexpected as PAESe has not shown any *in vitro* growth inhibitory or cytotoxicity up to 10 μ M. Although the mechanism is not known, we hypothesize the *in vivo* antitumor activity of PAESe may be associated with altering free radicals in tumor leading to differences in tumorigenic phenotype and/or enhancing *in vivo* immune function. Antioxidants are known to enhance immune function by increasing the number of immune cells such as macrophage, mononuclear cells, and lymphocytes like natural killer cells as well as the expression of interleukin-2 receptors [45]. Thus, the activity of chemotherapeutic agents could be more effective to tumor cells by immune-enhancing effect of PAESe unlike *in vitro* studies [45]. It should be noted that NCr mice are deficient in T cell so that a

complete inhibition of immune function is not provided. Another possible explanation for the antitumor effect of PAESe might be related to the effect of selenium that is a component of PAESe. Selenium is an essential cofactor of glutathione peroxidase, a well-known antioxidant enzyme that decreases oxidant-induced DNA damages. Selenium is also known to have antiangiogenic properties *in vitro* and *in vivo* through apoptosis and controlling matrix metalloproteinase activity and vascular endothelial growth factor levels [46]. However, the selenium is bound in PAESe, and we have no evidence to suggest that this compound is being degraded and free selenium is released. In addition, antioxidant can prevent DNA mutation and lipid peroxidation caused by oxidation that is highly related with the initiation and progression of malignancy [47]. Antioxidant can also reduce the expression of oncogenes as well as the activity of protein kinase C that promotes cancer progression [48].

The time-course of DOX-mediated cardio damage by free radicals and the mechanism underlying the *in vivo* antitumor activity are not known. We developed a long circulating PAESe liposome with saturated, high phase-transition lipids (DSPC), cholesterol, and surface coating with hydrophilic polymer (PEG-DSPE) (**Chapter 3**) and evaluated its antitumor activity using a tumor xenograft mouse model.

Nanoparticulate drug carriers are known to modulate drug disposition, which is responsible for the increased therapeutic efficacy and reduced toxicity of a variety of chemotherapeutic agents in animal models and clinically [21-24]. Sterically stabilized liposome (SSL), one such nanoparticulate drug carrier, has a prolonged circulating property. Stealth coating with hydrophilic polymer like polyethylene glycol (PEG) limits the ability of serum proteins to interact with carrier surface, resulting in the reduced

opsonization and rapid clearance [21, 49]. Cholesterol, one of major components for SSL, reduces the membrane fluidity above the lipid phase transition temperature as well as the permeability to aqueous solutes, which provide steric stability. Further, lipidic particles like SSL can extravasate and accumulate passively in tumor vasculature through diffusion by the enhanced permeability and retention (EPR) effect [50]. Tumor tissue has unique physiological features such as leaky vascular architecture and nonfunctional lymphatic drainage due to abnormal and uncontrolled growth of tumor formation [51]. Long circulating liposomes can remain in the body, eventually tumor interstitium for a prolonged time, resulting in accumulation of drug in tumor tissue. EPR effect is known to relevant to over 40 kDa nanoparticles or macromolecules, not to low-molecular weight compounds which covers most of drugs in use today [52].

Results showed that tumor volume of PAESe, DOX+PAESe, SSL-PAESe, and DOX+SSL-PAESe groups was not different significantly compared to DOX group. It was noteworthy that tumor volume appeared to be decreased significantly ($p < 0.05$) in DOX+PAESe, SSL-PAESe, and DOX+SSL-PAESe groups relative to saline control at day 33 even though the dose of SSL-PAESe (5 mg/kg) was the half dose of free PAESe (10 mg/kg). After day 33, variability in tumor volume increased. This was mediated in part by difficulty in assessing tumor volume, but also because significant weight loss or tumor burden required some animals to be sacrificed, particularly among the control group. Body weight of PAESe and SSL-PAESe treated mice was not altered significantly compared to control; however, PAESe alone appeared to decrease tumor volume. No significant differences were observed in tumor volume between animal groups treated with PAESe and DOX. Survival data also showed the groups treated with SSL-PAESe

(with or without DOX) lived longer than other groups while tumor volume of these groups (SSL-PAESe and DOX+SSL-PAESe) were significantly smaller than control and DOX group. Moreover, histological examination by H&E staining showed that there was no evidence of cardiotoxicity in groups treated with PAESe, DOX+PAESe, SSL-PAESe, and DOX+SSL-PAESe. It is important that the dose of SSL-PAESe was half of free formulation as is frequently pointed out. These results showed that the exposure of drug might be increased in tumor tissue, resulting in the improved antitumor or antioxidant activity of PAESe by encapsulation in long-circulating liposomes.

There results were further supported by our previous data (**Chapter 3**) that determined pharmacokinetic properties in plasma of animals administered with free (10 mg/kg) and SSL-PAESe (5 mg/kg). Marked differences in pharmacokinetic properties were observed between free and SSL-PAESe animal groups; Circulation half-life (101 hr) was significantly increased in animals administered with SSL-PAESe while PAESe was rapidly cleared with $\beta_{t1/2}$ of 8.78 min in free PAESe group. There were also significant decreases in elimination rate and clearance in SSL-PAESe group compared to free PAESe group.

We also determined the cardioprotective effect of PAESe following long-term exposure of DOX. Previously, we have shown that PAESe decreased early myocardial damage after DOX treatment [20]. Anthracycline-induced cardiotoxicity has been more commonly recognized even years to decades after treatment has ceased with an asymptomatic period [53]. This chronic cardiotoxicity is clinically the most important because it causes more serious clinical problems such as late-onset ventricular dysfunction, heart failure and arrhythmias that lead to increased mortality [54, 55]. Acute

cardiotoxicity, on the other hand, occur immediately after treatment, and is not as usual type under current treatment protocols. Acute toxicities mediated by DOX are related to transient arrhythmias or acute failure of the left ventricle [56, 57]. The cumulative dose of the drug is the major factor to incur the congestive heart failure secondary to cardiomyopathy. The potential of developing this cardiomyopathy is known to increase rapidly at total cumulative dose of over 550 mg/m² body surface area [1]. Several studies showed that there was a time-dependent histological change on cardiomyocytes, and congestive heart failure was established after long-term exposure of DOX *in vivo* animal model [58, 59]. Based on these results, the cardioprotection of PAESe was determined after long-term exposure of DOX along with 4 weeks interval to recover from bone marrow depression, which mimic the clinical setting for anthracycline therapy.

Results from histological staining and necrotic index demonstrated that PAESe has the protective effect against cardiotoxicity after long-term exposure of DOX. Intact myocardium was observed in all DOX+PAESe groups like as control group whereas evidence of cardiotoxicity was found in myocardium of DOX group with inflammatory foci composed of neutrophils and macrophages. Also, necrotic index of DOX group was higher than that of DOX+PAESe and control group. No significant differences were observed in body weight in all of the experimental groups because tumor was not involved in this study; thus there was no tumor-mediated weight loss. These data suggests that PAESe has a protective effect against chronic cardiotoxicity following cumulative exposure to DOX. This is an interesting result that may have clinical relevance because other antioxidants, such as vitamin E and N-acetylcysteine, prevent acute cardiotoxicity but not the chronic form of cardiotoxicity following treatment with DOX [60-62].

In conclusion, we demonstrated that PAESe, a novel selenium-based antioxidant, and its encapsulated form in sterically stabilized liposome (SSL-PAESe) had cardioprotective effect on free radical mediated DOX-induced cardiotoxicity and exerted *in vivo* antitumor activity. PAESe decreased evidence of cardiomyopathy after long-term DOX treatment, which is clinically the most important form of cardiotoxicity unlike other antioxidants. Encapsulated PAESe in long circulating liposome exerted the improved *in vivo* antitumor activity relative to free PAESe with extended survival even though the half dose was applied, which suggests that the enhanced circulation and exposure of PAESe following liposome encapsulation improves PAESe antitumor activity. Even though further studies are necessary to determine the relationship between *in vivo* antitumor effect and immune function of PAESe, it is clear that PAESe and SSL-PAESe have potential as chemoprotectants, and may be used to improve the clinical utility of DOX, as well as direct chemotherapeutic agent.

Table 4-1. Mean days survival

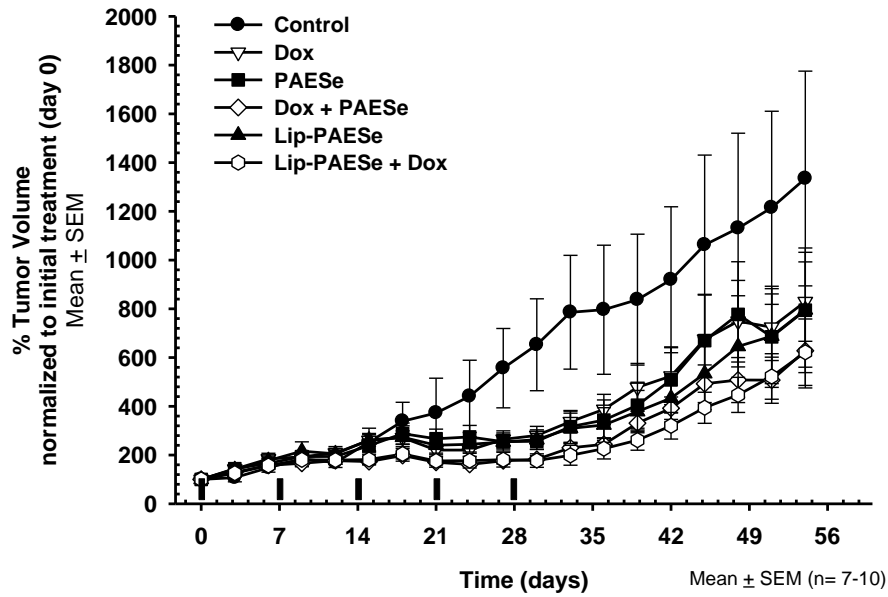
	Median days survival (Range)	% Increase in median survival vs. control	<i>p</i> value
Control	55 (35 – 81)	-	-
DOX	58 (41 – 89)	5	0.1765
PAESe	71 (26 – N/A)	29	0.0144
DOX+PAESe	75 (45 – N/A)	36	0.0021
SSL-PAESe	89 (55 – N/A)	62	0.0005
DOX+SSL-PAESe	72 (52 – N/A)	31	0.0006

p value: From statistical analysis of each group vs. control using Kaplan-Meier analysis

Table 4-2. Necrotic index

	# of section examined	# of necrotic foci with sections	necrotic index
Control (n=3)	2	0	0
	2	0	0
	2	0	0
DOX+PAESe (n=3)	2	0	0
	2	0	0
	2	0	0
DOX (n=4)	2	3	1.5
	2	3	1.5
	2	1	0.5
	2	1	0.5

(A)



(B)

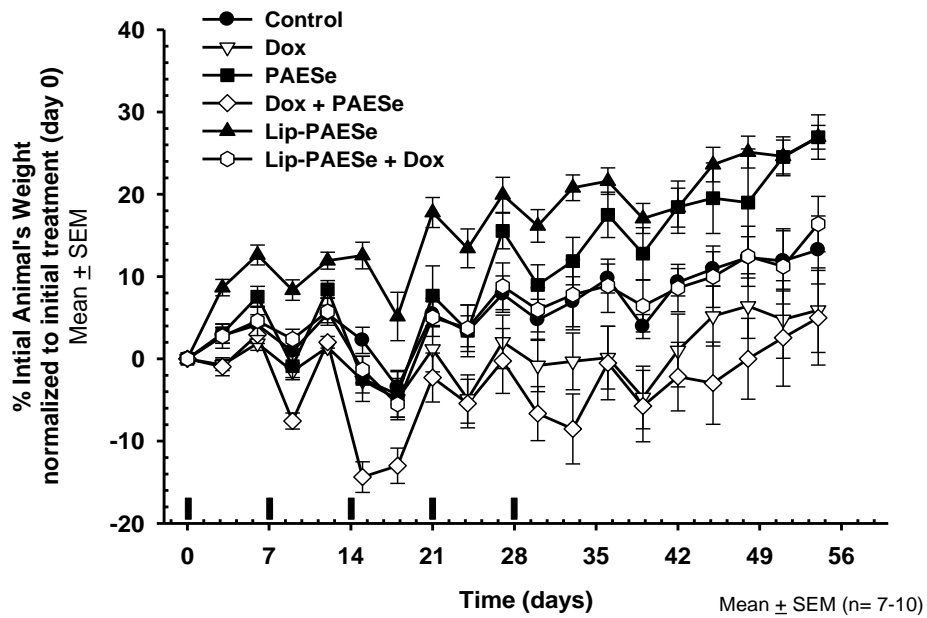


Figure 4-1. Effect of SSL-PAESE on tumor growth (A) and body weight (B) in a PC-3 xenograft model The effect of encapsulated PAESE in long circulating liposome (SSL-PAESE) on tumor growth (A) and body weight (B) was determined in a tumor (PC-3)

xenograft mouse model. After tumors reached 200 mm³, treatment was initiated with 5 mg/kg/week for DOX and 10 mg/kg/week for PAESe, and 5 mg/kg/week for SSL-PAESe by tail vein injection weekly. Tumor volume and body weight were monitored every three days, data are presented as means \pm SEM (n = 7-10) and were normalized to average tumor volume or body weight on day 0. An asterisk indicates a significant ($p < 0.05$) difference compared to control.

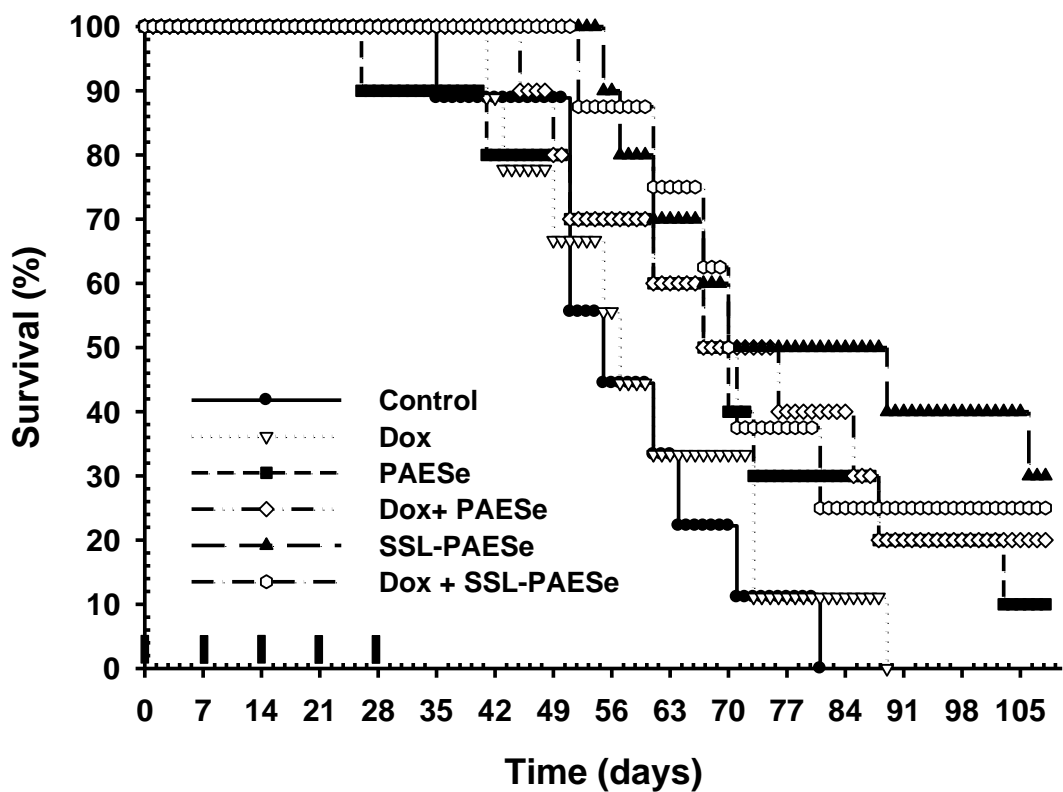


Figure 4-2. Survival (%) time profile The effect of encapsulated PAESe in long circulating liposome (SSL-PAESe) on survival was determined in a tumor (PC-3) xenograft mouse model. After tumors reached 200 mm³, treatment was initiated with 5 mg/kg/week for DOX and 10 mg/kg/week for PAESe, and 5 mg/kg/week for SSL-PAESe by tail vein injection weekly. Mice were monitored every day, and solid bars represent treatment day.

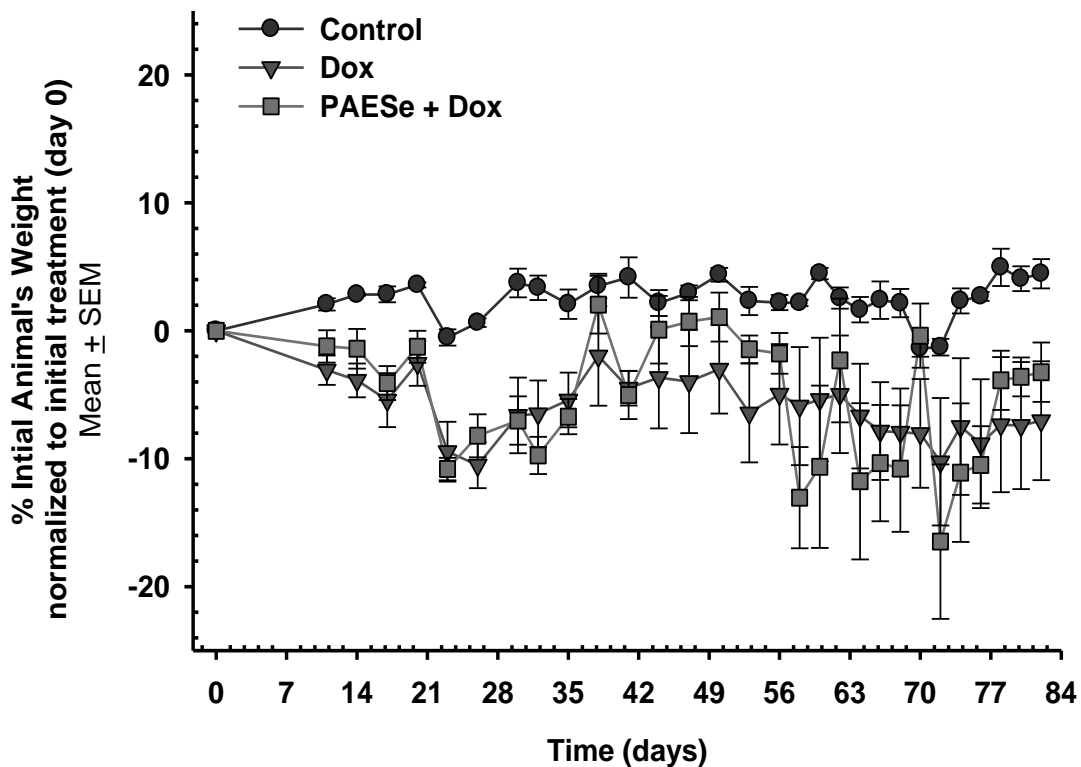


Figure 4-3. Body weight change of mice after long-term exposure of DOX Animals were treated with DOX (5 mg/kg) or DOX+PAESE (5+10 mg/kg) or normal saline (control) *via* tail vein injections weekly for 4 weeks (black rectangular boxes), following by a 4 week drug holiday. The same treatments were then repeated for an additional 3 weeks. Body weight was measure every 3 days for 12 weeks of total experiment period.

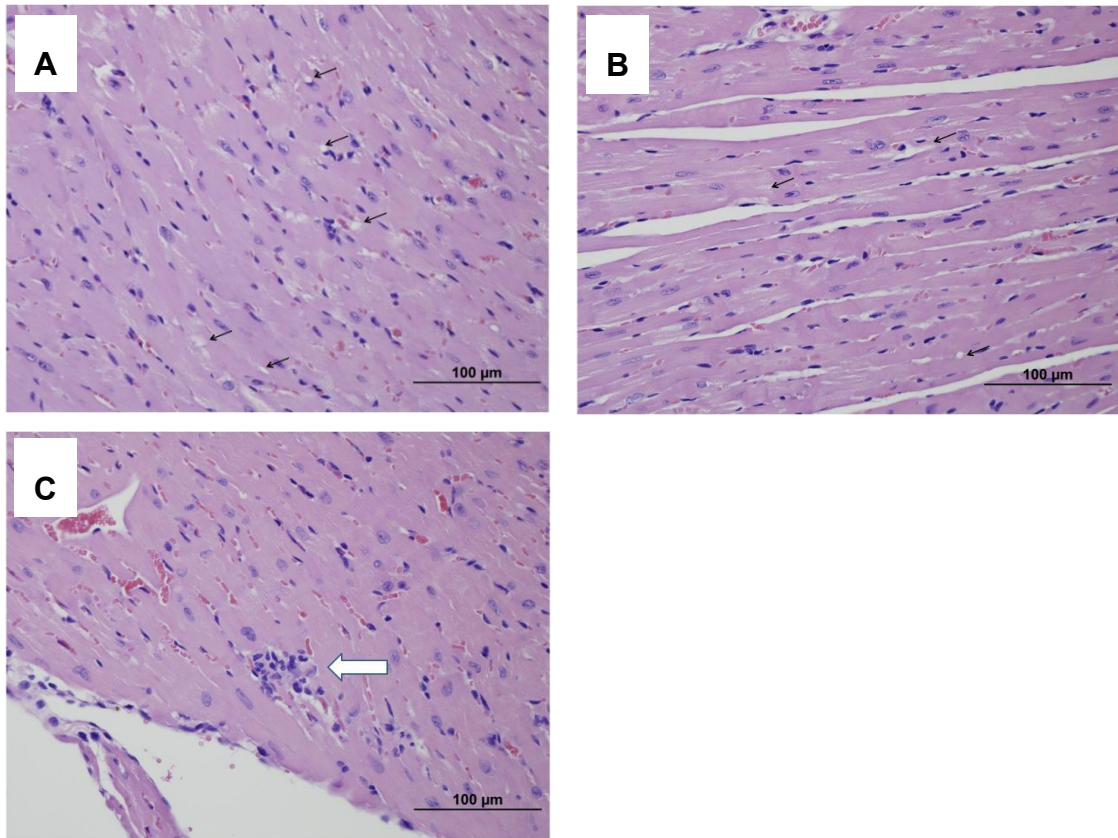


Figure 4-4. Histological micrographic images of the myocardium Athymic, NCr (*nu/nu*) mice (~ 25 g) were treated with 5 mg/kg of DOX or 5+10 mg/kg DOX + PAESE or normal saline *via* intravenous tail vein injections weekly for 4 weeks. The same treatments were repeated for an additional 3 weeks after a 4 week drug holiday. Mice were scarified 2 weeks after the last treatment, and hearts were collected and stained with H&E. Micrographs of the myocardium of the left ventricular free wall from a mouse treated with saline (A), DOX with PAESE (B), and DOX (C) were captured. In all DOX (C) treated group, inflammatory foci (white block arrow) were observed in the myocardium composed of neutrophils and macrophages. The slight vacuolization in the myocardiocytes (arrows) is an artifact of formalin fixation. (40 ×, scale bars = 100 μm).

Reference

1. Hande KR. Clinical applications of anticancer drugs targeted to topoisomerase II. *Biochimica et Biophysica Acta (BBA) - Gene Structure and Expression* 1998; **1400**:173-184.
2. Billingham ME, Mason JW, Bristow MR, Daniels JR. Anthracycline cardiomyopathy monitored by morphologic changes. *Cancer treatment reports* 1978; **62**:865-872.
3. Quiles JL, Huertas JsR, Battino M, Mataix J, Ramirez-Tortosa MC. Antioxidant nutrients and adriamycin toxicity. *Toxicology* 2002; **180**:79-95.
4. Chance B, Sies H, Boveris A. Hydroperoxide metabolism in mammalian organs. *Physiological Reviews* 1979; **59**:527-605.
5. Handa K, Sato S. Generation of free radicals of quinone group-containing anti-cancer chemicals in NADPH-microsome system as evidenced by initiation of sulfite oxidation. *Gann* 1975; **66**:43-47.
6. Shimpo K, Nagatsu T, Yamada K, Sato T, Niimi H, Shamoto M, et al. Ascorbic acid and adriamycin toxicity. *The American Journal of Clinical Nutrition* 1991; **54**:1298S-1301S.
7. Wahab MH, Akoul ES, Abdel Aziz AA. Modulatory effects of melatonin and vitamin E on doxorubicin-induced cardiotoxicity in Ehrlich ascites carcinoma-bearing mice. *Tumori* 2000; **86**:157-162.

8. Feleszko W, Mlynarczuk I, Balkowiec-Iskra EZ, Czajka A, Switaj T, Stoklosa T, et al. Lovastatin potentiates antitumor activity and attenuates cardiotoxicity of doxorubicin in three tumor models in mice. *Clinical Cancer Research: An Official Journal Of The American Association For Cancer Research* 2000; **6**:2044-2052.
9. Tebbi CK, London WB, Friedman D, Villaluna D, De Alarcon PA, Constine LS, et al. Dexrazoxane-associated risk for acute myeloid leukemia/myelodysplastic syndrome and other secondary malignancies in pediatric Hodgkin's disease. *Journal of Clinical Oncology* 2007; **25**:493-500.
10. Herman EH, Zhang J, Chadwick DP, Ferrans VJ. Comparison of the protective effects of amifostine and dexrazoxane against the toxicity of doxorubicin in spontaneously hypertensive rats. *Cancer Chemotherapy And Pharmacology* 2000; **45**:329-334.
11. May SW. Selenium-based drug design: rationale and therapeutic potential. *Expert Opinion on Investigational Drugs* 1999; **8**:1017-1030.
12. May SW. Selenium-based pharmacological agents: an update. *Expert Opinion on Investigational Drugs* 2002; **11**:1261-1269.
13. May SW, Pollock SH. Selenium-Based Antihypertensives: Rationale and Potential. *Drugs* 1998; **56**:959-964.
14. May SW, Wang L, Gill-Woznichak MM, Browner RF, Ogonowski AA, Smith JB, et al. An Orally Active Selenium-Based Antihypertensive Agent with Restricted CNS Permeability. *Journal of Pharmacology and Experimental Therapeutics* 1997; **283**:470-477.

15. De Silva V, Woznichak MM, Burns KL, Grant KB, May SW. Selenium Redox Cycling in the Protective Effects of Organoselenides against Oxidant-Induced DNA Damage. *Journal of the American Chemical Society* 2004; **126**:2409-2413.
16. Henle ES, Linn S. Formation, Prevention, and Repair of DNA Damage by Iron/Hydrogen Peroxide. *Journal of Biological Chemistry* 1997; **272**:19095-19098.
17. May SW, Herman HH, Roberts SF, Ciccarello MC. Ascorbate depletion as a consequence of product recycling during dopamine .beta.-monooxygenase catalyzed selenoxidation. *Biochemistry* 1987; **26**:1626-1633.
18. Overcast JD, Ensley AE, Buccafusco CJ, Cundy C, Broadnax RA, He S, et al. Evaluation of Cardiovascular Parameters of a Selenium-Based Antihypertensive Using Pulsed Doppler Ultrasound. *Journal of Cardiovascular Pharmacology* 2001; **38**:337-346.
19. Pollock SH, Herman HH, Fowler LC, Edwards AS, Evans CO, May SW. Demonstration of the antihypertensive activity of phenyl-2-aminoethyl selenide. *Journal of Pharmacology and Experimental Therapeutics* 1988; **246**:227-234.
20. Kang JY, Costyn LJ, Nagy T, Cowan EA, Oldham CD, May SW, et al. The antioxidant phenylaminoethyl selenide reduces doxorubicin-induced cardiotoxicity in a xenograft model of human prostate cancer. *Archives of Biochemistry and Biophysics* 2011; **515**:112-119.
21. Arnold RD, Mager DE, Slack JE, Straubinger RM. Effect of repetitive administration of Doxorubicin-containing liposomes on plasma pharmacokinetics

- and drug biodistribution in a rat brain tumor model. *Clinical Cancer Research* 2005; **11**:8856-8865.
22. Siegal T, Horowitz A, Gabizon A. Doxorubicin encapsulated in sterically stabilized liposomes for the treatment of a brain tumor model: biodistribution and therapeutic efficacy. *Journal of Neurosurgery* 1995; **83**:1029-1037.
 23. Gabizon A, Shiota R, Papahadjopoulos D. Pharmacokinetics and tissue distribution of doxorubicin encapsulated in stable liposomes with long circulation times. *Journal of the National Cancer Institute* 1989; **81**:1484-1488.
 24. Sharma US, Sharma A, Chau RI, Straubinger RM. Liposome-mediated therapy of intracranial brain tumors in a rat model. *Pharmaceutical Research* 1997; **14**:992-998.
 25. Arnold RD, Slack JE, Straubinger RM. Quantification of Doxorubicin and metabolites in rat plasma and small volume tissue samples by liquid chromatography/electrospray tandem mass spectroscopy. *Journal of Chromatography B* 2004; **808**:141-152.
 26. Davol PA, Frackelton AR. Targeting human prostatic carcinoma through basic fibroblast growth factor receptors in an animal model: Characterizing and circumventing mechanisms of tumor resistance. *The Prostate* 1999; **40**:178-191.
 27. Wong HL, Rauth AM, Bendayan R, Wu XY. In vivo evaluation of a new polymer-lipid hybrid nanoparticle (PLN) formulation of doxorubicin in a murine solid tumor model. *European Journal of Pharmaceutics and Biopharmaceutics* 2007; **65**:300-308.

28. Sakurai Y, Uruguchi T, Imazu H, Hasegawa S, Matsubara T, Ochiai M, et al. Changes in thymidylate synthase and its inhibition rate and changes in dihydropyrimidine dehydrogenase after the administration of 5-fluorouracil with cisplatin to nude mice with gastric cancer xenograft SC-1-NU. *Gastric Cancer: Official Journal Of The International Gastric Cancer Association And The Japanese Gastric Cancer Association* 2004; **7**:110-116.
29. Jaenke RS. An anthracycline antibiotic-induced cardiomyopathy in rabbits. *Laboratory Investigation; A Journal Of Technical Methods And Pathology* 1974; **30**:292-304.
30. Ito H, Miller SC, Billingham ME, Akimoto H, Torti SV, Wade R, et al. Doxorubicin Selectivity Inhibits Muscle Gene Expression in Cardiac Muscle Cells in vivo and in vitro. *Proceedings of the National Academy of Sciences of the United States of Ame* 1990; **87**:4275-4279.
31. Wang Y, Korth M. Effects of doxorubicin on excitation-contraction coupling in guinea pig ventricular myocardium. *Circulation Research* 1995; **76**:645-653.
32. Bristow MR, Kantrowitz NE, Harrison WD, Minobe WA, Sageman WS, Billingham ME. Mediation of subacute anthracycline cardiotoxicity in rabbits by cardiac histamine release. *Journal of Cardiovascular Pharmacology* 1983; **5**:913-919.
33. Fujita N, Hiroe M, Ohta Y, Horie T, Hosoda S. Chronic Effects of Metoprolol on Myocardial [beta]-Adrenergic Receptors in Doxorubicin-Induced Cardiac Damage in Rats. *Journal of Cardiovascular Pharmacology* 1991; **17**:656-661.

34. Revis NW, Marusic N. Glutathione peroxidase activity and selenium concentration in the hearts of doxorubicin-treated rabbits. *Journal of Molecular and Cellular Cardiology* 1978; **10**:945-948.
35. Keizer HG, Pinedo HM, Schuurhuis GJ, Joenje H. Doxorubicin (adriamycin): A critical review of free radical-dependent mechanisms of cytotoxicity. *Pharmacology & Therapeutics* 1990; **47**:219-231.
36. Olson RD, Boerth RC, Gerber JG, Nies AS. Mechanism of adriamycin cardiotoxicity: Evidence for oxidative stress. *Life Sciences* 1981; **29**:1393-1401.
37. Venditti P, Balestrieri M, De Leo T, Di Meo S. Free radical involvement in doxorubicin-induced electrophysiological alterations in rat papillary muscle fibres. *Cardiovascular Research* 1998; **38**:695-702.
38. Sarvazyan NA, Askari A, Huang WH. Effects of doxorubicin on cardiomyocytes with reduced level of superoxide dismutase. *Life Sciences* 1995; **57**:1003-1010.
39. Rajagopalan S, Politi PM, Sinha BK, Myers CE. Adriamycin-induced Free Radical Formation in the Perfused Rat Heart: Implications for Cardiotoxicity. *Cancer Research* 1988; **48**:4766-4769.
40. Saeki K, Obi I, Ogiku N, Shigekawa M, Imagawa T, Matsumoto T. Doxorubicin directly binds to the cardiac-type ryanodine receptor. *Life Sciences* 2002; **70**:2377-2389.
41. Doroshow JH. Effect of Anthracycline Antibiotics on Oxygen Radical Formation in Rat Heart. *Cancer Research* 1983; **43**:460-472.
42. Zhou S, Palmeira CM, Wallace KB. Doxorubicin-induced persistent oxidative stress to cardiac myocytes. *Toxicology Letters* 2001; **121**:151-157.

43. Cassidy SC, Chan DP, Rowland DG, Allen HD. Effects of doxorubicin on diastolic function, contractile reserve, and ventricular–vascular coupling in piglets. *Pediatric Cardiology* 1998; **19**:450-457.
44. Pearlman M, Jendiroba D, Pagliaro L, Keyhani A, Liu B, Freireich EJ. Dexrazoxane in combination with anthracyclines lead to a synergistic cytotoxic response in acute myelogenous leukemia cell lines. *Leukemia Research* 2003; **27**:617-626.
45. Patrick L. Selenium Biochemistry and Cancer: A Review of the Literature. *Alternative Medicine Review* 2004; **9**:239-258.
46. Jiang C, Jiang W, Ip C, Ganther H, Lu J. Selenium-induced inhibition of angiogenesis in mammary cancer at chemopreventive levels of intake. *Molecular Carcinogenesis* 1999; **26**:213-225.
47. Sundstrom H, Korpela H, Viinikka L, Kauppila A. Serum selenium and glutathione peroxidase, and plasma lipid peroxides in uterine, ovarian or vulvar cancer, and their responses to antioxidants in patients with ovarian cancer. *Cancer Letters* 1984; **24**:1-10.
48. Prasad KN, Cole WC, Kochupillai V, Kumar A. High doses of multiple antioxidant vitamins: essential ingredients in improving the efficacy of standard cancer therapy. *Journal of the American College of Nutrition* 1999; **18**:13-25.
49. Immordino ML, Dosio F, Cattel L. Stealth liposomes: review of the basic science, rationale, and clinical applications, existing and potential. *International Journal of Nanomedicine* 2006; **1**:297-315.

50. Maeda H. The enhanced permeability and retention (EPR) effect in tumor vasculature: the key role of tumor-selective macromolecular drug targeting. *Advanced Enzyme Regulation* 2001; **41**:189-207.
51. Bergers G, Benjamin LE. Tumorigenesis and the angiogenic switch. *Nature Review Cancer* 2003; **3**:401-410.
52. Maeda H, Sawa T, Konno T. Mechanism of tumor-targeted delivery of macromolecular drugs, including the EPR effect in solid tumor and clinical overview of the prototype polymeric drug SMANCS. *Journal of Controlled Release* 2001; **74**:47-61.
53. Freter CE. Doxorubicin cardiac toxicity manifesting seven years after treatment. Case report and review. *The American journal of medicine* 1986; **80**:483.
54. Schwartz RG, McKenzie WB, Alexander J, Sager P, D'Souza A, Manatunga A, et al. Congestive heart failure and left ventricular dysfunction complicating doxorubicin therapy. Seven-year experience using serial radionuclide angiocardiology. *The American journal of medicine* 1987; **82**:1109-1118.
55. Steinherz LJ, Steinherz PG, Tan CT, Heller G, Murphy ML. Cardiac toxicity 4 to 20 years after completing anthracycline therapy. *JAMA: The Journal Of The American Medical Association* 1991; **266**:1672-1677.
56. Steinberg JS, Cohen AJ, Wasserman AG, Cohen P, Ross AM. Acute arrhythmogenicity of doxorubicin administration. *Cancer* 1987; **60**:1213-1218.
57. Ferrans VJ. Overview of cardiac pathology in relation to anthracycline cardiotoxicity. *Cancer treatment reports* 1978; **62**:955-961.

58. Imondi AR, Della Torre P, Mazue G, Sullivan TM, Robbins TL, Hagerman LM, et al. Dose-response relationship of dexrazoxane for prevention of doxorubicin-induced cardiotoxicity in mice, rats, and dogs. *Cancer Research* 1996; **56**:4200-4204.
59. Bjelogrljic SK, Radic J, Jovic V, Radulovic S. Activity of d,l- α -Tocopherol (Vitamin E) against Cardiotoxicity Induced by Doxorubicin and Doxorubicin with Cyclophosphamide in Mice. *Basic & Clinical Pharmacology & Toxicology* 2005; **97**:311-319.
60. Breed JGS, Zimmerman ANE, Dormans JAMA, Pinedo HM. Failure of the antioxidant vitamin E to protect against adriamycin-induced cardiotoxicity in the rabbit. *Cancer Research* 1980; **40**:2033-2038.
61. Herman EH, Ferrans VJ, Myers CE, Van Vleet JF. Comparison of the effectiveness of (+/-)-1,2-bis(3,5-dioxopiperazinyl-1-yl)propane (ICRF-187) and N-acetylcysteine in preventing chronic doxorubicin cardiotoxicity in beagles. *Cancer Research* 1985; **45**:276-281.
62. Myers C, Bonow R, Palmeri S, Jenkins J, Corden B, Locker G, et al. A randomized controlled trial assessing the prevention of doxorubicin cardiomyopathy by N-acetylcysteine. *Seminars In Oncology* 1983; **10**:53-55.

Abbreviations

AUC	area under the plasma drug concentration-time curve
DOX	doxorubicin
DSPC	1,2-distearoyl-sn-glycero-3-phosphatidylcholine
DSPE-PEG	1,2-distearoyl-sn-glycero-3-phosphoethanolamine-N- [poly(ethylene glycol) 2000]
EPR	enhanced permeability and retention
FBS	fetal bovine serum
FDA	Food and Drug Administration
NADPH	reduced nicotinamide adenine dinucleotide phosphate
PAESe	phenyl-2-aminoethyl selenide
PC-3	androgen-independent human prostate cancer epithelial cells
PK	pharmacokinetic
ROS	reactive oxygen species
SEM	standard error of the mean
SSL	sterically stabilized liposomes
SSL-PAESe	sterically stabilized PAESe liposomes

CHAPTER 5

SUMMARY AND FUTURE STUDY

The overall goals of this dissertation were to determine the ability of phenyl-2-aminoethyl selenide (PAESe), a potent antioxidant, to mitigate doxorubicin (DOX) induced cardiotoxicity, without altering DOX antitumor activity.

In **Chapter 2**, we determined the protective effect of PAESe on DOX-mediated cardiotoxicity and its potential alter antitumor activity of DOX using *in vitro* and *in vivo* models of human cancer. We demonstrated that PAESe did not inhibit the growth of PC-3 and BT-474 cells at drug concentrations up to 10 μ M for 72 hr, however, concomitant use of PAESe decreased the oxidative-mediated cytotoxicity of a known oxidant, TBHP, but had limited effect on vincristine or DOX activity. PAESe decreased the concentration of intracellular reactive oxygen species (ROS) generated from TBHP and DOX. In an *in vivo* model, PAESe decreased early signs of DOX-induced cardiotoxicity, such as infiltration of neutrophil and macrophages into the myocardium. These data supported our *hypothesis* that PAESe reduces DOX-mediated cardiotoxicity while preserving antitumor effect of DOX. Unexpectedly we observed evidence that PAESe elicited direct antitumor activity in a tumor (PC-3) xenograft mouse model. This finding was not expected, as *in vitro* studies suggested that PAESe non-significantly reduced MTT and SRB staining at concentrations of 10 μ M following 72 hr exposure. It is possible the *in vivo* activity is due to differences in exposure, although this is not likely as the

pharmacokinetics (half-life and clearance) of a structurally similar compound was rapidly eliminated with short half-life (~10 min) and PAESe's half-life was determined to be less than 15 min (**Chapter 3**). Concomitant administration of PAESe also decreased body weight loss, a common toxicity associated with the use of DOX. This unexpected *in vivo* antitumor activity is believed related to its potent antioxidant activity. However, the mechanism(s) of action is unclear.

In **Chapter 3**, we developed a novel liquid chromatography tandem mass spectrometry (HPLC-MS/MS) method to determine the pharmacokinetic (PK) of PAESe. The HPLC-MS/MS analytical method was validated, and it had a lower limit of quantification of 50 nM and the acceptable range ($\pm 15\%$) of the accuracy and precision for intra-day and inter-day assay. We also encapsulated PAESe in sterically stabilized liposomes (SSL-PAESe) as a tool to understand the effect of altering systemic exposure and to evaluate their activity in tumor model (**Chapter 4**). The SSL-PAESe were developed with >80% encapsulation efficiency at drug:lipid ratio of 0.2:1.0 (mol:mol).

We demonstrated that encapsulation of PAESe in SSL altered the PK properties of PAESe, resulting in a significantly ($p < 0.05$) enhanced circulation half-life (690%), exposure (AUC, 6,787%) and decreased clearance (-99.3%). These results supported our *hypothesis* that encapsulation PAESe in sterically stabilized liposomes (SSL) increases the exposure of PAESe by long circulating property of SSL. The SSL-PAESe and new HPLC-MS/MS assay provided tools to examine the effect of different exposure profiles on cardiotoxicity and antitumor activity (**Chapter 4**). These tools will serve as basis for examining tissue/tumor distribution to optimize dosing schedules and gain mechanistic insights into PAESe cardioprotective and antitumor activity and can be used to optimize

formulations with optimal chemoprotective and/or antitumor activity.

In **Chapter 4**, we determined the effect of encapsulated PAESe in SSL on antitumor activity and survival *in vivo* using an established human prostate (PC-3) tumor xenograft model in athymic mice. We found that encapsulated PAESe in SSL exerted the improved *in vivo* antitumor activity relative to free PAESe with extended survival even though SSL-PAESe was administered at ½ the dose of free PAESe. In addition, no evidence of cardiotoxicity was observed in groups treated with PAESe and SSL-PAESe alone and in combination with DOX. These findings support our *hypothesis* that the long-circulating PAESe-liposomes improve antitumor efficacy and cardioprotectant properties. This effect is believed to be associated with the increased circulation time following encapsulation. Further, we also examined that PAESe decreased evidence of DOX-induced cardiomyopathy, such as disruption and fragmentation of myofibers after long-term DOX treatment, which is more commonly recognized and clinically the most important form of cardiotoxicity. These data support the hypothesis that PAESe would have a protective effect after long-term exposure of DOX.

Here, we showed that PAESe reduced cardiotoxicity of anthracyclines and unexpectedly had antitumor activity. These data support future studies for translation into clinical application.

Cardiotoxicity associated with anthracyclines is a major clinical challenge in cancer chemotherapy. The cardioprotective effect of PAESe should be determined for other anthracyclines (*e.g.*, Daunorubicin and Epirubicin) and other chemotherapeutics that lead to free radical induced cardiovascular damages. The activity should also be determined using other dosing schedules that are used in the clinical setting for prolonged

period in mice and other animal models that are more representative of human cardiotoxicity, such as the pig.

Cardiotoxicity is characterized by the occurrence of abnormalities in left ventricular ejection fraction (LVEF) and electrocardiographic interval changes, ventricular arrhythmias, coronary syndromes, pericarditis and myocarditis-like syndromes [1]. As future work, monitoring techniques such as electrocardiography and radionuclide angiocardigraphy can be applied to measure heart rate, left ventricular performance, slope of systolic and diastolic pressure to assess abnormalities in cardiac function. Electrocardiography is one of the standard approaches used for monitoring cardiac function, and radionuclide angiocardigraphy is widely used to evaluate early anthracycline-induced cardiotoxicity [2, 3]. The levels of serum enzyme can also be measured in order to enunciate the cardioprotective effect of PAESe. Serum enzymes such as creatine kinase (CK) and asparatate aminotransferase (AST) are major indicators to detect muscle damages [4]. Serum levels of cTnT (cardiac troponin T) can also be detected to diagnose cardiotoxicity such as myocardial infarction, acute myocarditis, and angina [5].

In addition, dose-response relationship can be evaluated to determine dose ratios of DOX and PAESe capable of providing maximal activity of PAESe. The time-course of DOX-mediated cardio damage by free radicals may also be examined to optimize the dose schedule.

The possible toxicity of PAESe should also be determined although the growth of PC-3 and BT-474 cells was not significantly inhibited (**Chapter 2**) and animal body weight of free- and SSL-PAESe group was not significantly different relative to control

(**Chapter 2, 4**). To this end, the HPLC-MS/MS assay we developed can be utilized to quantify PAESe in tumor, heart, and other organs so that the exposure response profile can be generated.

Further studies are necessary to clarify the mechanism of action for antitumor effect of PAESe. We suggested this unexpected antitumor effect might be associated with its potent antioxidant activity, which could alter *in vivo* immune function. This hypothesis is based on the observation that *in vitro* studies, in the absence of immunological cells, suggested there was limited effect on tumor growth. Although the *in vivo* studies were performed in immunocompromised animals, they are partially deficient in T cells, *i.e.*, do not have a complete absence of functional T cells, so that immune function might not be inhibited completely [6, 7]. Antioxidants are known to alter a magnitude of immune function by increasing the activity of immune cells and the expression immune-related cytokine signaling molecules [8-10]. In addition, antioxidant can also reduce the expression of oncogenes as well as the activity of protein kinase C that promotes cancer progression [11]. To this end, the effect of PAESe on *in vivo* immune function should be determined by examining the relations with cytokine signaling molecules like interleukins or cytotoxic T lymphocytes and natural killer cells that are essential effectors of anti-tumor immune responses *in vivo*.

Alternatively, PAESe may alter tumorigenicity by regulating oncogenic expression [12, 13]. Although *in vitro* studies (**Chapter 2**) suggested PAESe did not have direct antitumor activity, at 10 μ M and 72 hr exposure there was some cytotoxicity, albeit non-significant. Based on PK studies (**Chapter 3**) PAESe is rapidly eliminated from the systemic circulation, therefore if there are differences in exposure it is likely these are

mediated by indirect effects or time dependent (transduction) effects that occur after initial exposure. The antitumor activity of selenium may be related to its antioxidant activity. Glutathione peroxidase, another important antioxidant, is known to decrease oxidant-induced DNA damages, which are known to associate with malignancy [14-16].

The *in vivo* antitumor effect of PAESe was not significantly different between free- and SSL-PAESe group although circulation time and exposure (AUC) of SSL-PAESe group were markedly increased compared to free PAESe group (**Chapter 3 and 4**). Further, it is unlikely to have prolonged exposure *in vitro* since free drug is rapidly eliminated ($\beta_{1/2} = 8.78$ min) *in vivo*. These data further suggest that PAESe exposure (direct action) might not be responsible for the antitumor effect.

In conclusion, we demonstrated that PAESe, a novel selenium-based antioxidant, and its encapsulated form in sterically stabilized liposome (SSL-PAESe) were effective in providing cardioprotective effect on free radical mediated DOX-induced cardiotoxicity and unexpectedly showed potent *in vivo* antitumor activity. Although further studies are necessary to determine the mechanism underlying the antitumor activity of PAESe, this research is significant as clearly demonstrates that PAESe and SSL-PAESe have potential as chemoprotectants to improve the clinical usage of DOX, as well as direct chemotherapeutic agents.

Reference

1. Albini A, Pennesi G, Donatelli F, Cammarota R, De Flora S, Noonan DM. Cardiotoxicity of anticancer drugs: the need for cardio-oncology and cardio-oncological prevention. *JNCI: Journal of the National Cancer Institute* 2010; **102**:14-25.
2. Puri A, Maulik SK, Ray R, Bhatnagar V. Electrocardiographic and biochemical evidence for the cardioprotective effect of vitamin E in doxorubicin-induced acute cardiotoxicity in rats. *European Journal Of Pediatric Surgery: Official Journal Of Austrian Association Of Pediatric Surgery* 2005; **15**:387-391.
3. Hazari MS, Haykal-Coates N, Winsett DW, Costa DL, Farraj AK. A Single Exposure to Particulate or Gaseous Air Pollution Increases the Risk of Aconitine-Induced Cardiac Arrhythmia in Hypertensive Rats. *Toxicological Sciences* 2009; **112**:532-542.
4. DeAtley SM, Aksenov MY, Aksenova MV, Jordan B, Carney JM, Butterfield DA. Adriamycin-induced changes of creatine kinase activity in vivo and in cardiomyocyte culture. *Toxicology* 1999; **134**:51-62.
5. Herman EH, Lipshultz SE, Rifai N, Zhang J, Papoian T, Yu ZX, et al. Use of cardiac troponin T levels as an indicator of doxorubicin-induced cardiotoxicity. *Cancer Research* 1998; **58**:195-197.

6. Shankaran V, Ikeda H, Bruce AT, White JM, Swanson PE, Old LJ, et al. IFN gamma and lymphocytes prevent primary tumour development and shape tumour immunogenicity. *Nature* 2001; **410**:1107.
7. Maleckar JR, Sherman LA. The composition of the T cell receptor repertoire in nude mice. *Journal Of Immunology (Baltimore, Md.: 1950)* 1987; **138**:3873-3876.
8. Patrick L. Selenium Biochemistry and Cancer: A Review of the Literature. *Alternative Medicine Review* 2004; **9**:239-258.
9. Ames BN, Shigenaga MK, Hagen TM. Oxidants, Antioxidants, and the Degenerative Diseases of Aging. *Proceedings of the National Academy of Sciences of the United States of America* 1993; **90**:7915-7922.
10. Knight JA. Review: Free radicals, antioxidants, and the immune system. *Annals Of Clinical And Laboratory Science* 2000; **30**:145-158.
11. Prasad KN, Cole WC, Kochupillai V, Kumar A. High doses of multiple antioxidant vitamins: essential ingredients in improving the efficacy of standard cancer therapy. *Journal of the American College of Nutrition* 1999; **18**:13-25.
12. Schwartz JL, Antoniades DZ, Zhao S. Molecular and biochemical reprogramming of oncogenesis through the activity of prooxidants and antioxidants. *Annals Of The New York Academy Of Sciences* 1993; **686**:262-278.
13. Lin J. Suppression of protein kinase C and nuclear oncogene expression as possible action mechanisms of cancer chemoprevention by curcumin. *Archives of Pharmacal Research* 2004; **27**:683-692.

14. Ursini F, Bindoli A. The role of selenium peroxidases in the protection against oxidative damage of membranes. *Chemistry And Physics Of Lipids* 1987; **44**:255-276.
15. Clark L, Combs GJ, Turnbull B, Slate E, Chalker D, Chow J, et al. Effects of selenium supplementation for cancer prevention in patients with carcinoma of the skin. A randomized controlled trial. Nutritional Prevention of Cancer Study Group. *JAMA* 1996; **276**:1957-1963.
16. Jiang C, Jiang W, Ip C, Ganther H, Lu J. Selenium-induced inhibition of angiogenesis in mammary cancer at chemopreventive levels of intake. *Molecular Carcinogenesis* 1999; **26**:213-225.

Abbreviations

AST	asparatate aminotransferase
AUC	area under the plasma drug concentration-time curve
BT-474	human breast carcinoma cell
CK	creatine kinase
cTnT	cardiac troponin T
DOX	doxorubicin
HPLC-MS/MS	high-performance liquid chromatography – tandem mass spectrometry
MTT	3-(4,5-Dimethylthiazol-2-yl)-2,5-diphenyltetrazolium bromide
PAESe	phenyl-2-aminoethyl selenide
PC-3	human prostate carcinoma
PK	pharmacokinetic
ROS	reactive oxygen species
SRB	sulforhodamine B
SSL	sterically stabilized liposomes
SSL-PAESe	sterically stabilized PAESe liposomes
TBHP	<i>tert</i> -butylhydroperoxide